SIGNAL PROCESSING VIA NONLINEAR MICRO RING RESONATOR FOR OPTICAL COMMUNICATION

SOMSAK MITATHA

A THESIS SUBMITTED IN PARTIAL FULFILLMENT
OF THE REQUIREMENT FOR THE DEGREE OF
DOCTOR OF ENGINEERING IN ELECTRICAL
FACULTY OF ENGINEERING
KING MONGKUT'S INSTITUTE OF TECHNOLOGY LADKRABANG
2008

KMITL-2008-EN-D-016-151

SIGNAL PROCESSING VIA NONLINEAR MICRO RING RESONATOR FOR OPTICAL COMMUNICATION

SOMSAK MITATHA

A THESIS SUBMITTED IN PARTIAL FULFILLMENT

OF THE REQUIREMENT FOR THE DEGREE OF

DOCTOR OF ENGINEERING IN ELECTRICAL

FACULTY OF ENGINEERING

KING MONGKUT'S INSTITUTE OF TECHNOLOGY LADKRABANG

2008

KMITL-2008-EN-D-018-151

Thesis Certification

Faculty of Engineering

King Mongkut's Institute of Technology Ladkrabang

Thesis Title	Signal Processing via Nonlinear Micro Ring Resonator for Optical Communication
Student	Mr.Somsak Mitatha
Student ID.	~~45061213~~ 45160309
Degree	Doctor of Engineering
Program	Electrical Engineering
Thesis Advisor	Assoc.Prof.Dr.Kobchai Dejhan
Thesis Number	KMITL-2008-EN-D-018-151

EXAMINERS		SIGNATURES
Assoc.Prof.Dr.Kraisin	Songwatana	
Asst.Prof.Dr.Somkiat	Lerkvaranyu	
Assoc.Prof.Dr.Athikom	Roeksabutr	
Assoc.Prof.Dr.Fusak	Cheevasuvit	
Assoc.Prof.Dr.Kobchai	Dejhan	

Date 24 September 2008 **Time** 17.00-19.00

Place Building A , 3rd Floor, Conference Room No. 1

สถาบันเทคโนโลยีพระจอมเกล้าเจ้าคุณทหารลาดกระบัง

KING MONGKUT'S INSTITUTE OF TECHNOLOGY LADKRABANG

(Assoc.Prof.Dr.Kobchai Dejhan)

Dean

24 September 2008

หัวข้อวิทยานิพนธ์	การประมวลสัญญาณผ่านวงแหวนโพรงสั่นพ้องขนาดเล็กชนิดไม่เป็นเชิงเส้นเพื่อใช้ในการสื่อสารทางแสง
นักศึกษา	นายสมศักดิ์ มิตะถา
รหัสนักศึกษา	45061213
ปริญญา	ปริญญาวิศวกรรมศาสตรดุษฎีบัณฑิต
สาขาวิชา	วิศวกรรมไฟฟ้า
พ.ศ.	2551
อาจารย์ที่ปรึกษาวิทยานิพนธ์	รองศาสตราจารย์ ดร.กอบชัย เดชหาญ

บทคัดย่อ

วิทยานิพนธ์นี้นำเสนอการประยุกต์ของอุปกรณ์ชนิดไม่เป็นเชิงเส้นโดยใช้โพรงสั่นพ้องวงแหวนขนาดเล็กเพื่อใช้ในการประมวลผลสัญญาณทางแสงซึ่งสามารถประยุกต์ใช้กับการส่งข้อมูลลับและการสื่อสารแบบไร้สาย วิทยานิพนธ์นี้ได้นำเสนองานวิจัยแบ่งออกเป็น 4 หัวข้อดังนี้

หัวข้อแรกนำเสนอการออกแบบการป้องกันข้อมูลของสวิทช์ชิ่งแบบกลุ่ม โดยอาศัยพฤติกรรมที่ไม่เป็นเชิงเส้นของโซลิตอนในโพรงสั่นพ้องวงแหวนขนาดเล็ก การสร้างสัญญาณเดออสกำเนิดจากพฤติกรรมที่ไม่เป็นเชิงเส้นที่เรียกว่าปรากฏการณ์ของเคอร์ การควบคุมกำลังอินพุทและพารามิเตอร์บางตัวของอุปกรณ์สามารถกำหนดคุณลักษณะของสัญญาณเอาท์พุทได้ ผลลัพธ์ที่ได้แสดงให้เห็นถึงศักยภาพของอุปกรณ์เพื่อนำไปใช้งานเป็นตัวกรองทางแสงของแถบผ่านและแถบหยุด เพื่อป้องกันสัญญาณที่มีลักษณะเป็นกลุ่มข้อมูล หัวข้อที่สองนำเสนอพฤติกรรมที่ไม่เป็นเชิงเส้นที่รู้จักกันในชื่อไบเฟอเคชั่น ที่สามารถสร้างและใช้เป็นบิทหยุดและบิทเริ่มต้นในการเข้ารหัสป้องกันกลุ่มข้อมูลดิจิตอลที่นำมาประยุกต์ใช้งานในด้านสวิทช์ชิ่งทางแสง หัวข้อที่สามเสนอวิธีการเข้ารหัสทางดิจิตอลของสัญญาณเดออส และสัญญาณนี้สามารถแปลงเป็นรหัสดิจิตอลลอจิกพัลส์ 0 หรือ 1 โดยวิธีควอนไตซ์สัญญาณ สุดท้ายเป็นการเสนอระบบการกำเนิดสัญญาณแสงแบบเร็วและช้าโดยการการป้อนพัลส์โซลิตอนเข้าไปในโพรงสั่นพ้องวงแหวนขนาดเล็กแบบไม่เป็นเชิงเส้น ผลการจำลองที่แสดงแถบความถี่เร็วและช้าจะใช้เป็นสัญญาณเพื่อส่งไปในเครือข่ายสื่อสารทางแสงแบบไร้สาย การออกแบบอุปกรณ์ขนาดเล็กนี้ประยุกต์ใช้กับโทรศัพท์เคลื่อนที่ได้

Thesis Title	Signal Processing via Nonlinear Micro Ring Resonator for Optical Communication
Student	Mr. Somsak Mitatha
Student ID	45061213
Degree	Doctor of Engineering
Program	Electrical Engineering
Year	2008
Thesis Advisor	Associate Professor Dr. Kobchai Dejhan

ABSTRACT

This thesis presents the interesting results for application of the nonlinear device known as a nonlinear micro ring resonator to process the optical signal processing which can be applied to the secured data transmission and wireless communication applications.

We propose four topics. Firstly, propose a design of the secured packet switching using the nonlinear behaviors of soliton in a micro ring resonator. The chaotic signals are generated by a Kerr effects nonlinear type, where the control input power or device parameters can be used to specify the output signals. Results obtained have shown the potential of using such a proposed device for the tunable band-pass and band-stop filters, in which the packet switching data can be performed and secured. Secondly, propose the nonlinear behavior of light known as bifurcation which can be generated to form the start-stop bits of secure digital codes for optical packet switching data. Thirdly, propose digital encoding of chaotic signals in nonlinear micro ring resonator. The generated chaotic signals can be formed as the logical pulses "1" or "0" using the signal quantizing method. Finally, propose a system of the simultaneous fast and slow light generation using a soliton pulse propagating within the nonlinear micro ring resonators. Results show the selected down-link and up-link frequency bands are 500 MHz and 2 GHz, respectively. Such small device system can be implemented within the mobile telephone hand set.

ACKNOWLEDGMENTS

Firstly of all, I would like to express my guidance sincere gratitude to my advisor, Assoc. Prof. Dr. Kobchai Dejhan, for his attention, insight, encourage, guided, and support during this research and for being available at anytime to response my questions, which has been valuable. I am grateful to Assoc. Prof. Dr. Preecha Yupapin for introducing me the research topics, for the many insightful conversations, and his constant encouragement. Working with him has been a great learning experience.

I would like to thank Dr. Wuttinan Pornsuwanchareon for his constructive comments and simulation results. The nonlinear optical simulations in this thesis are the fruit of collaboration with him. This thesis would have not been possible without his help.

I would like to thank Dr. Prajak Saeung for helping me with my problems, for reading and giving comments on my thesis, for staying up with me just to give me moral support, and for so many other favors which made things simpler and enjoyable.

I would also like to thank every young members of the Advanced Research Center of Photonic Laboratory (ARCP) of the Department of Applied Physics, Faculty of Science, KMITL; whose support has created a friendly environment.

I would like to thank my committee members, Assoc.Prof.Dr. Fusak Cheevasuvit, Assoc.Prof. Dr. Athikom Roeksabutr, Assoc. Prof.Dr. Kraisin Songwatana, Asst.Prof.Dr. Somkiat Lerkvaranyu, for their assistance, helpful comments, and insightful suggestions.

I would like to thank my loving Assoc.Prof.Dr. Charay Surawatpanya and Mrs. Chaweewon Mongkolaphakij, who have taught me to achieve my goal and have always believed in me. Their unconditional love has been the greatest source of energy to me.

Finally, my greatest thanks are to my beloved family and parents whose caring, understand, and possible attitude have encouraged me to go forward during difficult times. Whose never-ending love and support made the completion of this work completed and my dream of a graduate education come true.

Somsak Mitatha

CONTENTS

CONTENTS (Cont.)

LIST OF TABLES

Table **Pages**

LIST OF FIGURES

LIST OF FIGURES (Cont.)

Figures **Pages**

CHAPTER 1

INTRODUCTION

1.1 The Optical Communication Network

The use of light for communication purposes dates back to the use of smoke and fire to convey a piece of information. There are many reasons that makes photons popular in information processing. Photons can accomplish certain functions better than electrons by virtue of their special properties. The very large bandwidth, ~1015 Hz, gives optics a potential speed for signal processing which is well beyond any electronics. The shortest optical pulses of <10 fs give light three order of magnitude advantage over the shortest electrical pulse [1]. When it comes to interconnects on a chip, the wiring capacitance will set the speed limits of integrated circuits. Besides, photons can pass through each others unperturbed in the absence of a nonlinear interaction, whereas electrons interact with each other even at a distance. In Table 1.1, we summarize the potential advantages and disadvantages of using optics in signal processing.

Table 1.1: Advantage and disadvantage of optics in signal processing.

Advantage of optics	Disadvantage of optics
- Large bandwidth ~ 10^{15} Hz	- High power requirement ~ 1 W peak power
- Low propagation loss	- Interfacing with electronics
- Low cross talk	- Wave front distortions
- High degree of parallelism	
- Small dimension	
- Ultra short pulses < 10 fs	
- Coherence properties	

The turn of new millennium witnessed an explosion in data-traffic volume, due to the ongoing increasing demand on the Internet. Therefore, all-optical switching devices have been looked at as key components for future high-speed optical communication systems. Such devices would enable highly parallel logic operations as well as ultrafast switching because of the instantaneous nature of virtual optical transitions [2]. With the recent advances in semiconductor fabrication, there has been a noticeable effort to bring those devices on semiconductor platforms to the real world. An ideal all-optical switch is the one that poses the following characteristics. It would only require as little as sub picojoule(pJ) of energy to switch with at least 20dB switching contrast. Beside compactness, it is desirable to integrate such a device with already established optoelectronics devices on a planar integrated photonic circuit. One category of devices that has a great potential to meet those requirements is microring resonators.

1.2 Signal Processing in Optical Networks

Networking applications such as data browsing, large file transfer, multimedia-on-demand, and videoconferencing require high quality transfer of data streams of different lengths and initial formats. Optical fiber provides a suitable medium in which it is possible to reach tremendous transmission rates over long distances [3]. The maximum information carrying capacity was estimated to be around 100 THz [4]. Very high data rates can be achieved using a combination of wavelength and time division multiplexing techniques (WDM and TDM). WDM involves sending many signals in parallel at closely spaced wavelengths along the same fiber, while TDM allows close spacing in time of bits in a single channel.

While there exist means to produce, transfer, and detect information at a very high bandwidth, there is a need for more agility in photonic networks. The agility of present-day optical networks is limited by the electronic nature of a very important function: the processing of data signals. Signal processing is responsible for switching and routing traffic, establishing links, restoring broken links, testing, and managing the network.

At present, important and functionally complex signal processing operations of switching and routing are carried out electronically. Electronic signal processing imposes two significant limitations on the functionality of optical networks: cost and opacity. Today, signal switching and routing requires converting the optical information into electrical signals, processing in the electronic domain, and converting back to the optical domain before retransmission. Such an operation requires detection, retiming, reshaping, and regeneration at each switching and routing

point. This necessitates complex and expensive electronic and electro-optical hardware at each routing and switching node.

The use of electronic signal processing places strict requirements on the format of data streams transferred and processed, thus making the signal processing opaque. Repetition rates of optical signals, power levels, and packet lengths have to be standardized before they can be processed electronically. In addition, since modern electronics can process information at repetition rates far below the fundamental limits of the optical transmission, electronics imposes limits on the ultimate transmission rate of a network.

The ability to perform signal processing operations entirely within the optical domain would eliminate the requirement of optical-electrical-optical conversions, while providing the agility and speed inherent to optical elements. Provisioning of services with a vast diversity of rates and duration of connections could be enabled. All-optical switching solutions would be transparent to bit rate and protocols. The speed of electronic devices would no longer limit network throughput: optical signal processing, in contrast with electronics, may provide ultrafast sub picoseconds switching times [5].

1.3 Optical Signal Processing using Nonlinear Optics

In contrast to the optical signal processing solutions discussed in the previous section, nonlinear optics can potentially support transparent and fast self-processing of signals. A variety of nonlinear optical signal processing functions can be realized with similar fundamental building blocks [6–8]. Nonlinear optical elements and devices can be either integrated in photonic circuits [9] or used in a free-standing configuration [10].

Nonlinear optics can enable signal processing without the requirement of external electrical, mechanical, or thermal control [11]. The response time of properly designed nonlinear optical devices is limited fundamentally only by the nonlinear response time of the constituent materials [5, 12–14]. Photons do not interact with each other in vacuum. In order to perform nonlinear optical signal processing operation the properties of a medium through which the light travels must be modified by the light itself. Optical signals then propagate differently as a result of their influence on the medium.

Nonlinear optical signal processing elements utilize the illumination-dependent real and imaginary parts of the index of refraction [11]. Depending on the material and spectral position, the refractive index and absorption of a given nonlinear material can either increase or decrease

with increasing illumination. A wide range of broadband and wavelength-selective nonlinear optical signal processing devices has been proposed and demonstrated.

The most commonly studied nonlinear optical switching elements are nonlinear Fabry-Perot interferometers, nonlinear Mach-Zehnder modulators, nonlinear directional couplers, optical limiters, and nonlinear periodic structures. A nonlinear Fabry-Perot interferometer consists of two mirrors separated by a nonlinear material. As the refractive index of the nonlinear material changes with an increased level of illumination, the effective path length of the resonator is altered. A nonlinear Fabry-Perot interferometer can be tuned out of, or into, its transmission resonance. When illuminated with the continuous-wave light, a nonlinear Fabry-Perot interferometer can exhibit optical bistability. Optical bistability is a phenomenon in which the instantaneous transmittance of the device depends both on the level of incident illumination and on the prior transmittance of the device. Such an element enables all-optical memory.

In a nonlinear Mach-Zehnder modulator and a nonlinear directional coupler, a part of the waveguide is made out of a nonlinear material. Changing the intensity of the incident light changes the effective path length experienced by the light. This, in turn, through phase interference, results in an illumination-dependent transmittance in a Mach Zehnder modulator, and an illumination-dependent coupling in a nonlinear directional coupler.

A number of techniques use nonlinear properties of materials to obtain power limiting, and associated with it, on-off switching. Such devices are based on total internal reflection [15], self-focusing [16], self-defocusing, or two photon absorption [17]. Nonlinear periodic structures combine the phenomena of nonlinear index change and distributed Bragg reflection. The intensity-dependent transmission and reflection properties of nonlinear periodic structures can be harnessed to yield various signal processing functions. Prior to this work it has been demonstrated that nonlinear periodic structures can support optical switching, optical bistability, and solitonic propagation of pulses. Nonlinear periodic structures offer many structural and material degrees of freedom allowing modification of the general character and specifics of their optical response.

1.4 Goal of the Thesis

A variety of nonlinear optical signal processing functions in microring resonator can be realized in many applications. For examples, the Kerr effect, four wave mixing (FWM) can be used to communication high microwave frequency (THz), bistability can be implemented for the

switching, bifurcation can be start bit for data communication, the add/drop multiplexing can be used cancellation chaotic signal and the chaos of nonlinear system can be chaotic coding.

Microring resonators with these applications are thus need careful and exact design for their correct operation. A direct result of the progress in fabrication techniques is the increased need of the accurate models for characterizing the nonlinear devices. For very simple devices, analytical tools provide a framework for quick low cost feasibility studies and allow for design optimization before devices are fabricated.

The primary goal of this thesis investigates the design and simulation nonlinear characteristics of ring resonator architectures. The discrete-time signal processing (DSP) approach is systematic and intuitive for the design of nonlinear optical devices and also found that very useful for deriving an algorithm transfer functions in Z-domain for modeling ring resonator filters. Second goal is to design of the secured packet switching using the Kerr effects nonlinear type of soliton in a microring resonator for communication security application. Third goal is to generate start-stop bits as the secured codes using bifurcation nonlinear in a microring resonator for optical packet switching application. Another objective is to generate the logical pulses "1" or "0" from chaotic signals using the signal quantizing method for optical digital encoding application. Finally, is to generate the simultaneous fast and slow light using a soliton pulse propagating within the nonlinear micro ring resonators.

1.5 Scope of the Thesis

With the growing importance of microring resonators for a variety of applications, it becomes necessary to devise a model which is directly interpretable in physical terms, and which is essentially free of any fit parameters. In this thesis, we restrict ourselves to the design of 2-D a multiple ring resonator filters and analyze the nonlinear characteristics in general. In this thesis, we employ the discrete-time signal processing (DSP) approach to design and analyze nonlinear optical filters. DSP is employed here for the analytical derivation of the optical transfer functions in Z-domain of filters. The present analysis is restricted to directional couplers and waveguides characterized by various parameters, the power coupling coefficient, power coupling loss, the radius of the ring waveguide and attenuation coefficient.

1.6 Organization of the Thesis

This thesis presents a novel design and simulated characteristics for characterizing nonlinear optical ring resonator filters. The organization is as follows:

- The current chapter gives an introduction to the subject of the thesis and generalized signal processing in optical networks.
- Chapter 2 describes some of phenomena of nonlinear optic.
- Chapter 3 discusses analytical approach of signal processing which is used to characterize nonlinear devices, theoretical background and enhanced nonlinearity in microring resonator.
- Design nonlinear devices by using nonlinear behavior in microring resonator filters and all essential parameters describing the nonlinear characteristics are extracted in chapter 4 and 5.
- Finally, Chapter 6 presents a summary of the results of the thesis and a discussion of future research.

CHAPTER 2

PHENOMENA OF NONLINEAR OPTIC

The use of semiconductor materials as nonlinear optical elements bridges the gap between optics and electronics. It opens the possibility for integrating the laser sources, signal processing elements, and detectors on the same platform. In this regard, the III-V binary semiconductors, such as GaAs and InP, have acquired great attention in the last few decades because they are direct bandgap materials and possess higher nonlinear coefficients than their competing materials. Another attractive feature of binary semiconductors is that they can be combined or alloyed to form ternary or quaternary compounds. Doing so, makes it possible to vary the bandgap of the material continuously together with its band structure, electronic, and optical properties. As an example, the bandgap energy of the ternary compound $Al_xGa_{1-x}As$ depends on the mole fraction x. Another important quaternary compound that we will consider is $In_{1-x}Ga_xAs_yP_{1-y}$. Therefore, one can design ternary and quaternary compounds to be transparent for optical channel waveguides or active for lasers and amplifiers at the 1550 nm communication window.

In this chapter, we will discuss different nonlinear processes that affect the performance of semiconductor microring resonators as all-optical signal processing tools.

2.1 Nonlinear Susceptibility

Nonlinear optics is the study of phenomena that occur as a consequence of the modification optical properties of a material under intense illumination. Typically, only laser light is sufficiently intense to modify the optical properties of a material. Nonlinear optical phenomena are nonlinear in the sense that the induced material polarization is nonlinear in the electric field [18]. The general equation that describes the optical field evolution in a dielectric material is given by

$$\nabla^2 \mathrm{E} - \frac{1}{c^2}\frac{\partial^2 \mathrm{E}}{\partial t^2} = -\mu_0 \frac{\partial^2 \mathrm{P(E)}}{\partial t^2} \tag{2.1}$$

where the polarization $\vec{P}$ characterizes the medium and it is a function of the electric field. In the case of weak nonlinear behavior of the medium, the polarization can be expressed by a Taylor polynomial as

$$\vec{P} = \underbrace{\varepsilon_0 \vec{E} + \varepsilon_0 \chi^{(1)} : \vec{E}}_{linear\ P_L} + \underbrace{\varepsilon_0 \chi^{(2)} :: \vec{E} \cdot \vec{E} + \varepsilon_0 \chi^{(3)} ::: \vec{E} \cdot \vec{E} \cdot \vec{E} + \ldots}_{nonlinear\ P_{NL}}, \tag{2.2}$$

where dielectric dispersion is ignored. $\chi^{(1)}$ is the linear susceptibility, :represents the inner tensor product and the second and the third-order tensor $\chi^{(2)}$ and $\chi^{(3)}$ are responsible for the second harmonic generation, and the third-order harmonic generation, respectively.

2.2 Nonlinear Refraction (Optical Kerr Effect)

The optical Kerr effect (i.e. nonlinear refraction index) results from the third order nonlinear susceptibility $\chi^{(3)}$, which is a fourth rank tensor.

An optical wave is a real quantity and usually expressed as

$$\vec{E}(t) = \mathrm{Re}\left\{\vec{E} \exp j(\vec{k} \cdot \vec{r} + \omega t)\right\} \tag{2.3}$$

or similarly as

$$\vec{E}(t) = \frac{1}{2}\vec{E} \exp j(\vec{k} \cdot \vec{r} + \omega t) + c.c. \tag{2.4}$$

where c.c. represents the complex conjugate of the preceding term. Thus, an x-polarized optical wave, propagating in the z-direction in an isotropic medium, is represented mathematically as

$$\vec{E}(t) = \frac{1}{2}E_x \hat{x} \exp j(kz + \omega t) + c.c. \tag{2.5}$$

The third order polarization (mediated by $\chi^{(3)}$) in a material leads to a nonlinear intensity dependent contribution to its refractive index; i.e., the refractive index of the material changes as the incident intensity on the material changes. The susceptibility tensors in isotropic material can

be further simplified as $\chi^{(2)}=0$, due to inversion symmetry; the third order nonlinear susceptibility will only have one contributing term χ_{xxxx} since the light is x-polarized and there are no means for sourcing additional polarization components.

The linear and nonlinear induced polarizations are

$$P_L=\varepsilon_0(1+\chi^{(1)})E, \tag{2.6}$$

$$\begin{aligned} P_{NL} &= P^{(3)} \\ &= \varepsilon_0\chi_{xxxx}(\omega;-\omega,\omega,\omega)E^*EE \\ &\quad + \varepsilon_0\chi_{xxxx}(\omega;\omega,-\omega,\omega)EE^*E \\ &\quad + \varepsilon_0\chi_{xxxx}(\omega;\omega,\omega,-\omega)EEE^* \\ &= 3\varepsilon_0\chi_{xxxx}|E|^2E \\ &= \frac{3}{4}\varepsilon_0\chi_{xxxx}|E_x|^2E \end{aligned} \tag{2.7}$$

respectively. Hence,

$$P=P_L+P_{NL}=\varepsilon_0\left(1+\chi^{(1)}+\frac{3}{4}\varepsilon_0\chi_{xxxx}|E_x|^2\right)E$$

The total dielectric constant is

$$\varepsilon_r^{tot}=\varepsilon_r+\Delta\varepsilon_r$$

where $\varepsilon_r=1+\chi^{(1)}=n_o^2$ and $\Delta\varepsilon=\frac{3}{4}\chi_{xxxx}|E_x|^2$ after comparing with the expression for P.

The refractive index is related to the dielectric constant as:

$$n=\sqrt{\varepsilon_r+\Delta\varepsilon_r}\approx\sqrt{\varepsilon_r}+\frac{\Delta\varepsilon_r}{2\sqrt{\varepsilon_r}}=n_0+\frac{3\chi_{xxxx}}{8n_0}|E_x|^2 \tag{2.8}$$

The intensity dependent refractive index for a nonlinear material is given by

$$n = n_0 + n_2 |E|^2 \tag{2.9}$$

Comparing Eq.(2.8) and Eq.(2.9), the nonlinear refractive index is directly determined by the third-order susceptibility as

$$n_2 = \frac{3\chi_{xxxx}}{8n_0} = \frac{3\chi^{(3)}}{8n_0} \tag{2.10}$$

which characterizes the strength of the optical nonlinearity. The intensity I of an optical wave is proportional to $|E|^2$ as $I = \frac{1}{2\eta}|E|^2$ where η is the impedance of the medium. When comparing the optical response in the same medium, $I = |E|^2$ is taken for simplification.

2.3 Four Wave Mixing

When the signal at difference frequencies propagates through the medium, besides Cross-Phase Modulation (XPM), another important effect occurs: four-wave mixing (FWM) [21].

Four-wave mixing is a nonlinear effect arising from a third-order optical nonlinearity, as is described with a $\chi^{(3)}$ coefficient. It can occur if at least two different frequency components propagate together in a nonlinear medium such as an optical fiber. Assuming just two input frequency components ω_1 and ω_2 (with $\omega_2 > \omega_1$), a refractive index modulation at the difference frequency occurs, which creates as additional frequency components (Fig 2.1). In effect, two new frequency components are generated: $\omega_3 = \omega_1 - (\omega_2 - \omega_1) = 2\omega_1 - \omega_2$ and $\omega_4 = \omega_2 + (\omega_2 - \omega_1) = 2\omega_2 - \omega_1$

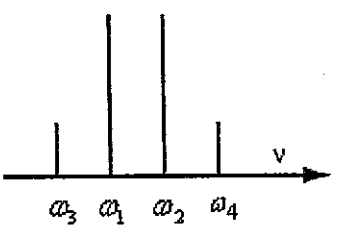

Fig. 2.1 Generation of new frequency components via four-wave-mixing

Four-wave mixing (FWM) is a parametric interaction among waves satisfying a given phase relationship called phase matching. Different phenomena may be originated by FWM process depending on the relation among interaction frequencies. If three optical fields with carrier frequencies ω_i (i = 1, 2, 3) propagate inside the medium simultaneously, it appears that the third-order polarization vector has several components: three components have the frequencies of the input fields, the others have an angular frequency ω_4 given by

$$\omega_4 = \omega_1 \pm \omega_2 \pm \omega_3 \tag{2.11}$$

If no field is present in the medium at the frequency ω_4, a new field component is created at this frequency. If a field at the frequency ω_4 is already present in the medium, it will be affected by the nonlinear interaction between the fields at ω_i, which causes crosstalk in multi-channel communication systems.

The phase-mismatch among all for waves is given by

$$\Delta\beta = \beta(\omega_1) + \beta(\omega_2) - \beta(\omega_3) - \beta(\omega_4) \tag{2.12}$$

where $\beta(\omega)$ is the propagation constant for an optical field with frequency ω. Assuming that the frequencies to be closely and equally spaced (i.e., $\omega_1 = \omega_2 - \Delta\omega$, $\omega_3 = \omega_2 - 2\Delta\omega$, $\omega_1 = \omega_2 - \Delta\omega$) and by applying Taylor series expansion of all β s about the frequency ω_2, gives

$$\Delta\beta = 2\beta_2(\Delta\omega)^2 \tag{2.13}$$

where $\beta_2 = \partial^2\beta / \partial\omega^2$ is the group velocity dispersion (GVD). When $\beta_2 = 0$ we set perfect shave phase matching and thus an efficient FWM. This situation is desirable for applications such as all-optical signal processing, wavelength conversion, pulse compression, etc. FWM in optical materials can also be used for generating spectrally inverted signal through the process of optical phase conjugation (OPC), which is useful for dispersion compensation. However, in the WDM systems FWM causes a transfer of power from each channel to its neighbors. Such the power transfer not only results in the power loss for the channel but also induces inters channel crosstalk

that degrades the system performance severely. This problem can be minimized using the technique of dispersion management, in which the dispersion is kept locally high even though it is low on average.

2.4 Optical Chaos

Optical Chaos is observed in many nonlinear optical systems. One of the most common examples is a ring resonator. One of the most seminal works is published by Ikeda (Physical Review Letters, 1982) where chaotic behavior in a ring resonator was proposed and experimentally confirmed. Optical Chaos was an exciting field of research in the mid-1980s and was expected at that time to lead to production of all optical devices including all optical computers. Researchers realized later the inherent limitation of the optical systems due to the non-localized nature of photons compared to highly localized nature of electrons. Research in Optical Chaos has seen a recent resurgence in the context of studying synchronization phenomena, and in developing techniques for secure optical communications [22-23].

2.5 Optical Bistability

The phenomenon of Optical Bistability (OB) arises from a combination of the nonlinearity in the radiation-matter interaction and of a feedback mechanism [24-26]. Generally, there are two classes of OB: absorptive and dispersive OB. Absorptive OB occurs whenever the input wavelength is close to the atomic resonance of the material. An increase in the input power produces an increase in saturation, i.e., in the degree of transparency of the medium. This allows the internal field of the cavity to increase, which in return increases the saturation. Such positive feedback loop causes the switch-up process. When the input power is decreased, the internal field is intense enough to maintain the saturation. As a consequence, the transmitted power is held "ON" and one obtains a hysteresis curve. Typically, InGaAsP can be designed to have the band edge around 1.45 μm and thus show absorptive OB when pumped at 1.55 μm. On the other hand, dispersive OB occurs whenever the input wavelength is tuned far away from the atomic resonance and hence the material is transparent. The frequency of the incident field is kept near one of the cavity frequencies, but detuned enough so that the transmission is low. An increase in the input intensity produces an increase in the intensity of the internal field. Because the refractive index is a function of intensity, this changes the optical length of the medium in such a way that the cavity

resonance is driven closer to the input frequency. In return, it increases the internal field intensity. Thus, again, we have a positive feedback loop which produces up-switching. When the incident power is decreased, the internal field is intense enough to maintain resonance between the cavity and the input frequency, and therefore one again obtains a hysteresis. An example of this phenomena is shown in Fig. 2.2 where the input wavelength is at 1.55 μm. The characteristic of bistability hysteresis can be implemented as optical switching.

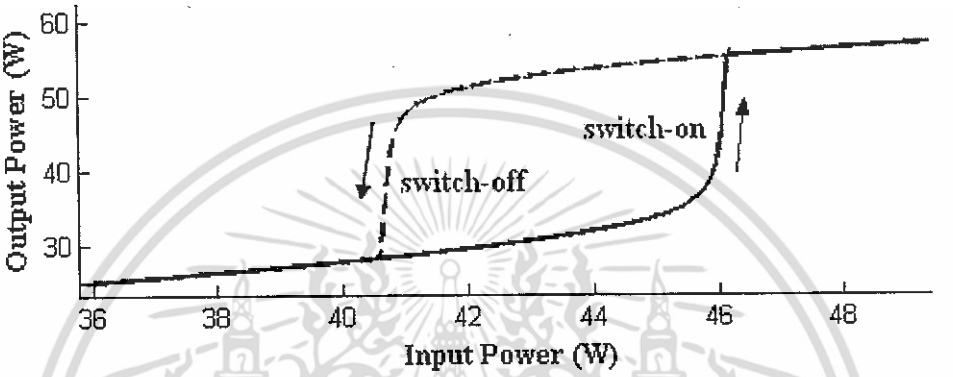

Fig. 2.2 The output power versus the input power showing the bistability hysteresis used as switch "on" and "off".

2.6 Optical Bifurcation

Bifurcation theory is the mathematical study of how and when the solution of a problem changes from only being one possible solution to be two, which is called a bifurcation. Most commonly used in the mathematical study of dynamical systems, a bifurcation occurs when a small smooth change made to the parameter values (the bifurcation parameters) of a system causes a sudden 'qualitative' or topological change in its long-term dynamical behavior. Bifurcations occur in both continuous systems and discrete systems [27, 28].

The study of how the character of fixed points change as parameters of the system change is called bifurcation theory. (Recall that the term bifurcation is used to describe any sudden changes in the dynamics of the system. When a fixed point changes character as parameter values change, the behavior of trajectories in the neighborhood of that fixed point will change. Hence the term bifurcation is appropriate here.) Being able to classify and understand the various possible bifurcations is an important part of the study of nonlinear dynamics.

2.7 Optical Soliton

How can we make beams that maintain their shape and size along propagation? As explained in the previous section, the phase between the different plane waves constructing the beam should be invariant along propagation. In a linear medium, the phase between the different plane waves depends solely on the propagation angle. It is clear then, that if all the plane wave components have the same angles; they will also have the same phase velocity and no phase different will be acquired during propagation. If we represent the propagation direction of these plane waves by arrows, these arrows will creates a cone in space. The associated beam will propagate in this linear medium with no broadening while maintains it's shape and dimensions. This type of beams is called "Bessel beams" since their field is described by Bessel function.

In a nonlinear medium, however, each plane wave is influenced by all the others. This is because the index change is a function of the total intensity. For some nonlinearities it is possible to find an ensemble of plane waves which will delay the phase velocity of the on axis components (in comparison with the of axis components) Consequently, the phase delay between the different propagating plane waves (explained in the previous section) will be compensated by the other waves via the medium nonlinearity.

If the nonlinearity is such that the index at the beam center is higher than in the dark regions, then the plane wave that propagates on axis will experience the highest index and will propagate slower from those off axis. This high index experienced by the on axis wave can compensate for it's linear tendency to propagate faster (because it is on axis). One example in which the index of refraction fully compensates for the shorter trajectory is a hyperbolic secant solution in a Kerr type medium. The plane waves that construct the hyperbolic secant index profile (induced by the beam via the nonlinearity) have all the same phase velocity along propagation, and hence their interference (the hyperbolic secant shape) also maintains its shape and size as it propagates.

To look on solitons from the mathematical perspective, one has to find a stationary wave solution of governing nonlinear wave equation. The mathematical aspects of solitons are out of the scope of this thesis. Hence at this point, I will give just the final solution. For the exact mathematical derivation, the reader may refer to [29-31].

We start from the Maxwell equations with the following assumptions:

• The electric field in the propagation direction is negligible in comparison with the transverse electric field (paraxial approximation).

• The electro-magnetic wave is monochromatic and its frequency is ω.

• The transverse electric field is $E(x,y,z,t)=\psi(x,y,z)\exp[j(\omega t-kz)]$ where the slowly varying field $\psi(x,y,z)$ changes much slower than $\exp[j(\omega t-kz)]$.

• The change in the refractive index is much smaller than 1.

For beams in Kerr-type medium (for which the index of refraction is the following function of the intensity: $n(I)=n_0+n_2 I$, one can start from the Maxwell equations and derive the nonlinear Schrödinger equation:

$$\frac{\partial}{\partial z}\psi(x,y,z)=\left[\frac{j}{2k}\left(\frac{\partial^2}{\partial x^2}+\frac{\partial^2}{\partial y^2}\right)+\frac{jkn_2}{n_0}\left|\psi(x,y,z)\right|^2\right]\psi(x,y,z) \qquad (2.14)$$

Here, z is the propagation direction, k is the wave vector, and ψ is the slowly-varying amplitude of the electric field. Among all solutions for Equation (2.14) there is one family of particular interest:

$$\psi=\sqrt{\psi_0}\,\mathrm{sech}\left[\frac{x}{W_0}\right]\exp\left[j\left(\frac{z}{4z_0}\right)\right] \qquad (2.15)$$

Where $W_0=\sqrt{\frac{2n_0}{n_2}}\frac{1}{k\psi_0}$ and $Z_0=\frac{kW_0^2}{2}$. We can see that the intensity of this subfamily ($I(x,y)=|\psi|^2$) is z independent. For any chosen peak power, ψ_0, we can find a sech solution with appropriate width (the width, W_0, is a function of the peak intensity and is wider for lower peak intensities). All solutions of this sub-family (equation (2.15)) will keep their shape and size invariant along propagation. Yet, in order to observe such solitons in nature, it is not enough to have a steady state mathematical solution in hand: one should also check for the stability of this steady state solution to noise and to deviations from ideal initial condition. If the solution exemplifies a state of stationary propagation - only then it can be considered as a soliton.

2.8 Summary

This chapter introduced the fundamental concepts of different nonlinear behaviors include soliton signal which used as input for launching into micro ring resonator. Consequently, we understand of the behaviors and enable design for the nonlinear devices as mention in chapter 4 and 5. The next chapter discusses theoretical background and also detailed of enhanced nonlinearity in both single and double ring resonators.

CHAPTER 3

THEORETICAL BACKGROUND

This chapter, I will describe the theoretical background of this thesis. To begin, the meaning, the advantage and the history of ring resonator involve the material system that was used for the planar waveguide are discussed in section 3.1, 3.2 and 3.3, respectively. Section 3.4 discusses the basic concept of optical add/drop filter. Section 3.5 discusses the key to analyzing optical filters using Z-transforms. In section 3.6 and 3.7 discuss enhanced nonlinearity in ring resonators.

3.1 What is a Ring Resonator?

A ring resonator is simply a waveguide shaped into a ring structure as shown in Fig. 3.1. When an input electric field, E_i is coupled to the ring waveguide through an external bus waveguide, a positive feedback is induced and the field inside the ring resonator, E_r starts to build up. Coupling between the straight and the ring waveguide is achieved through the evanescent wave. Therefore, the gap and coupling length between them determine how much power is coupled from the straight waveguide to the ring waveguide and vise versa. The feedback mechanism is simply induced by the ring waveguide and therefore there is no need for any Bragg gratings, mirrors, or distributed feedback waveguides which are more difficult to fabricate. In such configuration, only certain wavelengths will be allowed to resonate inside the ring waveguide, thus frequency selectivity is obtained.

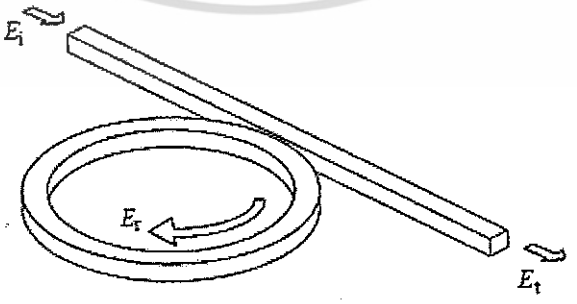

Fig. 3.1 Schematic diagram for a ring resonator coupled to a single waveguide.

3.2 Why Micro Ring Resonators?

Now we can summarize the advantages attained by microring resonators over other conventional optical cavities:

• Geometry:

The ring geometry by itself is unique. The ring waveguide supports a traveling wave rather than a standing wave. Hence, coupling can be at any point on the ring circumference. Furthermore, it allows more than one waveguide to be coupled to the ring. Therefore, multiplexing, demultiplexing, and routing can be achieved with no need for external circulators.

• Simplicity:

Fabrication of microring resonators is straightforward. There is no need for any mirrors, Bragg gratings, or distributed feedback waveguides to achieve the positive feedback.

• Materials:

There is no need for any exotic materials to fabricate microring resonators. Semiconductors fabrications are well developed and their high refractive indices allow smaller radii bends to be feasible. Bending losses decrease exponentially with increasing core-cladding refractive index contrast. This made high index contrast a fundamental requirement for very large scale integration (VLSI) photonics [32]. A 2 μm microring resonator with a finesse of 100 will have a cavity lifetime of 10 ps. Therefore, 100 GHz data can be processed by such a device. Semiconductors also allow micro rings to be integrated with other optoelectronics devices such as micro lasers, amplifiers, and detectors.

3.3 The Ring Resonator – History

The proposal to use an integrated ring resonator for a bandpass filter has been made in 1969 by E. A. Marcatili [32]. The layout of the channel dropping filter is shown in Fig. 3.2. The transmission properties of the used guide consisting of a dielectric rod with rectangular cross section, surrounded by several dielectrics of smaller refractive indices have been described by E. A. Marcatili [33].

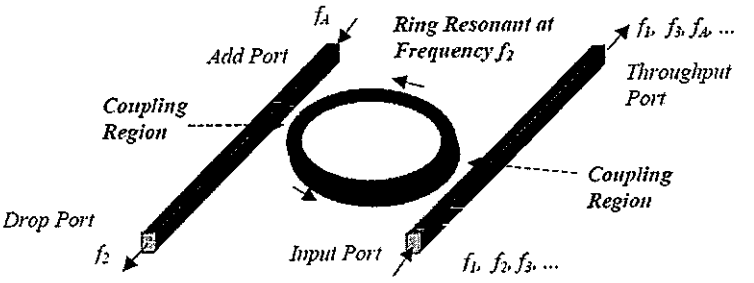

Fig. 3.2 Ring resonator channel dropping filter.

A general architecture for an autoregressive planar waveguide optical filter was demonstrated for the first time in 1996 [34]. The autoregressive lattice filters which were designed and fabricated consisted of one and two stages using Ge-doped silica waveguides.

A signal flow chart transformation for evaluating the filter transfer functions was demonstrated. Purely passive single ring resonator filters shown in Fig. 3.1 have been realized in the material system AlGaAs-GaAs [35, 36] and Si-SiO_2 [37] and Si_3N_4- SiO_2 [38]. The radius of the used ring resonators is between 5 μm and 30 μm and the free spectral range (FSR) achieved is between 20 nm and 30 nm. Passive ring resonators in the form of a racetrack have been realized in the material system GaInAsP [39] and AlGaAs-GaAs [40]. The filter performance is limited by bending and scattering losses in the resonator. These losses could be compensated by using or adding an active material.

3.4 Optical Add/Drop Ring Resonator Filter

A ring resonator consists of a waveguide in a closed loop. The loop can be any closed shape, such as a circle, ellipse, racetrack, etc. The ring is placed near one or two bus waveguides (Fig. 3.3). Typically, the input signal consists of one or more WDM channels. Signals on the input bus couple evanescently to the resonator. If a channel wavelength is resonant in the resonator, i.e., it encounters an integral multiple of 2π in phase over a round-trip, the signal intensity builds up in the ring, it couples to the output bus, and is "dropped." At the same time, a signal on the same wavelength can be added via the add port. The resonator thus functions as an add/drop multiplexer.

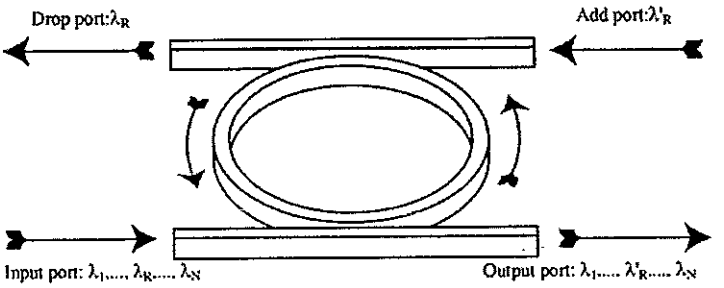

Fig. 3.3 Schematic diagram for a ring resonator coupled to two waveguides as an add/drop filter.

An incident optical signal composed of multiple wavelengths $(\lambda_1,\ldots,\lambda_R,\ldots,\lambda_N)$ at the input port coupled into the ring and for a resonant wavelength (λ_R), the energy builds up in the resonator despite the small coupling and eventually the signal is coupled into the drop port. Symmetrically, a new signal at resonant wavelength (λ_R') at the add port couples to the output port through the ring. As a result, such a configuration constitutes a very compact add/drop filter where a channel can be dropped from the WDM spectrum and replaced by a new signal on the same channel. Note that waves with a wavelength away from resonance will not repeat themselves in the ring and the coupled field interferes destructively with the wave in the resonator leading to little energy in the resonator and little dropped power. Residual dropped power at non-resonant wavelengths is possible due to imperfections and can induce inter-band crosstalk that is detrimental to WDM applications. Moreover, if the input channel at λ_R is not completely extinguished, will result in intra-band crosstalk. These issues will be studied and can be theoretically overcome by varying coupling parameters, inducing loss/gain in the ring and inserting additional rings between the two waveguides.

3.5 The Z-Transform Description

The filter functions arise from the interference of two or more waves that are delayed relative to each other. The incoming signal is split into multiple paths by a division of the wave front or the amplitude. Diffraction gratings are an example of wave front division, while directional couplers and partial reflectors are examples of amplitude division. After traveling along different paths, the fields are combined and interference occurs. For interference, the optical waves must have the same polarization, the same frequency and be temporally coherent over the longest delay length. When signals are recombined, their relative phases determine whether they interfere constructively or destructively. The phase Φ for each path is the product of the distance

traveled, L and the propagation constant, β i.e., $\Phi = \beta L$ where $\beta = 2\pi n_e / \lambda$, which is expressed in terms of the refractive index n for a diffraction-based delay line or an effective index n_e for a waveguide delay line [40].

The individual optical path lengths are typically integer multiples of the smallest path length difference. The unit delay is defined as $T = L_u n / c$ where L_u is the smallest path length and is called the unit delay length. The refractive index is assumed to be independent of wavelength. The key to analyzing optical filters using Z-transforms is that each delay be an integer multiple of a unit delay length L_u. The phase for each path is then expressed as a multiple of βL_u, so $\Phi_p = p\beta L_u$, where p is an integer. The total transverse electric field for N paths is the sum over each optical path length given by

$$E_{out} = E_o e^{-j\Phi_0} + E_1 e^{-j\Phi_1} + E_2 e^{-j\Phi_2} + \ldots + E_{N-1} e^{-j\Phi_{N-1}}. \tag{3.1}$$

To obtain a Z-transform of E_{out}, we express the phase as a multiple of the unit delay T. Using $\Omega = 2\pi\nu$ where $c = \nu\lambda$

$$\beta L_u = \frac{2\pi n L_u}{\lambda} = \frac{2\pi\nu n L_u}{c} = \frac{\Omega L_u n}{c} = \Omega T.$$

This gives $\Phi_p = p\beta L_u = p\Omega T$. Therefore Eq. 3.1 becomes,

$$E_{out} = E_o e^{-j0} + E_1 e^{-j\Omega T} + E_2 e^{-j2\Omega T} + \ldots + E_{N-1} e^{-j(N-1)\Omega T}. \tag{3.2}$$

For dispersion-less line, unit delay T is a constant and using $z = e^{j\Omega T}$ in Eq. 3.2, we get

$$E_{out} = E_o + E_1 z^{-1} + E_2 z^{-2} + \ldots + E_{N-1} z^{-(N-1)}. \tag{3.3}$$

Because the delays are discrete multiples of the unit delay, the frequency response is periodic. One period is defined as the Free Spectral Range (FSR) and is given by $FSR = 1/T$. The normalized frequency $f = \omega / 2\pi$ is related to the optical frequency by $f = (\nu - \nu_c)T$ or $f = (\Omega - \Omega_c)T / 2\pi$. The center frequency $\nu_c = c / \lambda_c$ is defined so that the product of refractive

index and unit length is equal to an integer number of center wavelengths, i.e., $m\lambda_c = nL_u$ where m is an integer. Propagation loss of a delay line is accounted for by multiplying z^{-1} by $x = e^{-\alpha L/2}$ where α is the average loss per unit length and L is the delay path length.

For a more realistic case for a delay line with dispersion, the FSR is given as:

$$FSR = 1/T = \frac{c}{n_g L_u}, \tag{3.4}$$

where $n_g = n_{eff} + f_o\left(dn_{eff}/df\right)_{f_o} = n_{eff} + \lambda_o\left(dn_{eff}/d\lambda\right)_{\lambda_o}$ is called the *group refractive index* evaluated at either center frequency f_o or center wavelength λ_o.

The optical circuits are assumed to be linear and time invariant. They can be analyzed with Z-transforms using waveguide delays and directional couplers for splitting and combining signals. A schematic diagram of a directional coupler is shown in Fig. 3.4. The lines in the figure indicate waveguides of finite width and height. Two waveguides are brought close together so that their evanescent fields overlap. A power coupling ratio κ is associated with each directional coupler. For an input on one port, the power coupled to the cross-port is κ times the input power. The length of the region where the waveguides are coupled determines the coupling ratio. The input/output relation can be expressed using a 2x2 transfer matrix $\Phi_{cplr}(\kappa)$ as shown in Eq. 3.5, where κ is the power coupling ratio, and E_n^i and E_n^o, for n = 1, 2 represent the coupler input and output fields respectively.

The coupling ratio is assumed to be wavelength independent and hence the matrix elements are constants. The through and the cross-port transmission terms are given by $c = \cos\theta = \sqrt{(1-\gamma)(1-\kappa)}$ and $-js = -j\sin\theta = -j\sqrt{(1-\gamma)\kappa}$, respectively, where γ is the coupling loss and θ is equal to the coupling strength integrated over the coupling length. A complex number $-j$ represents a $-(\pi/2)$ phase shift for the cross coupled light fields.

$$\begin{bmatrix} E_1^o \\ E_2^o \end{bmatrix} = \Phi_{cplr}(\kappa)\begin{bmatrix} E_1^i \\ E_2^i \end{bmatrix}, \quad \Phi_{cplr}(\kappa) = \begin{bmatrix} c & -js \\ -js & c \end{bmatrix}. \tag{3.5}$$

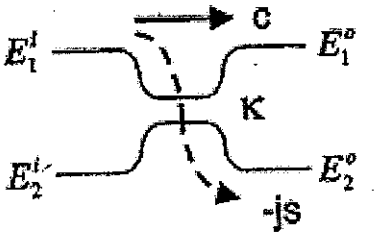

Fig. 3.4 Directional coupler and I/O relations.

The basic filter structures require at least two paths for interference. The output is then the sum of each optical path. The transfer function from any input port to any output port can be written by inspection using the transmission of each path segment. The directional coupler transmission is given by $-js$ for the cross port and c for the through port. The transmission for each delay path is expressed in terms of the unit delay. A filter's transmission is then written by summing all paths between a particular input and output port.

3.5.1 Single Coupler Ring Resonator Filter (SCRR)

A ring resonator is simply a waveguide shaped into a ring structure as shown in Fig. 3.5. To determine optical filter transfer function in Z-domain, the requirements of optical filters are considered to be satisfied are:

1) Linearity of all optical components.

2) Time invariance of all optical components.

3) Optical components must be lumped (i.e. not distributed).

The effects such as backscatter of light along the length of an optical fiber or waveguide, or saturation of an optical amplifier are therefore not considered here (the former is a distributed phenomenon; the latter is a nonlinear effect).

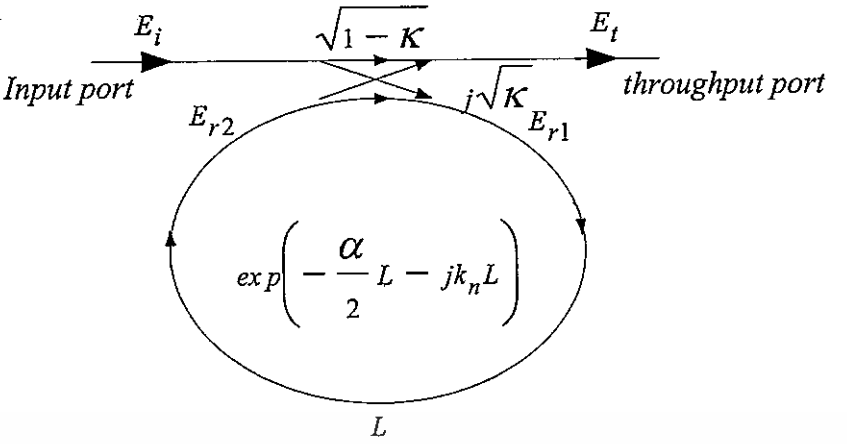

Fig. 3.5 Schematic diagram for SCRR filter.

The transfer function of this configuration is derived using Z-transform analysis. The circumference of the ring is L ($L = 2\pi R$, the radius is R), the coupling coefficient of the coupler is κ. The Z-transform parameter is represented by $z^{-1} = \exp^{-jk_nL}$ where $k_n = \frac{2\pi}{\lambda} n_{eff}$ is the propagation constant and n_{eff} is the effective index of the waveguide. The one round trip loss is $a = \exp^{-\alpha L/2}$, α is the intensity attenuation coefficient inside the waveguide [unit $length^{-1}$]. The transmitted or throughput field at the output of the straight waveguide, E_t and inserted electric field, E_i relations can be derived as followed:

$$E_t = (1-\gamma)^{1/2} \times \left[E_i \cdot \sqrt{1-\kappa} + j \cdot E_{r2} \sqrt{\kappa} \right]. \tag{3.6}$$

$$E_{r1} = (1-\gamma)^{1/2} \times \left[j \cdot E_i \cdot \sqrt{\kappa} + E_{r2} \cdot \sqrt{1-\kappa} \right]. \tag{3.7}$$

$$E_{r2} = E_{r1} \cdot a\, z^{-1}. \tag{3.8}$$

Using three equations above E_t / E_i can be calculated:

$$\frac{E_t}{E_i} = (1-\gamma)^{1/2} \times \left[\frac{\sqrt{1-\kappa} - (1-\gamma)^{1/2} \cdot a z^{-1}}{1 - (1-\gamma)^{1/2} \cdot \sqrt{1-\kappa} \cdot a z^{-1}} \right]. \tag{3.9}$$

The transfer function in Eq. (3.9) indicates that a ring resonator is very similar to a Fabry-Perot cavity. In the particular case shown in Fig. 3.5, the corresponding Fabry-Perot cavity would have an input mirror with a field reflectivity and a fully reflecting output mirror. However, the field propagating inside the ring cavity is a traveling wave in contrast to the Fabry-Perot cavity which resonates a standing wave.

In the following, new parameter will be used for simplification:

$$\begin{aligned} D &= (1-\gamma)^{1/2} \\ x &= D \cdot \exp^{-\alpha L/2} \\ c &= \sqrt{1-\kappa} \\ \phi &= k_n \cdot L \end{aligned} \tag{3.10}$$

The intensity relation for the output port is given by:

$$T = \frac{I_t}{I_i}(\phi) = \left|\frac{E_t}{E_i}\right|^2 = D^2 \cdot \left[1 - \frac{\left(1-x^2\right)\cdot\left(1-c^2\right)}{\left(1-x\cdot c\right)^2 + 4\cdot x\cdot c\cdot sin^2\left(\frac{\phi}{2}\right)}\right] \tag{3.11}$$

3.5.2 Double Coupler Ring Resonator Filter (DCRR)

Consider the architectures of double coupler ring resonator which sometime called add/drop filters as illustrated in Fig. 3.6, which are constructed by 2×2 optical couplers.

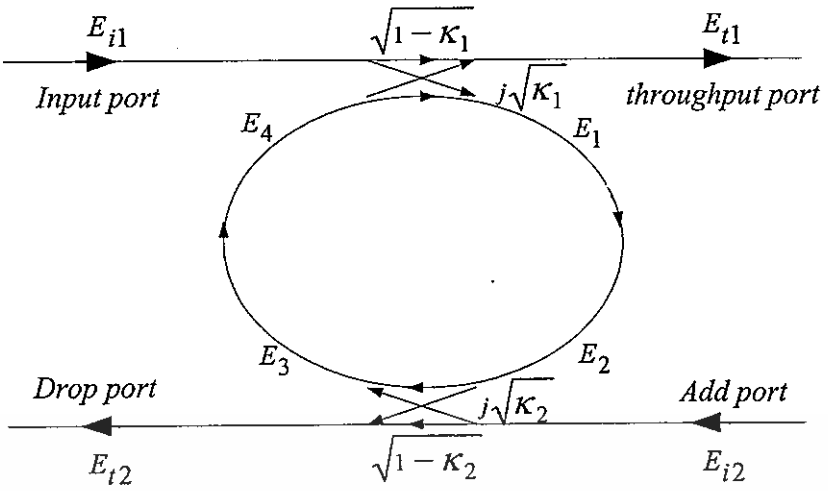

Fig. 3.6 The architecture of DCRR or add/drop filter.

Similarly, the optical transfer functions of the ring resonator filters at the throughput port and drop port for an input port E_{i1} can be derived as followed. For the first coupler (κ_1), we have

$$E_{t1} = \sqrt{1-\gamma_1}\left[j\sqrt{\kappa_1}E_4 + \sqrt{1-\kappa_1}E_{i1} \right] \tag{3.12}$$

$$E_1 = \sqrt{1-\gamma_1}\left[j\sqrt{\kappa_1}E_{i1} + \sqrt{1-\kappa_1}E_4 \right] \tag{3.13}$$

where γ and κ_1 are the loss and the coupling coefficients, respectively. The incoming light of E_{i1} and E_4 are coupled through the first coupler to the output light E_{t1} and E_1 and the output light E_1 is transmitted through the ring becomes output light E_2. According to light transmission theory in linear optical systems, we obtain the following relation between E_1 and E_2

$$E_2 = E_1 e^{-\frac{\alpha L}{2}\frac{2}{2} - jk_n\frac{L}{2}} \tag{3.14}$$

where the transmission line length is $\frac{L}{2}$. The second coupler (κ_2) have the following relations:

$$E_{t2} = E_1 e^{-\frac{\alpha L}{2}\frac{2}{2} - jk_n\frac{L}{2}} \cdot j\sqrt{1-\gamma_2}\sqrt{\kappa_2} \quad \text{at } E_{i2} = 0 \tag{3.15}$$

$$E_3 = E_1 e^{-\frac{\alpha}{2}\frac{L}{2} - jk_n\frac{L}{2}} \sqrt{1-\gamma_2}\sqrt{1-\kappa_2} \tag{3.16}$$

Using the transmission theory, we obtain E_4 in terms of E_3

$$E_4 = E_3 e^{-\frac{\alpha}{2}\frac{L}{2} - jk_n\frac{L}{2}} \tag{3.17}$$

$$E_1 = \frac{E_{i1} j\sqrt{1-\gamma_1}\sqrt{\kappa_1}}{1-\sqrt{1-\gamma_1}\sqrt{1-\kappa_1}\sqrt{1-\gamma_2}\sqrt{1-\kappa_2}e^{-\frac{\alpha}{2}L - jk_nL}} \tag{3.18}$$

$$E_4 = \frac{E_{i1} j\sqrt{1-\gamma_1}\sqrt{\kappa_1}}{1-\sqrt{1-\gamma_1}\sqrt{1-\kappa_1}\sqrt{1-\gamma_2}\sqrt{1-\kappa_2}e^{-\frac{\alpha}{2}L - jk_nL}}\sqrt{1-\gamma_2}\sqrt{1-\kappa_2}e^{-\frac{\alpha}{2}L - jk_nL} \tag{3.19}$$

By using the upper equations, the transfer function for throughput port and drop port in Fig. 3.6 can thus be expressed as

Throughput port:

$$\begin{aligned}\frac{E_{t1}}{E_{i1}} &= \frac{-(1-\gamma_1)\kappa_1\sqrt{1-\kappa_2}e^{-\frac{\alpha}{2}L - jk_nL} + \sqrt{1-\gamma_1}\sqrt{1-\kappa_1}}{1-\sqrt{1-\gamma_1}\sqrt{1-\kappa_1}\sqrt{1-\gamma_2}\sqrt{1-\kappa_2}e^{-\frac{\alpha}{2}L - jk_nL}} \\ &= \frac{-(1-\gamma_1)(1-\kappa_1)\sqrt{1-\gamma_2}\sqrt{1-\kappa_2}e^{-\frac{\alpha}{2}L - jk_nL}}{1-\sqrt{1-\gamma_1}\sqrt{1-\kappa_1}\sqrt{1-\gamma_2}\sqrt{1-\kappa_2}e^{-\frac{\alpha}{2}L - jk_nL}} \\ &= \frac{-\sqrt{1-\gamma_2}\sqrt{1-\kappa_2}e^{-\frac{\alpha}{2}L - jk_nL} + \sqrt{1-\gamma_1}\sqrt{1-\kappa_1}}{1-\sqrt{1-\gamma_1}\sqrt{1-\kappa_1}\sqrt{1-\gamma_2}\sqrt{1-\kappa_2}e^{-\frac{\alpha}{2}L - jk_nL}}\end{aligned} \tag{3.20}$$

Drop port:

$$\frac{E_{t2}}{E_{i1}} = \frac{-\sqrt{1-\gamma_1}\sqrt{1-\gamma_2}\sqrt{\kappa_1\cdot\kappa_2}e^{-\frac{\alpha}{2}\frac{L}{2} - jk_n\frac{L}{2}}}{1-\sqrt{1-\gamma_1}\sqrt{1-\kappa_1}\sqrt{1-\gamma_2}\sqrt{1-\kappa_2}e^{-\frac{\alpha}{2}L - jk_nL}} \tag{3.21}$$

The intensity relations for the throughput and drop port can be obtained by normalizing the transfer functions in Eqs. (3.20) and (3.21) which are given by

$$\frac{I_{t1}}{I_{i1}}=\left|\frac{E_{t1}}{E_{i1}}\right|^2=\frac{\begin{array}{c}1-(1-\gamma_1)\kappa_1-2\sqrt{1-\gamma_1}\sqrt{1-\kappa_1}\cdot\sqrt{1-\gamma_2}\sqrt{1-\kappa_2}e^{-\frac{\alpha}{2}L}cos(k_nL)\\ +(1-\gamma_2)(1-\kappa_2)e^{-\alpha L}\end{array}}{\begin{array}{c}1+(1-\gamma_1)(1-\kappa_1)\cdot(1-\gamma_2)(1-\kappa_2)e^{-\alpha L}\\ -2\sqrt{1-\gamma_1}\sqrt{1-\kappa_1}\cdot\sqrt{1-\gamma_2}\sqrt{1-\kappa_2}e^{-\frac{\alpha}{2}L}cos(k_nL)\end{array}} \tag{3.22}$$

$$\frac{I_{t2}}{I_{i1}}=\left|\frac{E_{t2}}{E_{i1}}\right|^2=\frac{(1-\gamma_1)(1-\gamma_2)\cdot\kappa_1\kappa_2e^{-\frac{\alpha}{2}L}}{\begin{array}{c}1+(1-\gamma_1)(1-\kappa_1)\cdot(1-\gamma_2)(1-\kappa_2)e^{-\alpha L}\\ -2\sqrt{1-\gamma_1}\sqrt{1-\kappa_1}\cdot\sqrt{1-\gamma_2}\sqrt{1-\kappa_2}e^{-\frac{\alpha}{2}L}cos(k_nL)\end{array}} \tag{3.23}$$

For simplification, the calculation of the intensity relation does not take into account of coupling losses ($\gamma=0$) and the following parameters:

$$\begin{aligned}x&=exp\left(-\frac{\alpha}{2}L\right)\\ c_1&=\sqrt{1-\kappa_1}\\ c_2&=\sqrt{1-\kappa_2}\end{aligned} \tag{3.24}$$

The intensity relations Eqs. (3.22) and (3.23) are then given by

$$\frac{I_{t1}}{I_{i1}}(\phi)=\left|\frac{E_{t1}}{E_{i1}}\right|^2=1-\frac{\left(1-c_1^2\right)\cdot\left(1-c_2^2x^2\right)}{\left(1-c_1c_2x\right)^2+4c_1c_2xsin^2\left(\frac{\phi}{2}\right)} \tag{3.25}$$

$$\frac{I_{t2}}{I_{i1}}(\phi)=\left|\frac{E_{t2}}{E_{i1}}\right|^2=\frac{\left(1-c_1^2\right)\cdot\left(1-c_2^2\right)\cdot x}{\left(1-c_1c_2x\right)^2+4c_1c_2xsin^2\left(\frac{\phi}{2}\right)} \tag{3.26}$$

3.6 Enhanced Nonlinearity in Single Ring Resonator

In section 3.6 and 3.7, we will carefully study such enhancement and its projection on the dynamic performance of the microring resonator for all-optical switching applications. We will concentrate on the reduction achievable in the switching power of a microring due to the resonant condition.

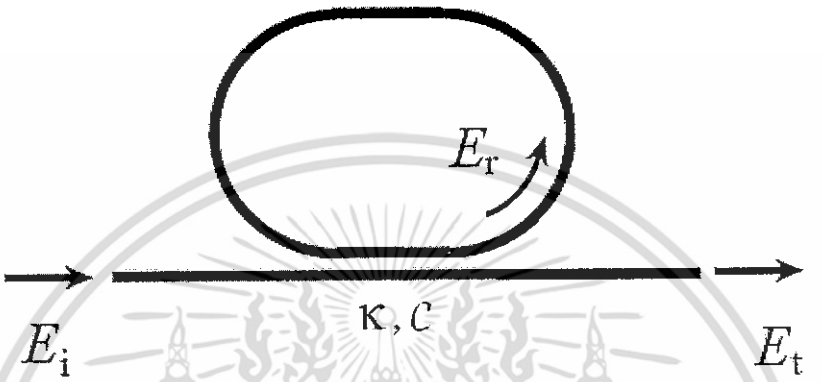

Fig. 3.7 The waveguide layout of SCRR.

For a small range of detuning, i.e., much smaller than the 3-dB bandwidth of the microring resonance, a small signal analysis approach is enough to understand the dynamic behavior of the resonator and to determine its switching enhancement. In such analysis, we will assume that the linear parameters of the microring resonator are constants with respect to time. Without loss of generality, we will consider the SCRR filter case in Fig. 3.7 that we have introduced in section 3.5.1. At the steady state, the field transmittance of the filter is given by

$$\frac{E_t}{E_i} = \frac{c - a e^{j\phi_0}}{1 - ca\, e^{j\phi_0}}. \tag{3.27}$$

where $a = \exp(-\alpha L/2)$ is the round trip field attenuation of the microring, c is the field transmittance coefficient, and $\phi_0 = \beta L$ is linear phase shift in the ring. β is the wave propagation constant associated with the fundamental mode supported by the ring waveguide, and L is the circumference of the ring. One useful feature of a ring resonator is that the original power gets to build up in the ring and keeps circulating inside the ring. The buildup factor B, which is defined as the ratio of the power circulating inside the ring to the input power, is given by [41]

$$B = \frac{P_r}{P_i} = \frac{1-c^2}{1+c^2a^2-2ca\cos\phi_0} \tag{3.28}$$

where P_i is the input power, P_r is the average power inside the ring. Under conditions that the incident light is on resonance with the ring and the loss is negligible ($a = 1$), the maximum value of the buildup factor $B_{\max} = (1+c)/(1-c)$. Thus, when c is very close to unity, the power circulating inside the fiber ring becomes very high. This power buildup can induce nonlinear effects if the ring possesses an intensity-dependent nonlinear refractive index n_2 that results from the third-order susceptibility ($\chi^{(3)}$) of the waveguide material [41]. The nonlinear refractive index n_2 can be included in the single-pass phase shift as

$$\phi = \phi_0 + \phi_{NL} \cong \beta L + \gamma L_{eff} P_r \tag{3.29}$$

where $L_{eff} = [1-\exp(-\alpha L)]/\alpha$, is the effective interaction length due to the loss and γ is the nonlinearity coefficient (related to n_2 by $\gamma = 2\pi n_2 / \lambda A_{eff}$, where λ is the input wavelength and A_{eff} is the effective core area of the waveguide). ϕ_0 and ϕ_{NL} are the single-pass linear and nonlinear phase shifts, respectively. In such a nonlinear case, ϕ_0 in Eq. (3.28) should now be replaced by ϕ. Thus, by substituting Eq. (3.29) into Eq. (3.28), we obtain a transcendental equation for the single-pass phase shift as

$$\phi(P_i, \phi_L) = \phi_L + \gamma L_{eff} \frac{1-c^2}{1+c^2a^2-2ca\cos\phi(P_i, \phi_L)} P_i \tag{3.30}$$

The nonlinear response of switching device can be evaluated by the derivative of phase shift ϕ with respect to input power P_i. This derivative can be expressed as

$$\frac{d\phi}{dP_r} = \frac{d\phi}{d\phi_0}\frac{d\phi_0}{dP_r}\frac{dP_r}{dP_i} \approx \frac{8Ln_2}{\pi\lambda A_{eff}} F^2 \tag{3.31}$$

where F is resonator finesse [41].

3.7 Enhanced Nonlinearity in Add/Drop Ring Resonator

The transmission equation from input port to drop port for the DCRR as shown in Fig. 3.6 is given by

$$\frac{E_{t2}}{E_{i1}} = \frac{s_1 s_2 \sqrt{\gamma} e^{j\phi_0}}{1 - c_1 c_2 \gamma e^{j\phi_0}} \tag{3.32}$$

where c_1, s_1 and c_2, s_2 are the coupling coefficients for the two couplers respectively. Critical coupling condition for the DCRR is defined to be $\left|E_{t2} / E_{i1}\right|^2 = 1$, i.e. all light goes through the drop port, which gives $s_{2c} = \sqrt{1 - c_1^2 e^{-\alpha L}}$. Since $s_{2c} = s_1$, symmetric DCRR (with two identical couplers) will operate at noncritical coupling. The phase shift of the drop port field (E_{t2}) is

$$\phi = \pi + \phi_0 + \arctan\left[\frac{c^2 \gamma \sin\phi_0}{1 - c^2 \gamma \cos\phi_0}\right] \tag{3.33}$$

Similar to SCRR, the nonlinear effect can be included by applying equation (3.29) to the computation of ϕ as follow.

$$\phi = \phi_0 + \frac{2\pi n_2 \frac{L}{2} P_2}{\lambda A_{eff}} + \frac{2\pi n_2 \frac{L}{2} P_4}{\lambda A_{eff}} \tag{3.34}$$

where P_2 and P_4 are circulating powers, respectively.

3.8 Summary

The main goal of this chapter suggests nonlinear enhancement in micro ring resonator and we then can get the nonlinear transfer functions which used to characterize the nonlinear behaviors such as chaos, bifurcation, and bistability. Each behavior can be implemented for design of many applications as describe in chapter 4.

CHAPTER 4

THEORETICAL RESULTS

In this chapter, we design the optical devices result from nonlinear behaviors such as chaos, bistability, and bifurcation based microring resonator. The results of nonlinear device design can be applied for optical communication network including secured information transmission in optical link and data coding using chaotic signal, secured codes as start-stop bits using bifurcation.

4.1 High Capacity Packet Switching Using Soliton Pulse

Soliton has been the popular subject of study for years, where many subjects such as mathematics, physics and engineering have been used to study and investigate [42-44], where one of the most popular behaviors is called the "optical soliton". The advantage of using optical soliton in optical communication is that the power is gained and also used for non-dispersion propagation in long distance communication link. Apart from long distance link, we still need the transformation security, where the combination between the long distance link and security are required in the practical communication networks. Recently, the chaotic signal generated by using light pulse traveling in a nonlinear microring resonator can be performed the secured transmission in optical link have proposed [45]. In this section, the combination behaviors between chaos and soliton are employed to implement the secured information in the communication system. Initially, the information can be secured by the use of chaotic signals, where the long distance link can also be employed by the soliton property.

Fig. 4.1(a) shows the diagram of nonlinear microring resonator used for generating chaotic signals. The chaotic signals generated due to Kerr effects nonlinear type which the input signal of soliton is launched in a microring resonator. Since the nonlinearity of the micro ring is of the Kerr-type, which the refractive index is given by

$$n = n_0 + n_2 I = n_0 + (\frac{n_2}{A_{eff}})P \tag{4.1}$$

where n_0 and n_2 are the linear and nonlinear refractive indexes, respectively. I and P are the optical intensity and optical field power, respectively. The effective mode core area of the fiber is A_{eff} . Here, the input optical field is set in the form of soliton pulse which has expression as Eq. .

Meanwhile, the obtained signals will be selected as secured channels for optical communication networks. Fig. 4.1(b) shows the design microring resonator via an add/drop filter device used for the multi-users. When the input signal is launched into the communication systems, the multi-users can retrieve the required signals by the drop ports while those that pass through unaffected.

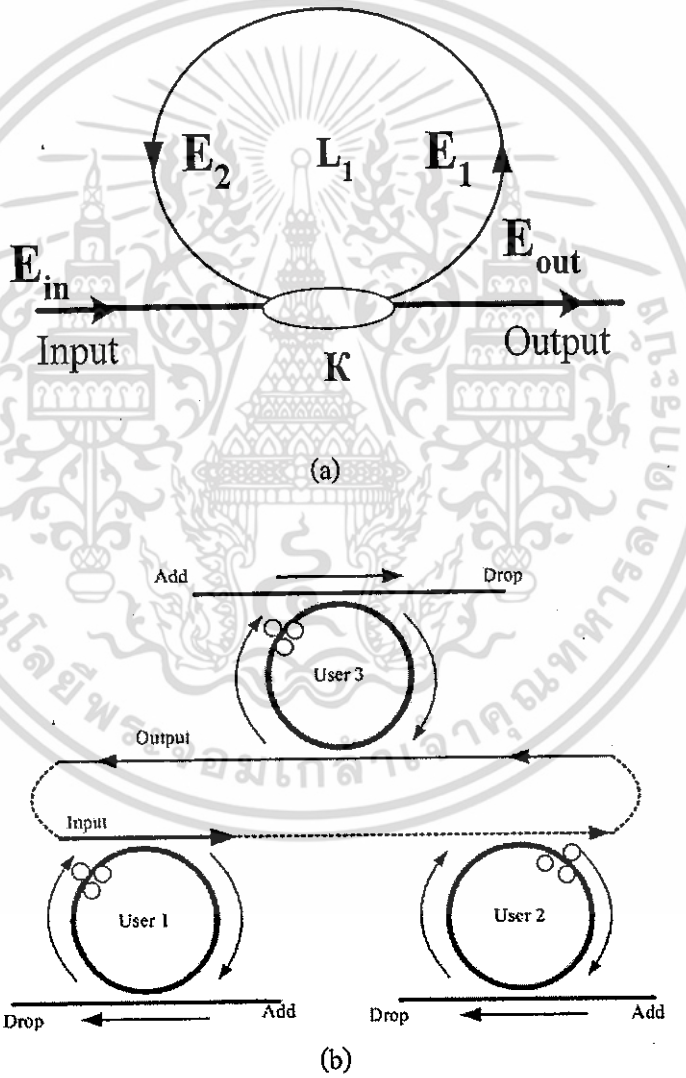

Fig. 4.1 The diagram of microring resonator (a) with single coupler, (b) with multi-user via an add/drop devices used in the optical network.

The wave form of the soliton pulse used as input signal, having pulse width of 50 ps is shown in Fig. 4.2(a), which is input into nonlinear microring as Fig. 4.1(a). While Fig. 4.2(b) shows the output signal generated from the microring resonator due to Kerr effect, where the chaotic wave form is realized. Here, the radius of the ring is set equal 10 μm.

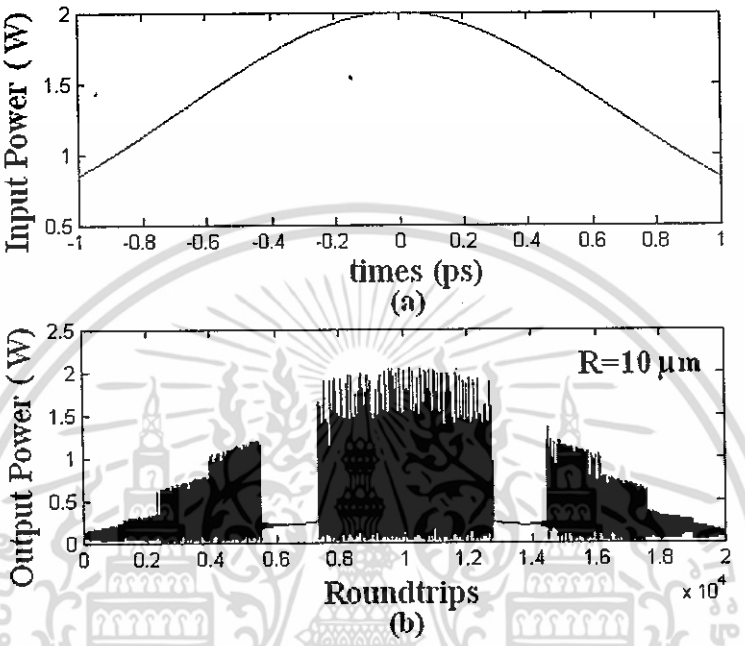

Fig. 4.2 The soliton pulse input and the chaotic signal output generated from microring resonator.

The characteristics of the chaotic signal output by varying the intense of input powers are shown in Fig. 4.3. The input powers (A) in Fig. 4.3(a)-(d) are set equal 2, 3, 4, and 5 W, respectively. We found that in Fig. 4(a), the chaotic soliton behavior is seen when the roundtrips of input soliton are in the range of 9,000-11,000. Similarly, in Figs. 4(b)-(d), with the input peak powers 3-5 W, the chaotic signals are occurred when the soliton circulated within the ring between 8,000-12,500 roundtrips. In this work, we choose input power of 2 W for our investigation.

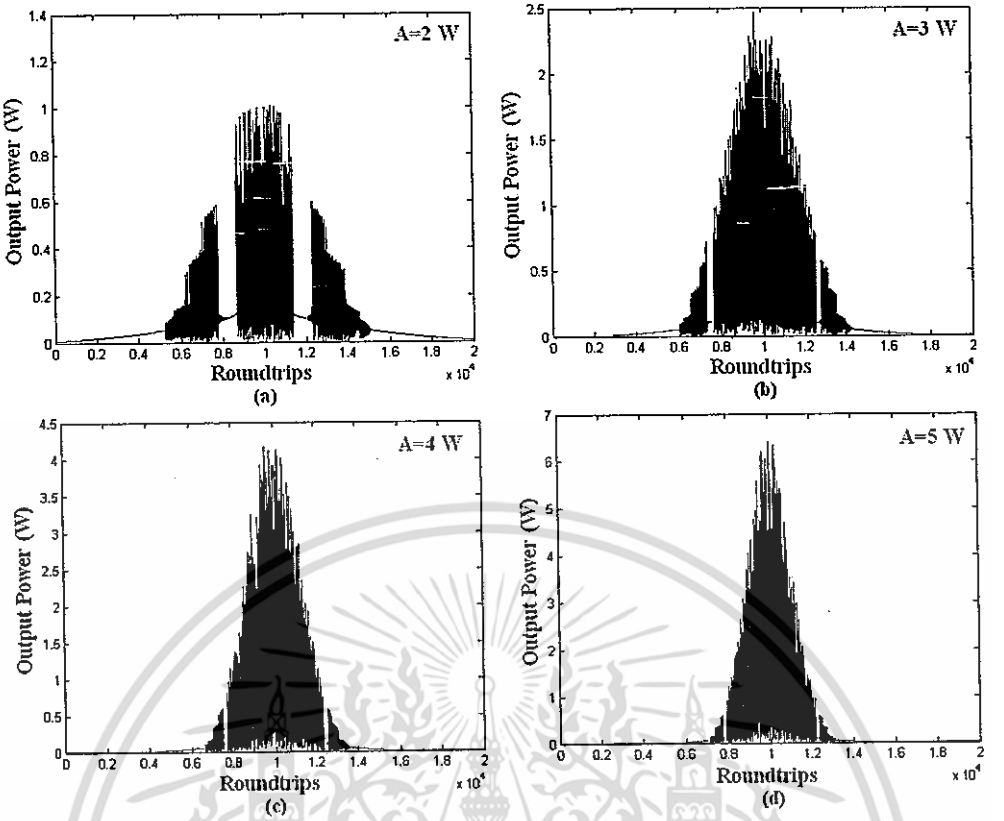

Fig 4.3 The generation of chaotic signal by varying input peak powers (A), (a) 2 W, (b) 3 W, (c) 4 W, and (d) 5 W.

Fig. 4.4 shows generation of chaotic signal with different ring radii. Fig. 4.4(a), the soliton chaotic behavior is occurred with mostly constant output intensity, when the roundtrips are in the range of 6,000-14,000, and the ring radius is 7 μm. When the ring radius is adjusted to 10 μm, we found that the soliton chaotic is realized with the roundtrips between 7,800-12,800 as shown in the Fig. 4.4(b). In Fig.4.4(c) and (d), the results of the different ring radii of 12 μm and 15 μm have shown that the soliton behaviors are neglected, which means only chaotic oscillation is seen.

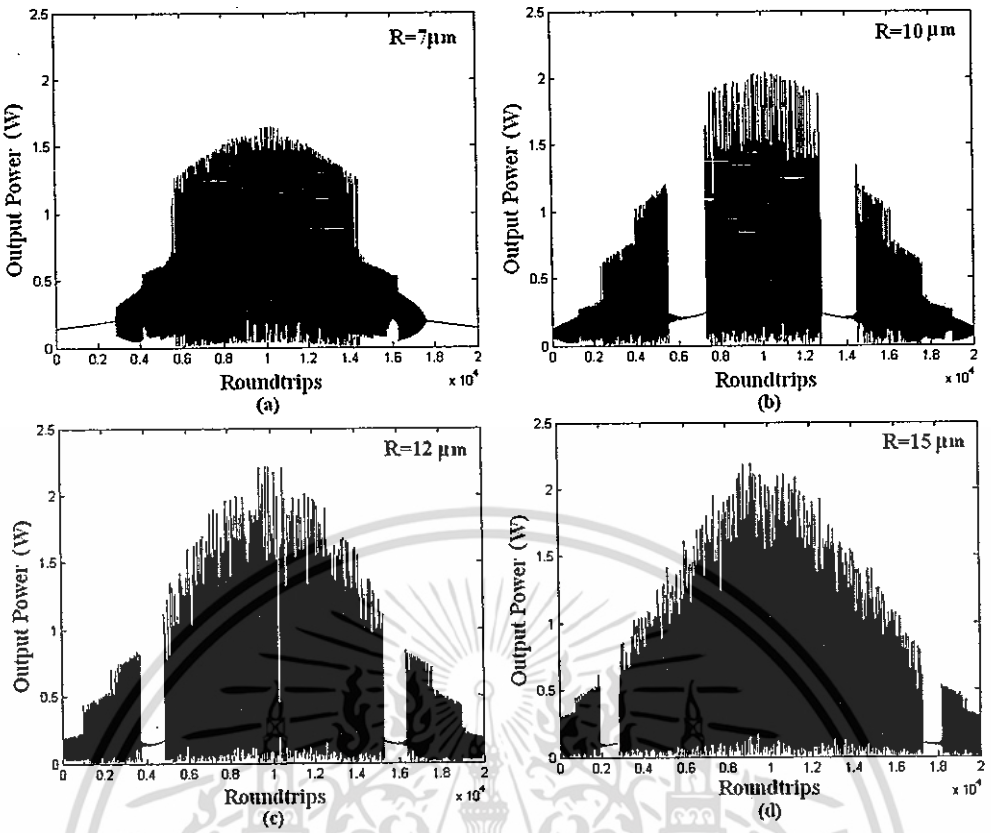

Fig 4.4 The generation of chaotic signal by varying ring radii of ring resonator, (a) 7 μm, (b) 10 μm, (c) 12 μm, and (d) 15 μm.

Results of the different coupling coefficients from 0.1-0.4 are shown in Fig. 4.5. Fig. 4.5(a) and Fig. 4.5(b) shows that the soliton chaotic behaviors are seen with the roundtrips between 4,500-15,500 and 6,100-14,000 with the coupling coefficients are 0.1 and 0.2, respectively. While the chaotic soliton is not properly occurred in Fig. 4.5(c) and Fig 4.5(d), with the coupling coefficient $K = 0.3$ and $K = 0.4$, respectively.

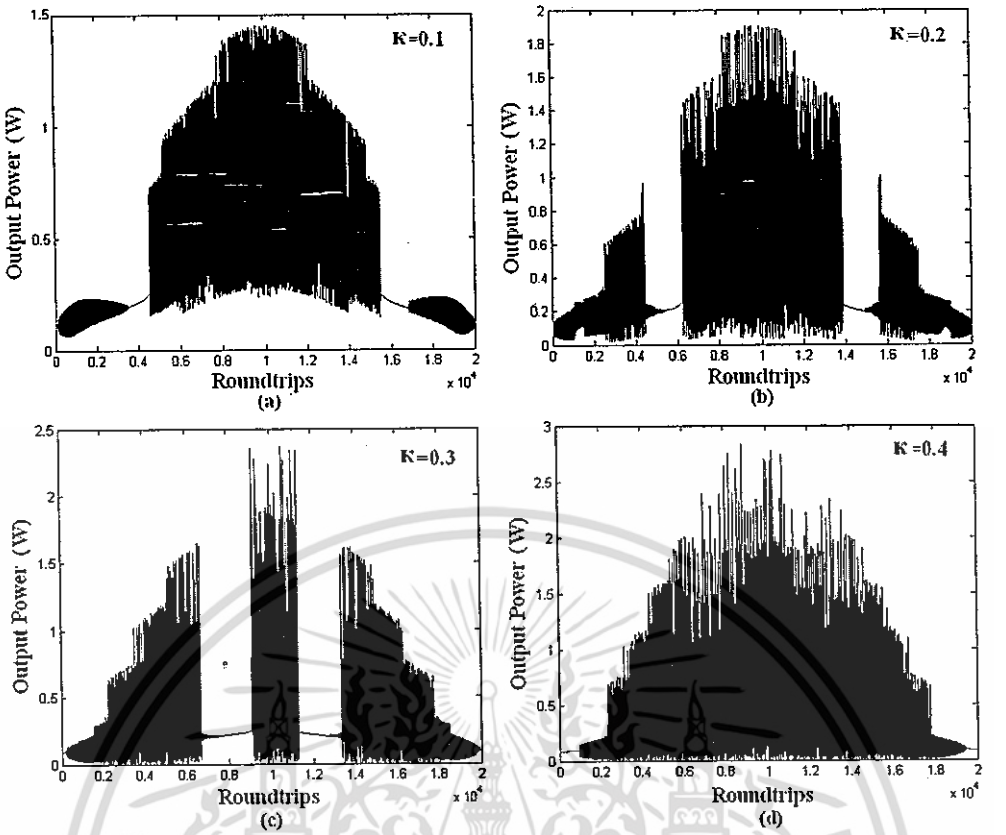

Fig. 4.5 The generation of chaotic signal by varying couple coefficient (K), (a) K = 0.1, (b) K = 0.2, (c) K = 0.3, and (d) K = 0.4.

4.2 Packet Switching Start-Stop Bits Generation

Nonlinear behaviors of light in optical ring resonator such as chaos, bistability and bifurcation become benefits in several aspects which have been proposed [46]. There are more useful applications investigated and confirmed by Yupapin [45, 47], where the chaotic behavior of light in fiber optic/microring device could be used to process the information security. They have also shown that such a device could be implemented within the mobile telephone device and system, where the telephone conversation security is plausible. In this section, the bifurcation behavior of light in a microring device is investigated, where the bifurcation is generated to form the secured codes for information security use.

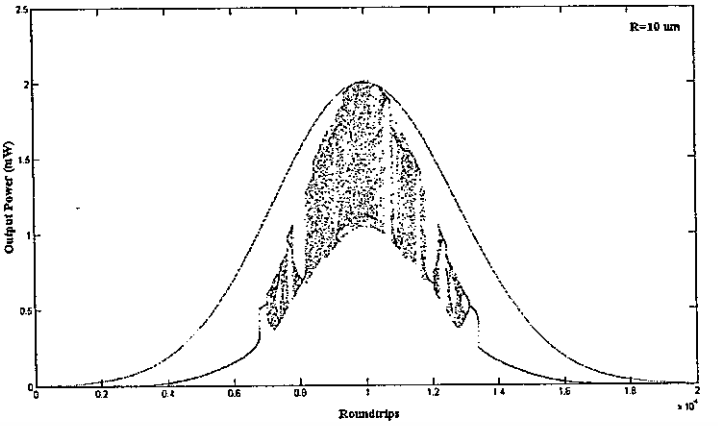

Fig. 4.6 Graph of the input power (solid line) and the output power (nonlinear signals) of the ring resonator.

Nonlinear behavior of light traveling in a single microring resonator is described in section 4.1. Here, the system parameters for generating bifurcation were set as λ_0 = 1.55 μm, n_0 = 3.34, A_{eff} = 30 μm^2, α = 0.02 $dBkm^{-1}$, γ = 0.1, and R_1 = 10-13 μm. The coupling coefficients of coupler are varied from κ = 0.0225-0.030. The nonlinear refractive index of ring resonator is $n_2 = 2.2 \times 10^{-13}$ m^2W^{-1}, and plot 20,000 iterations of round-trips within the ring.

The input signal is input into the device, which is the continuous wave (CW) known as Gaussian wave form. Fig. 4.6 shows the chaotic signal generation within a microring device, which is shown the basic behaviors such as bifurcation, chaos and bistability. Generally, the nonlinear signals generated within a microring resonator are characterized and described as following details. Initially, two routes of the chaotic signals are split by the behavior called bifurcation, where sometime the bistability behavior is occurred between bifurcation and chaos. To perform the security bits in this technique, firstly, the start bit is formed as state "0" or "1" by the first two bifurcation values where one bit is formed by one route of the bifurcation. Then the security bit is followed by chaotic codes, which is formed after the chaotic signals. Where the chaotic signals/codes between the start and stop bits (i.e. bifurcation) can be several codes or packet of codes.

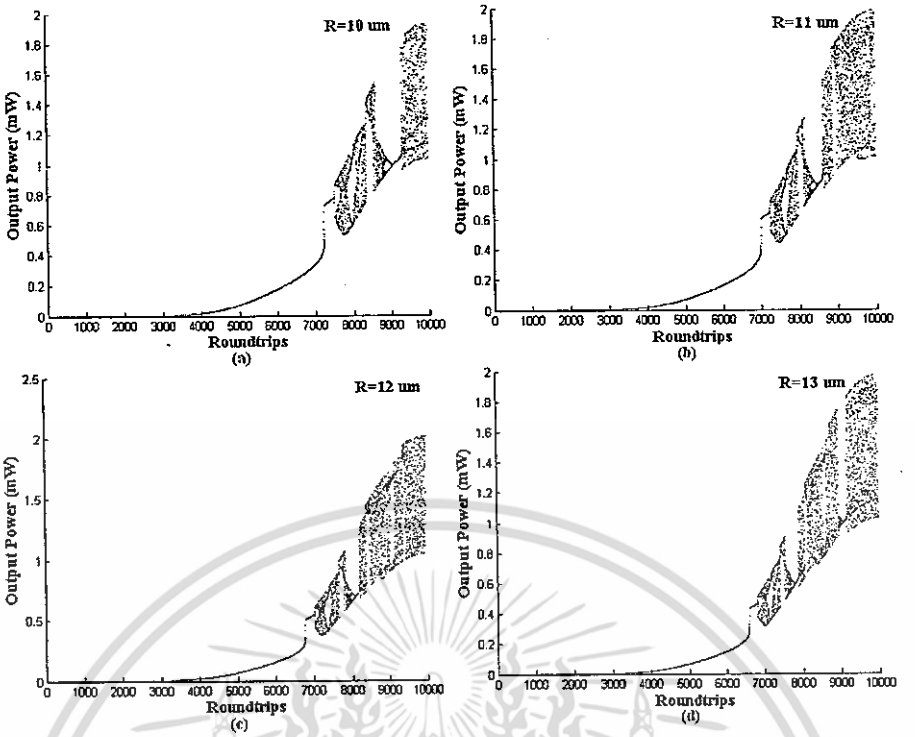

Fig. 4.7 Nonlinear characteristics of light wave within a microring resonator with different ring radii (R), (a) 10 μm, (b) 11 μm, (c) 12 μm, and (d) 13 μm.

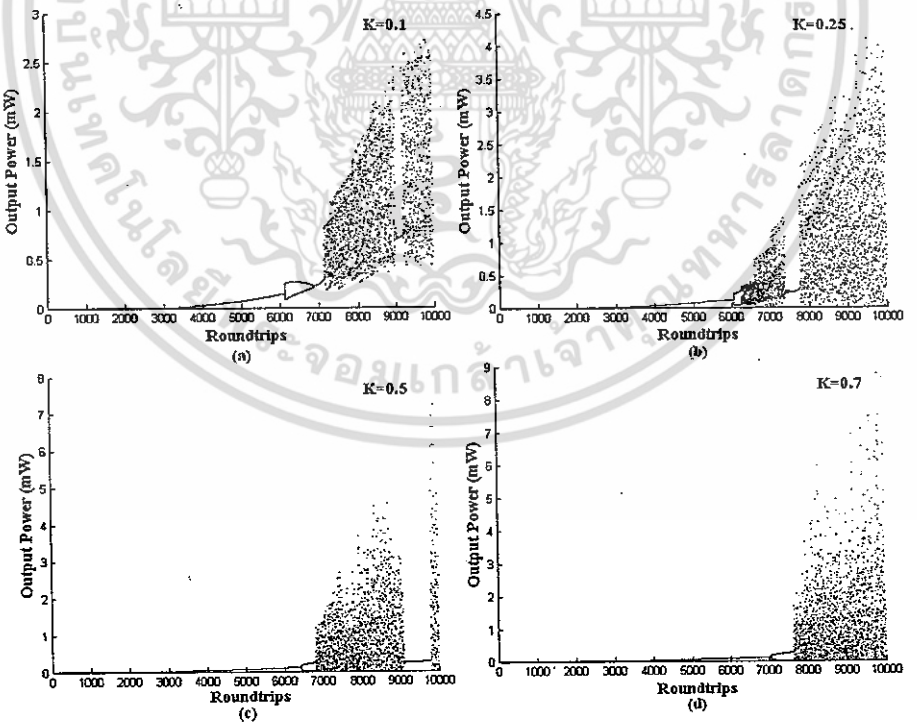

Fig. 4.8 Nonlinear characteristics of light within a microring resonator with different couple coefficient (K), (a) K = 0.1, (b) K = 0.25, (c) K = 0.5, and (d) K = 0.7

Figs. 4.7 and 4.8 show theoretical results of the nonlinear behaviors with some different parameters, for instance, the input power, ring radii and coupling coefficients. We found that from both Figures, the starting points for realizing nonlinear behaviors such as chaos, bistability, and bifurcation are different. Fig. 4.9 shows several set of data which is formed as start and stop bits due to the bifurcation behaviors. The 1st period generates the start and stop bits to use as switching for packet signals at the 7,000-7,400 roundtrips of circulating light. The 2nd period realizes the start and stop bits of the packet signals at the 7,500-7,800 roundtrips. While the 3rd and 4th periods generates the start and stop bits at the 7,900-8,000 and 8,400-9,000 roundtrips, respectively. The one roundtrip time is calculated equal to 2.9×10^{-12} second. These characteristics could be designed as the device for security purpose. Where the start and stop bits could be performed and used incorporating the required packet of data in the transmission line or network.

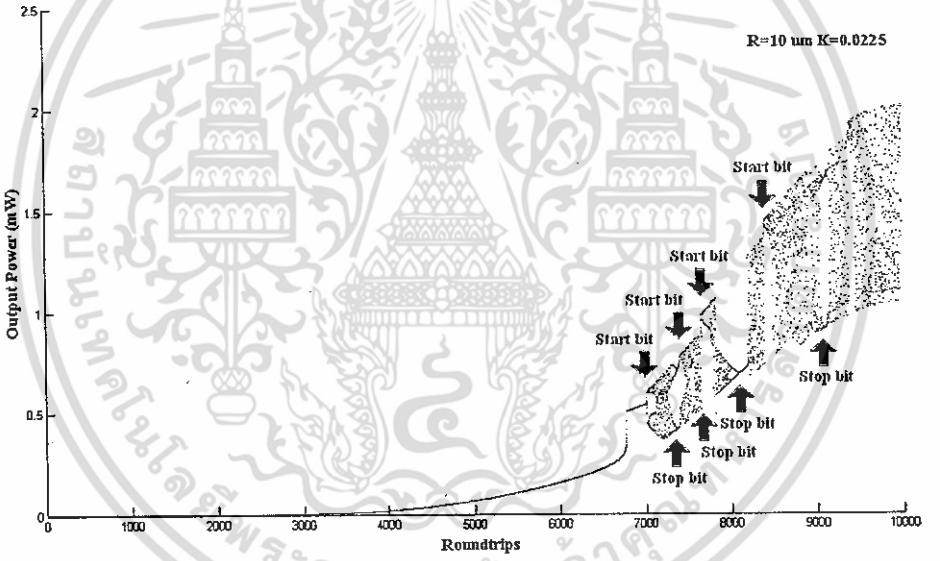

Fig. 4.9 The 4th order of start and stop bits generation obtained from bifurcation of microring resonator, when R= 10 μm, κ = 0.0225.

4.3 Chaotic Signal Generation and Coding

Chaotic behavior has been studied as a nonlinear property in the areas such as mathematics, physics electronics, and communications. The benefit of such a property can be accepted, for instance, the chaotic communication has recently attracted great interest because of its potential applications in secure and confidential communications, where it uses a noise-like broadband chaotic waveform as a carrier. The message coding, and the nonlinear effect of the coding process and control chaotic signal encoding will study in this section.

The chaotic encoding methods are processed by sampling, quantizing, and chaotic synchronization. The selected input signals can be used to control the required chaotic encoding, which can be distributed into the optical transmission link. The most important advantage of the proposed system is the easy implementation comparing to the well known secure communication technique called quantum cryptography, which will be extremely difficult in the realistic system, while the requirement in term of security is acceptable. Eventually, the required information can be retrieved when the decode technique and the tunable filters are employed by the required clients. The basic theory of a microring resonator is reviewed, the chaotic quantizing and coding and control are presented in details.

The chaotic signal can be generated using nonlinear single ring resonator as in Fig. 4.1(a). When the parameters of the system are set to $\lambda_0 = 1.55\ \mu$m, $n_0 = 1.54$, and $A_{eff} = 30\ \mu m^2$, where the waveguide ring resonator loss (α) is 0.5 dBmm^{-1}, and ring radius R = 10 μm. The coupling coefficient of the coupler is fixed to $\kappa = 0.0225$. The nonlinear refractive index is set equal to $n_2 = 2.2 \times 10^{-15}$ m^2/W, and the data of 10,000 iterations of roundtrips inside the optical microring is plotted. We assume that $\phi_L = 0$ for simplicity; however, the change in phase is slightly altered by the optical output, which means the dispersion can be neglected when the resonant output is occurred. The chaotic signals can be electronically formed by the digital codes as the following details. The quantitatively present logic coding can be expressed by

$$u(v) = \begin{cases} 0.....v < 3.5\ mW \\ 1.....v \geq 3.5\ mW \end{cases}$$

Furthermore, when $u(v)$ represents the logic states, v is the signal power. The quantization and re-quantization can be processed by similar transfer characteristics. We assume that the quantizing involved is infinite, which means that the system input signal is never clipped by saturation of the quantizing. In this case, the corresponding transfer functions of the quantizing output to its input can be expressed analytically in terms of the quantizing step size as details in references [48]. The chaotic signals mentioned below can be used to form the digital codes. Fig. 4.10 illustrates a flow chart of the chaotic encoding procedures. When the program is operated, i.e. "START," then the program logical coding begins. Firstly, the reduction of the threshold and maximum powers is required, which are ranged from 3.5 mW to 4 mW. Secondly, "Yes" and "NO" form the logics "1" and "0", respectively. Lastly, "END" is the process of the final step. In

practice, the design microring resonator with its suitable parameters can be used to generate the chaotic signals, which can be electronically coded.

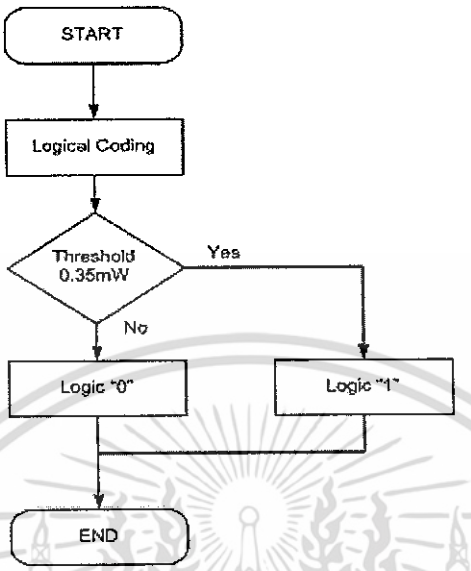

Fig. 4.10 Flow chart of a chaotic coding algorithm.

The signal quantization can be further understood by using the approximation method in which the chaotic signal can be encoded. The quantizing plots of the various input powers are ranged from 1.8 to 1.82 mW as shown in Fig. 4.11. These plots show the improvement of the approximation method as shown in Fig. 4.11(a)–(c), and deterioration until or the least-square method in Fig. 4.11(d) is introduced. Where (a) shows the relationship between the input and output signals; (b) the red line (solid line) is the power reduction with the threshold power of 3.5 mW; (c) the signal after threshold power condition uses; and (d) the output signal of when the approximation method is employed. The logical code with the logic state "1" or "0" is generated from the previous description, after the chaotic behaviors of the device is characterized; the next step is that the random coding can be generated by controlling the input optical power, which then enters into the microring device. The required chaotic codes can be electronically generated.

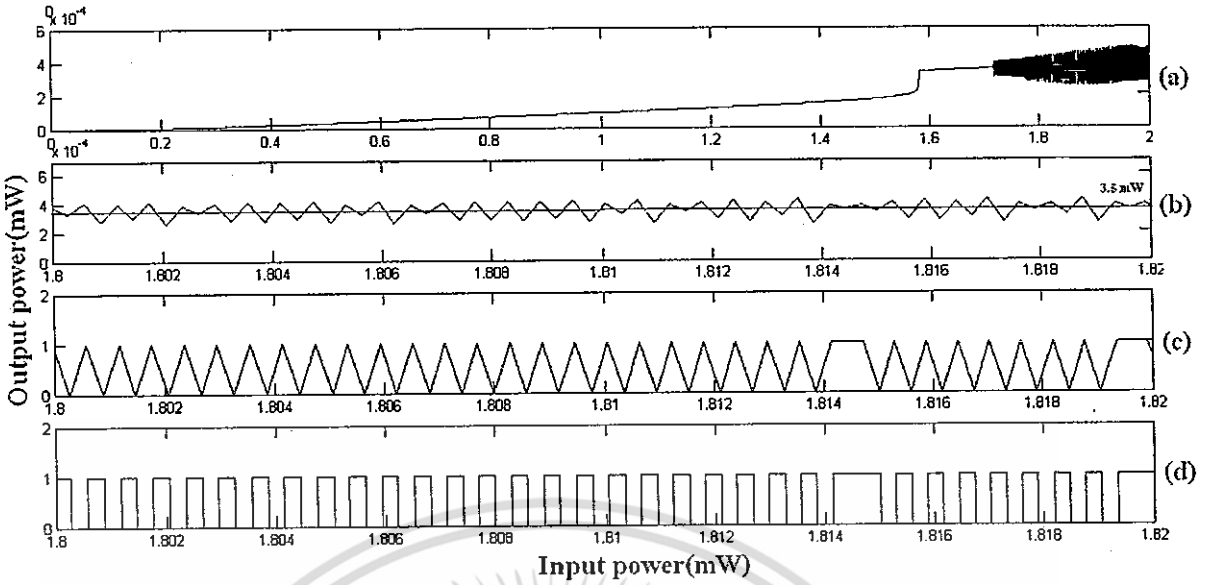

Fig. 4.11 The chaotic signal and digital coding using the approximation method.

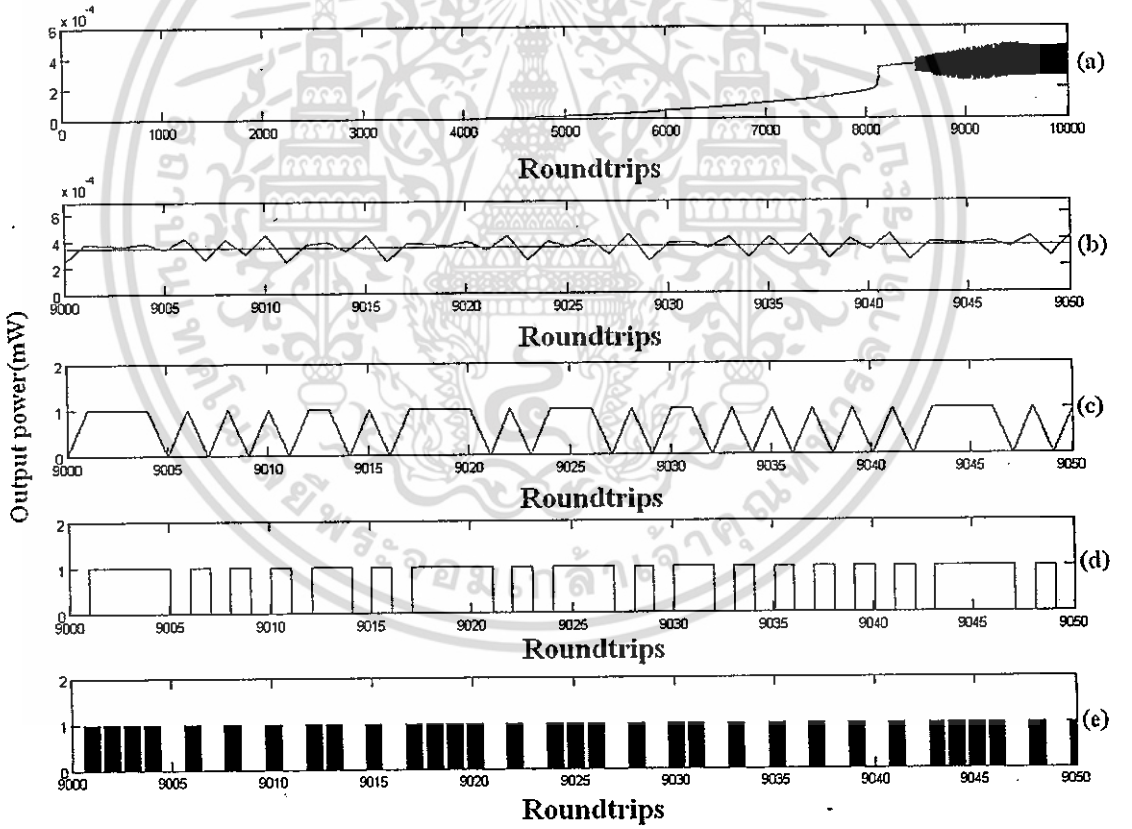

Fig. 4.12 Chaotic codes: [01111010101011010111110101110101101010101011110101].

The chaotic coding generation can be processed as following. Firstly, the chaotic signals can be generated within the microring resonator by controlling the optical input power, which can be specified by the roundtrip numbers, i.e. circulation time. Secondly, the electronically encoding

processes are performed by the following steps: (i) the chaotic coding with the threshold power is marked by using the least-square method; (ii) the clipping signals is introduced; and (iii) the chaotic code generation is completed by using the approximation and sampling methods. The first chaotic code generation is as shown in Fig. 4.12, where Fig. 4.12(a) shows the relationship between the output signals and the roundtrips, in which the chaotic behavior occurs when the roundtrip is 10,000, and the optical power is 0.5 mW. In Fig. 4.12(b) the threshold power is 3.5 mW, and the encoding roundtrips are ranged between 9000 and 9050.

Fig. 4.12(c)-(e) Show the clipping signals using the least-square method and the chaotic codes using the approximation method. The logic codes are [01111010101011010111101011101 01101010101011110101], which are 50 logic codes, and a roundtrip time is found to be 29 x 10^{-12} sec, i.e. is in order of ps.

Similarly, Fig. 4.13 is the result which is described as the following figure captions. Fig. 4.13 (a), the optical output power is 0.5 mW, with 10,000 roundtrips, where the threshold power is 0.40 mW with the encoding roundtrips that range between 9000 and 9050 as shown in Fig. 4.13 (b); where 4.13(c) shows the clipping signals, and the least-squares method is applied as shown in Fig. 4.13(d). There are 50 logic codes obtained with a bit time of 29 x 10^{-12} s as shown in Fig. 4.13(e).

Fig. 4.14, the chaotic signals are generated using the microring part, while the chaotic codes (digital codes) are electronically performed by the encryption data. The signals are multiplexed and transmitted via either wire or wireless links to the required receivers. The transmitted signals are received and then de-multiplexed, where the synchronously decryption to the encryption data is processed before the chaotic codes being intercepted by the specific users via the design chaotic filters.

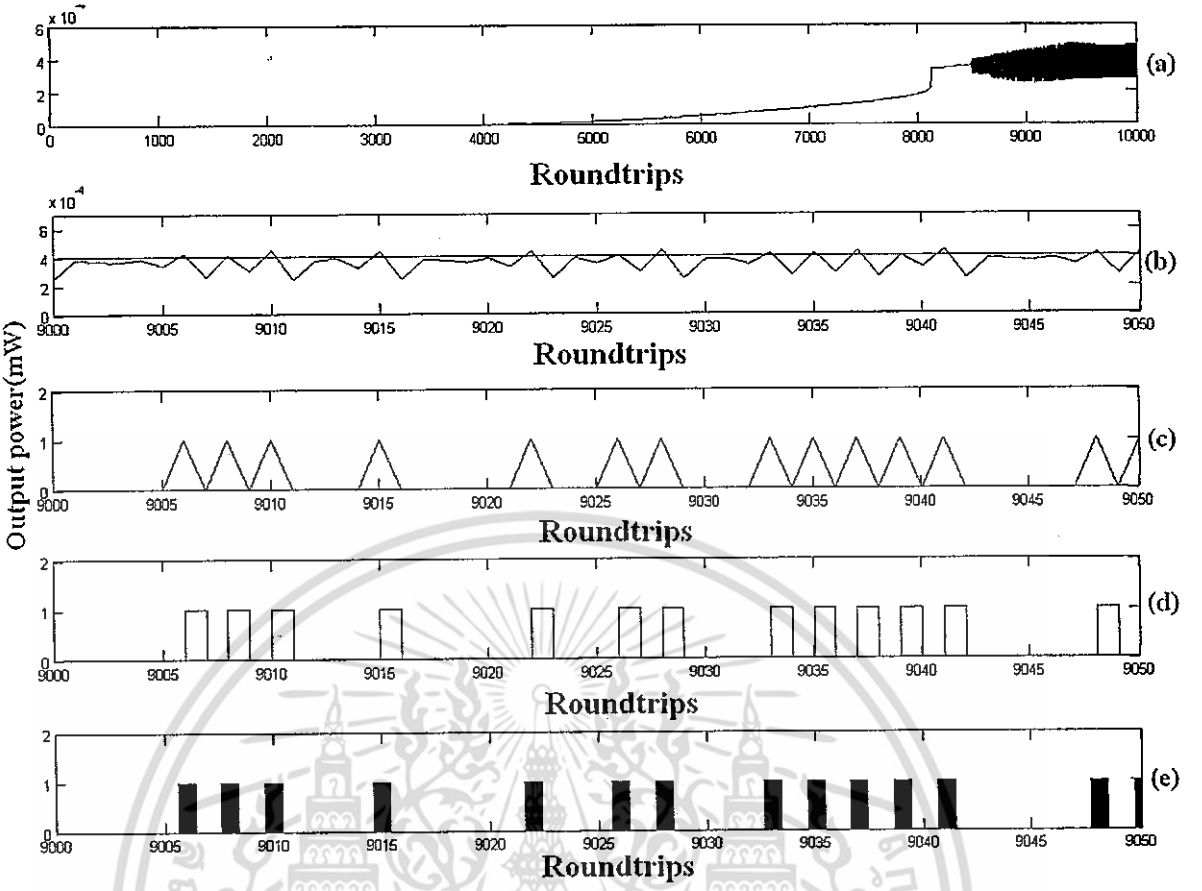

Fig. 4.13 Chaotic codes: [0000001010100001000000100010100001010101010000000101].

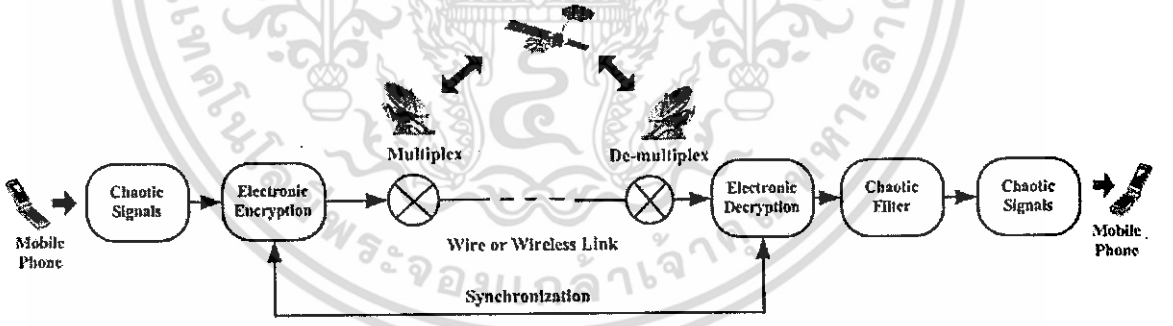

Fig. 4.14 Schematic diagram of the synchronous encryption and the encryption system.

4.4 Summary

In section 4.1, I have proposed the use of a microring resonator to design the optical packet switching, which is useful, easy to design and implemented. Where the chaotic signals can be generated using nonlinear effect and used as the high capacity and secured packet of data by using the chaotic encoding signals; for examples, such device can be applied into the mobile telephone hand set, computing system, telecommunication networks, etc.

In section 4.2, I have demonstrated the use of a microring resonator as the device for security purpose. Where the start and stop bits result from bifurcation effect could be performed and used incorporating the required packet of secured data in the transmission line or network.

Finally, section 4.3 describes the use of a microring resonator to generate the chaotic codes, where the advantages of such a device are the signals randomly encoded, easy to design and implement, the control optical power could be selected, and finally, the tunable filters can be employed. In an application, such a proposed device can be fabricated and implemented in the communication, for example, a mobile telephone hand set, a computing system, telecommunication networks, etc.

CHAPTER 5

FAST AND SLOW LIGHT GENERATIONS

In this chapter, we propose a new system of the simultaneous fast and slow light generation using a soliton pulse propagating within the nonlinear microring resonators result from Kerr effect. This proposed system can be implemented for the mobile telephone hand set, where the harmonic waves of the frequency bands can be selected to form the up-down-link converters, which means the frequency converter can be performed a single system.

5.1 Introduction

Mobile telephone has been brought to the world for two decades, where there are some technologies involved in many areas of research. Up to date, the searching for new devices and technologies are still needed. For instance, Yupapin and Suwancharoen have reported the use of chaotic signals generated by microring resonator for communication security [49], where the transmission signals could be secured by using the analog or digital methods. The increasing in the channel capacity could be achieved by the technique called the chaotic encoding and packet switching [50], where the information could be secured with highly capacity [51, 52]. Recently, Chaiyasoonthorn et al [53] have reported the interesting results when the ultra fast pulse with pulse width of as could be easily generated by using a soliton pulse traveling in the nonlinear microring resonators. The interesting idea is that the system is very small which is capable to implement within the mobile telephone hand set, whereas the required applications can be employed. This chapter, we present the other application, where the technique of up-link and down-link can be integrated within a small device called the microring devices. Several systems of optical wireless up-down-link converters have been reported [54, 55], however, there is no such a system that can be performed the link within a single system. Our proposed system can be implemented within the mobile telephone handset, where the links can be performed using the frequency bands generated by the technique called chaotic filtering, where the required frequency bands can be selected and used.

Optical soliton is recognized as a powerful laser pulse, which is used to generate the chaotic filter characteristics, especially, when it propagates within the nonlinear microring resonators [53]. When the soliton pulse is input into the multi-stage microring resonators as

shown in Fig. 5.1, the input optical field (E_{in}) in the form of soliton pulse is expressed by an Eq. (5.1).

$$E_{in} = ASech\left[\frac{T}{T_0}\right]\exp\left[\left(\frac{z}{2L_D}\right)\right] \tag{5.1}$$

where A and z are the optical field amplitude and propagation direction, respectively. $L_D = T_0^2/|\beta_2|i$ is the dispersion length of the soliton pulse. This solution describes a pulse that keeps its temporal width invariant as it propagates and thus is called a temporal soliton. T_o is known, once we can find the proper peak intensity $\left(\frac{|\beta_2|}{\gamma T_0^2}\right)$ that will make this pulse a soliton. For example, when the microring resonator is at the 1550 nm wavelength, with the 12 W peak power, then T_0 is 50 nm long, which is a pulse of about 2 millimeter long (in z). For the soliton pulse in the microring device, a balance should be achieved between the dispersion lengths $L_D = \frac{T_o^2}{|\beta_2|}$ and the nonlinear length $L_{NL} = \frac{1}{\gamma\psi_0}$, which are the length scales over which dispersive or nonlinear effects make the beam become wider or narrower. For a soliton pulse, there is balance between the two and hence $L_D = L_{NL}$.

$$n = n_0 + n_2 I = n_0 + (\frac{n_2}{A_{eff}})P \tag{5.2}$$

Where n_0 and n_2 are the linear and nonlinear refractive indexes, respectively. I and P are the optical intensity and optical field power, respectively. The effective mode core area of the device is A_{eff}. Thus, the normalized output of the light field can be expressed as,

$$\left|\frac{E_{out}}{E_{in}}\right|^2 = (1-\gamma)^2\left[1 - \frac{\kappa\left[1-(1-\gamma)^2\tau^2\right]}{1+(1-\gamma)^2(1-\kappa)\tau - 2(1-\gamma)\sqrt{1-\kappa}\tau\cos\phi}\right]. \tag{5.3}$$

The close form of equation (5.3) indicates that a ring resonator in the particular case to very similar to a Fabry-Perot cavity, which has an input and output mirror with a field reflectivity, 1-κ, and a fully reflecting mirror. Where n_0 and n_2 are the linear and nonlinear refractive

indices respectively and the coupling coefficient is κ., $x = \exp^{\frac{-\alpha L}{2}}$ represents the one roundtrip losses coefficient, Where $\phi_0 = kLn_o$ and $\phi_{NL} = kLn_2|E_{in}|^2$ are the linear and nonlinear phase shifts respectively and $k = 2\pi / \lambda$ is the wave propagation number in a vacuum.

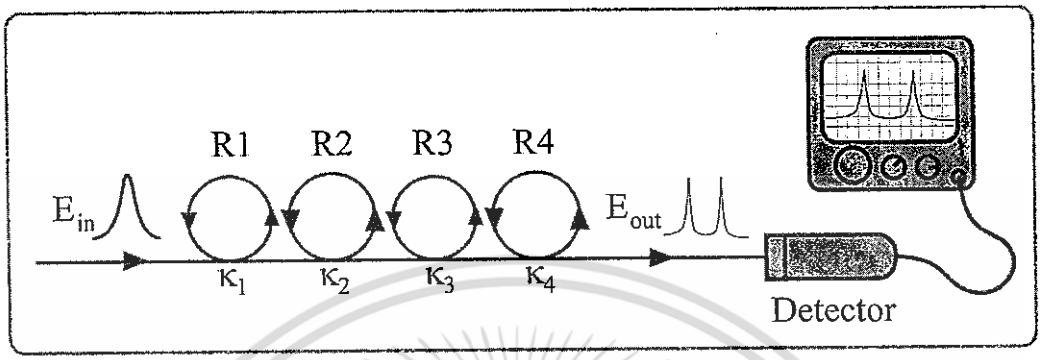

Fig. 5.1 Schematic diagram of a simultaneous fast and slow light generation. R_{1-4} and κ_{1-4} are ring radii and coupling coefficients respectively.

The basic proposed system of the simultaneous fast and slow light generation is shown in Fig. 5.1. The single mode soliton pulse becomes various modes (noisy signals) after circulating within the first microring device due to the Kerr nonlinear effects of light in the microring resonator. The chaotic filtering characteristics of the signals are formed by the other rings. By using the material parameters (InGaAsP/InP), the specified frequency bands can be obtained using the appropriate ring parameters; finally, we ended up with the following details. The soliton waveform with the center frequency at 2 GHz is input into the first microring resonator (R_1). The optical power is fixed to be 550 mW, f_0 = 2 GHz, n_0 = 3.34, n_2 = 2.2 x 10^{-17} m^2W^{-1}, A_{eff} = 0.50 μm^2, α = 0.5 dBmm^{-1}, and γ = 0.1, with 20,000 roundtrips. The chaotic signals are generated within the first ring (R_1), where the broad frequency band is observed in ring R_2. The clearer filtering signals are seen in ring R_3 and R_4.

5.2 Theoretical Results and Discussion

Fig. 5.2 shows graph of the simultaneous fast and slow light generation for up-down-link converters. Where the parameters are R_1 = 10 μm, κ_1 = 0.9713, R_2 = 10 μm, κ_2 = 0.9718, R_3 = 10 μm, κ_3 = 0.9718, R_4 = 15 μm, and κ_4 = 0.9728. The down-link and up-link converters are shown in Fig. 5.3 and 5.4, respectively. Fig. 5.3 shows graph of fast and slow light generation for down-link converter. The used parameters are R_1 = 10 μm, κ_1 = 0.9713,

$R_2 = 10\ \mu m$, $\kappa_2 = 0.9718$, $R_3 = 10\ \mu m$, $\kappa_3 = 0.9718$, $R_4 = 15\ \mu m$, and $\kappa_4 = 0.9728$. Fig. 5.4 shows graph of fast and slow light generation for up-link converter. The parameters used are $R_1 = 10\ \mu m$, $\kappa_1 = 0.9713$, $R_2 = 10\ \mu m$, $\kappa_2 = 0.973$, $R_3 = 10\ \mu m$, $\kappa_3 = 0.9732$, $R_4 = 15\ \mu m$, and $\kappa_4 = 0.9777$.

In application, the upstream and downstream communication information can be linked via a single system of devices as shown in Fig. 5.1, for the up-down-link converters. In principle, the communication signals are formed by the signal interchanging devices known as Electrical to Optical (E/O) and Optical to Electrical (O/E) converters. In the system the up-link and down-link frequency bands can be simultaneously generated, therefore, the next step is that the specified frequency band will be selected (filtered) to form the required link converters. By using the proposed system, the wide range of the spread wavelength domain can also be generated and available, which means that the wavelength multiplexing, especially, dense wavelength division multiplexing (DWDM) via optical wireless link is plausible.

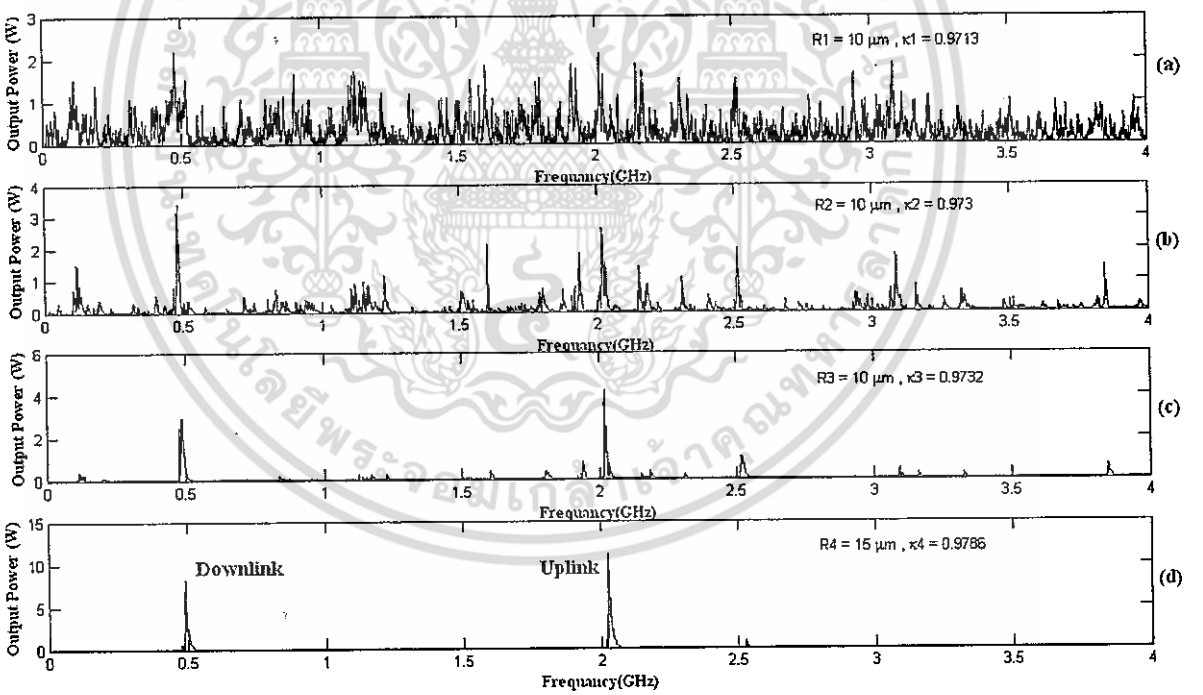

Fig. 5.2 Graph of simultaneous fast and slow light generation for up-down-link converters, (a) noisy chaotic signals, (b) frequency bands, (c) filtering signals, (d) Up-down-link signals.

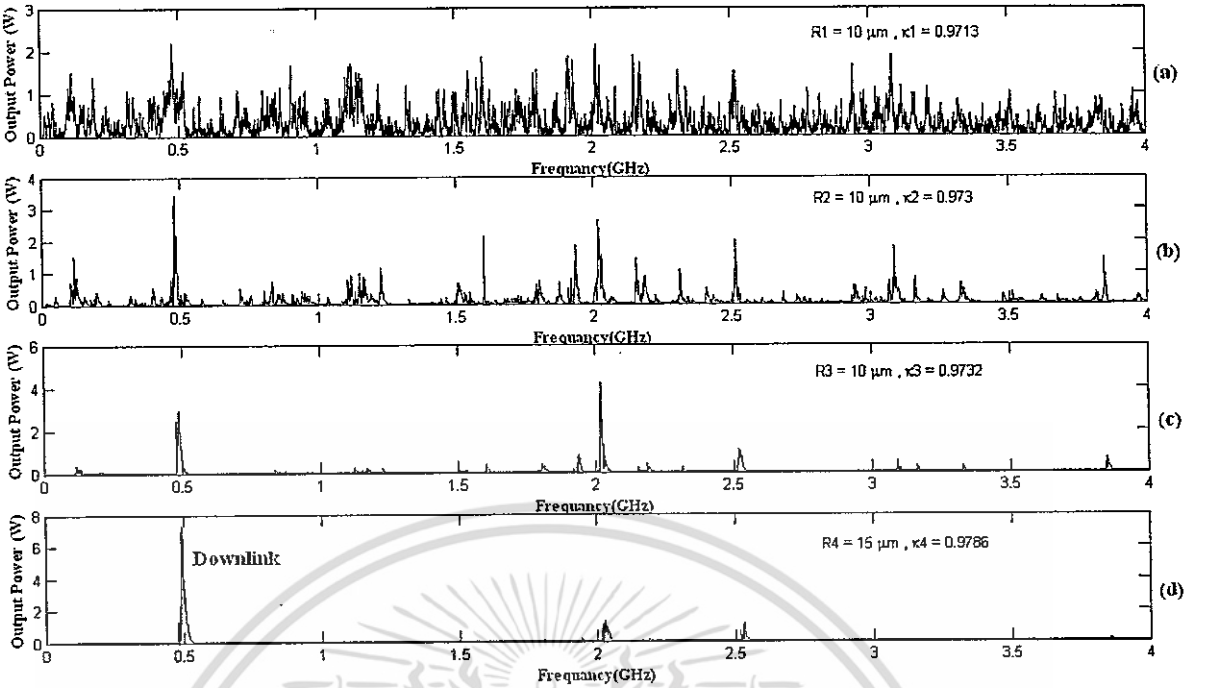

Fig. 5.3 Graph of fast and slow light generation for down-link converter, (a) noisy chaotic signals, (b) frequency bands, (c) filtering signals, (d) down-link signal (500MHz).

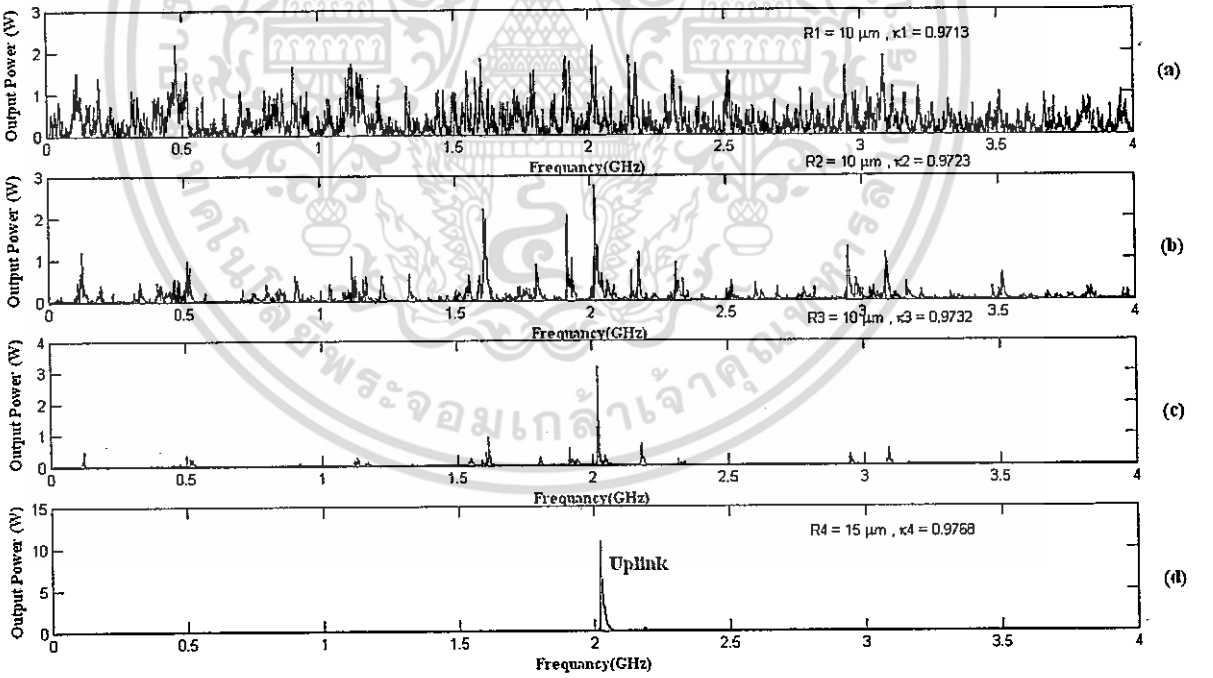

Fig. 5.4 Graph of fast and slow light generation for up-link converter, (a) noisy chaotic signals, (b) frequency bands, (c) filtering signals, (d) up-link signal (2GHz).

5.3 Summary

In this section, the very interesting results that the simultaneous fast and slow light could be generated by using the nonlinear microring devices. The system is consisted of a series of four nonlinear microring devices. We have shown that the two different frequency bands could be selected, and normally used in the up-down-link converters in optical wireless link system. The key advantages of the system are the simultaneous generation of up and down link frequency bands, and the frequency band generation can be formed in the single system.

CHAPTER 6

CONCLUSIONS

◈ High Capacity Packet Switching

We proposed a new design of the secured packet switching using the nonlinear behaviors of soliton in a micro ring resonator, where the nonlinear penalty of light traveling in the device becomes benefit. The chaotic signals are generated by a Kerr effects nonlinear type of soliton in a micro ring resonator, where the control input power can be used to specify the output filtering signals. Some device parameters are chosen and simulated using the Z-transform model. The potential of using such a device for communication security is performed and discussed. Results obtained have shown the potential of using such a proposed device for the tunable band-pass and band-stop filters, in which the packet switching data can be performed and secured.

◈ Packet Switching Start-Stop Bits Generation

The use of a microring resonator performed as the device for security purpose has been demonstrated. Where the start and stop bits could be performed and used incorporating the required packet of data in the transmission line or network. In practice, the microring device, light source and nonlinear materials are available and realized in commercial market. Which means this technique is one of our choices for communication security that could be plausible in realistic applications that will be implemented and used in the near future.

◈ Chaotic Signal Generation and Coding

The use of a microring resonator to generate the chaotic codes, where the advantages of such a device are (i) the signals randomly encoded, (ii) easy to design and implement, (iii) the control optical power could be selected, and finally, (iv) the tunable filters can be employed. In an application, such a proposed device can be fabricated and implemented in the communication. For example, a mobile telephone hand set, a computing system, telecommunication networks, etc. The chaotic signals can be encoded by using the electronically synchronized technique, where the required message can be successfully decoded by subtracting the chaotic oscillation. This is operated by the receiver on the transmitted signal using the least-squares method. We have

demonstrated that the chaotic signal is logically encoded using the waveforms of the transmitter and chaotic signal of the receiver output. Thus, we can conduct a secure transmission of a message by logical coding using the electronic quantizing, and coding by using the microring incorporating in the communication transmission. In either case, the completed or generalized chaotic quantizing control and chaotic signals encoding can be applied to the systems for chaotic communications for a long distance communication when the loss in the optical power is the issue of implementation. Therefore, such a proposed technique can overcome the problem of signal degradation because of the digital signal that can be recovered easier than the analog ones. In practice, the optical repeater is required into the system, where the signal recovery and noise reduction are required to be taken into account. For further applications, the more advantage method, called quantum chaos, may be the new area of investigation in the near future.

◈ Fast and Slow Light Generation

The very interesting results that the simultaneous fast and slow light could be generated using the nonlinear microring devices has been proposed. The system is consisted by series of four nonlinear microring devices. We have shown that the two different frequency bands could be selected, which are normally used in the up-down-link converters in optical wireless link system. The key advantages of the system are the simultaneous generation of up and down link frequency bands, and the frequency band generation can be formed in the single system. Further more, there are more frequency bands available, which will be suitable to implement more applications as well.

In conclusions, the future trend of using such present work is discussed, where the application such as quantum encoding and super high channel capacity for wavelength division multiplexing (WDM) will also be discussed as well.

LIST OF PUBLICATIONS

1. **S. Mitatha**, S. Thongmee, K. Dejhan, and P.P Yupapin, **"High Capacity Packet Switching With a Soliton Pulse in a Nonlinear Micro Ring Resonators"**, SmarMat-08 & IWOFM-2, Chiang Mai, 2008. (Impact Factor:2007:NA) ***(Article in press)***
2. **S. Mitatha**, S. Chaiyasoonthorn, K. Dejhan, and P.P Yupapin, **"AttoSecond Pulse and Beyond Generation Based on Muti-stage Micro Ring Resonators"**, SmarMat-08 & IWOFM-2, Chiang Mai, 2008. (Impact Factor:2007:NA) ***(Article in press)***
3. **S. Mitatha**, K. Dejhan, P.P Yupapin, and N.Pornsuwanchareoen, **"High Capacity and Security Packet Switching Using the Nonlinear Effects in Micro Ring Resonators"**, International Journal of Light and Electron Optics,2008.(Impact Factor:2006:0.585) ***(Article in press)***
4. **S. Mitatha**, K. Dejhan, P.P. Yupapin, and N. Suwancharoen, **"Chaotic Signal Generation and Coding using a Nonlinear Micro Ring Resonator"**, International Journal of Light and Electron Optics,2008. (Impact Factor:2006:0.585) ***(Article in press)***
5. **S. Mitatha**, K. Dejhan, P.P Yupapin, and N.Pornsuwanchareoen, **"Fast and Slow Light Generation via NMRRs for Optical Wireless Links"**, Proceeding on NOCA-3, August Bangkok, 2008.
6. **S. Mitatha**, K. Dejhan, P.P. Yupapin and W. Suwancharoen, **"Packet Switching Start-Stop Bits Generation Based on Bifurcation Behavior of Light in Micro Ring Resonator"**,International Journal of Light and Electron Optics, 2008. (Impact Factor: 2006:0.585) ***(Submitted).***
7. **S. Mitatha**, K. Dejhan, P.P. Yupapin and W. Suwancharoen, **"Fast and Slow Light Generation via Nonlinear Micro Ring Resonators for Optical Wireless Links"**, Microwave and Optical Technology Letter, 2008. (Menu Script ID:MOP-08-0893 ,Impact Factor:2006:0.6) ***(Submitted).***

REFERENCES

[1] R.W. Eason and A. Miller. "Nonlinear optics in signal processing." London, U.K.: Champan & Hall, 1993

[2] M. N. Islam. "Fiber switching devices and systems." New York, NY: Cambridge University Press, 1992

[3] E. Cotter, J. K. Lucek, and D. D. Marcenac. "Ultra-high-bit-rate networking: From the transcontinental backbone to the desktop." IEEE Comm. Mag., vol. 34, 1997. pp. 90-95

[4] P. P. Mitra and J. B. Stark. "Nonlinear limits to the information capacity of optical fiber communications." Nature, vol. 411, 2001. pp. 1027

[5] P. W. Smith. "On the physical limits of digital optical switching and logic elements." The Bell Sys. Tech. J., vol. 61, 1982. pp. 1975-1983

[6] L. Brzozowski and E. H. Sargent. "Nonlinear distributed-feedback structures as passive optical limiters." J. Opt. Soc. of America B., vol. 17, 2000. pp. 1360-1365

[7] L. Brzozowski and E. H. Sargent. "Optical signal processing using nonlinear distributed feedback structures." IEEE J. Quantum Electron., vol. 36, 2000. pp. 550-555

[8] L. Brzozowski and E. H. Sargent. "Nonlinear disordered media for broad-band optical limiting." IEEE J. Quantum Electron., vol. 36, 2000. pp. 1237-1242

[9] P. W. Smith, I. P. Kaminov, P. J. Maloney, and L. W. Stulz. "Self-contained integrated bistable optical devices." Appl. Phys. Lett., vol. 34, 1979. pp. 62-65

[10] P. W. Smith and E. H. Turner. "A bistable Farbry-Perot resonator." Appl. Phys. Lett., vol. 30, 1977. pp. 280-281

[11] B. E. A. Saleh and M. C. Teich. "Fundamentals of Photonics." New York: Wiley, 1991

[12] P. W. E. Smith and L. Qian. "Switching to optical for a faster tomorrow." IEEE Circuits and Devices Mag., vol. 15, 1999. pp. 28-33

[13] P. W. E. Smith. "All-optical devices: materials requirements." in Nonlinear Opt. Prop. Adv. Mats., vol. 1852, 1993. pp. 2-9

[14] G. I. Stegeman. "All-optical devices: materials requirements." in Nonlinear Opt. Prop. Adv. Mats., vol. 1852, 1993. pp. 75-89

[15] I. C. Khoo, M. Wood, and B. D. Guenther. "Nonlinear liquid crystal optical fiber array for all-optical switching/limiting." in LEOS '96 9th Annual Meeting, vol. 2, 1996. pp. 211-212

[16] G. L. Wood, W. W. Clark III, M. J. Miller, G. J. Salamo, and E. J. Sharp. "Evaluation of passive optical limiters and switches." in Materials for Optical Switches, Isolators, and Limiters, vol. 1105, 1989. pp. 154-181

[17] R. Bozio, M. Meneghetti, R. Signorini, M. Maggini, G. Scorrano, M. Prato, G. Brusatin, and M. Guglielmi. "Optical limiting of fullerene derivatives embedded in sol-gel materials." in Photoactive Organic Materials. Science and Applications. Proceedings of the NATO Advanced Research Workshop, vol. 572, 1996. pp. 159-174

[18] B. E. Little and S. T. Chu. "Toward very large-scale integrated photonics." Opt. & Photon. News, vol. 11, 2000. pp. 24-29

[19] R. W. Boyd. "Nonlinear Optics." 2nd ed. Academic Press, Inc., 2003

[20] G.P. Agrawal. "Nonlinear Fiber Optics." Academic Press, San Diego, CA, 2001

[21] Fan Yi Lin and Meng Chiao Tsai. "Chaotic communication in radio over fiber transmission based on optoelectronic feedback semiconductor laser." Opt Exp., vol. 15, no. 2, Jan 2007. pp. 302-311

[22] K.Ikeda, H. Daido and O. Akimoto. "Optical turbulence: Chaotic behavior of transmitted light from a ring cavity." Phys. Rev. Lett., vol. 45, 1980. pp. 709-712

[23] D. A. B. Miller, S. D. Smith, and A. Johnston. "Optical bistability and signal amplification in a semiconductor crystal: Applications of new low-power nonlinear effects in InSb." Appl. Phys Lett., vol. 35, no. 12, 1979. pp. 658–660

[24] P. Mandel, S. Smith, and B. Wherrett. "From Optical Bistability Towards Optical Computing." North-Holland, 1987

[25] H. M. Gibbs. "Controlling Light with Light." Academic Press Inc., 1985

[26] K. Otsuka. "Pitchfork bifurcation and all-optical digital signal processing with a coupled-element bistable system." Opt. Lett., vol. 14, no. 1, 1989. pp. 72-74

[27] L. M. Zhao, D. Y. Tang, F. Lin and B. Zhao. "Observation of period-doubling bifurcations in a femtosecond fiber soliton laser with dispersion management cavity." Opt. Exp. vol. 12, no. 19, 2004. pp.4573-4578

[28] A. Hasegawa and Y. Kodama. "Signal transmission by optical solitons in monomode fiber." Proc. IEEE., vol. 69, no. 9, Sept 1981. pp.1145–1150

[29] S. Blair. "Optical soliton-based logic gates." Ph.D. dissertation, University of Colorado, 1998

[30] E. Infeld and G. Rowlands. "Nonlinear waves solitons and chaos." Cambridge university press, 2000

[31] E. A. J. Marcatili. "Bends in Optical Dielectric Guides." Bell. Syst. Tech. J., vol. 48, September1969. pp. 2103-2132.

[32] E. A. J. Marcatili. "Dielectric Rectangular Waveguide and Directional Coupler for Integrated Optics." Bell. Syst. Tech. J., vol. 48, September 1969. pp. 2071-2101.

[33] C. K. Madsen and J. H. Zhao. "A General Planar Waveguide Autoregressive Optical Filter." IEEE J. Lightwave Tech., vol. 14, no. 3, March 1996. pp. 437-447

[34] S. C. Hagness et al.. "FDTD Microcavity Simulations: Design and Experimental Realization of Waveguide-Coupled Single-Mode Ring and Whispering-Gallery-Mode Disk Resonators." IEEE J. Lightwave Tech., vol. 15, no. 11, November 1997. pp. 2145-2165

[35] D. Rafizadeh et al.. "Waveguide-coupled AlGaAs/GaAs microcavity ring and disk resonators with high finesse and 21.6 nm free spectral range." Opt. Lett., vol. 22, no. 16, August 1997. pp. 1244-1246

[36] B. E. Little et al. "Ultra-Compact Si-SiO_2 Microring resonator Optical Channel Dropping Filters." IEEE Photon. Techn. Lett., vol. 10, no. 4, April 1998. pp. 549-551

[37] D. J. W. Klunder et al., "Vertically and laterally waveguide-coupled cylindrical microresonators in Si_3N_4 on SiO_2 technology." Appl. Phys. B 73., November 2001. pp. 603-608

[38] B. Vanderhaegen et al., "High Q GaInAsP ring resonator filters." ECIO'99, Torino Italy, April 1999. pp. 381-384

[39] M. K. Chin et al., "GaAs Microcavity Channel-Dropping Filter based on a Race-Track Resonator." IEEE Photon. Techn. Lett., vol. 11, no. 12, December 1999. pp. 1620-1622

[40] C. K. Madsen and J. H. Zhao, "Optical Filter Design and Analysis: A Signal Processing Approach." New York: Wiley, 1999

[41] J. E. Heebner and R.W. Boyd. "Enhanced all-optical switching by use of a nonlinear fiber ring resonator." Opt. Lett., vol. 24, no. 12, 1999. pp. 847–849

[42] J.C. Bronski, M. Segev, and M.I. Weinstein. "Mathematical frontiers in optical solitons." PNAS., vol. 98, no. 23, 2001. pp. 12872–12873

[43] C. L. Bai. "Soliton structures with non-propagating behavior in three-dimensional system." Chaos, Solitons and Fractals, vol. 36, 2008. pp. 253–262

[44] D.S. Ricketts, X. Li, and D. Ham. "Electrical soliton oscillator." IEEE Trans. Micro. Theory and Techniques, vol. 54, no. 1, 2006. pp. 373–382

[45] P.P. Yupapin and W. Suwancharoen. "Chaotic signals control and cancellation using a microring resonator incorporating an optical add/drop multiplexer." Opt. Comm., vol. 280, 2007. pp. 343–350

[46] P.P. Yupapin, W. Suwanchareon and S. Suchat. "Nonlinearity penalties and benefits of light traveling in a fiber optic ring resonator." Int. J. of Light and Electron Optics., 2007. DOI:10.1016/j.ijleo.2007.07.009

[47] P. Saeung and P.P. Yupapin. "A Design of Optical Ring Resonator Filters for WDM Applications." J. Nonlinear Optical Phys. and Mat., vol. 17, no. 2, 2008.

[48] J. van Howe and Chris Xu. "Ultrafast optical delay line using soliton propagation between a time-prism pair." Opt. Exp., vol. 13, 2005. pp. 1138

[49] P.P. Yupapin, P. Saeung and W. Suwancharoen, Guided Wave Optics and Photonics: Microring Resonator Design for Telephone Network Security, Nova Science Publisher, New York, 2008, ISBN: 978-1-60456-838-7.

[50] P.P. Yupapin, W. Suwanchroen and S. Pipatsart, A Novel Technology for Mobile Telephone Networks and Security, Mobile Telephones : Networks, Applications, and Performance, Editors : Alvin C. Harper and Raymond V. Buress, Nova Science Publishers, 2008. ISBN : 978-1-60456-436-5.

[51] S. Mitatha, K. Dejhan, P.P. Yupapin and N. Pornsuwancharoen, International Journal of Light and Electron Optics, 2008.[Article in press]

[52] S. Mitatha, K. Dejhan, P.P. Yupapin and N. Pornsuwancharoen, International Journal of Light and Electron Optics, 2008.[Article in press]

[53] S. Chaiyasoonthorn, O. Saneujit, W. Suwancharoen and P.P. Yupapin, J. Advance Materials Research, 2008. [Article in press].

[54] M. T. Zhou, J.D. Zhang, A.B. Sharma, Y. Zhang, S. Xiao, M. Fujise, Opt. Commun., 269, 69(2007).

[55] M. T. Zhou, Q.J. Wang, B. Luo, Y.X. Guo, L.C. Ong, Y. Zhang, Y. Zhang, Y.C. Soh, R. Miura, Opt. Commun. 281, 2572(2008).

APPENDIX

❖ Full Paper's Publications

1. **S. Mitatha**, K. Dejhan, P.P Yupapin, and N.Pornsuwanchareoen, **"High Capacity and Security Packet Switching Using the Nonlinear Effects in Micro Ring Resonators".,** International Journal of Light and Electron Optics,2008.(Impact Factor:2006:0.585) *(Article in press)*

2. **S. Mitatha**, K. Dejhan, P.P. Yupapin, and N. Suwancharoen, **"Chaotic Signal Generation and Coding using a Nonlinear Micro Ring Resonator"**, International Journal of Light and Electron Optics, 2008. (Impact Factor:2006:0.585)***(Article in press)***

3. **S. Mitatha**, K. Dejhan, P.P. Yupapin and W. Suwancharoen, **"Fast and Slow Light Generation via Nonlinear Micro Ring Resonators for Optical Wireless Links"**, Microwave and Optical Technology Letter, 2008. (Impact Factor:2006:0.6) ***(Submitted).***

XML:ver:5.0.1 5 jena | IJLEO : 50616 | Prod.Type:FTP pp.1–11(col.fig.:1–10) | ED:MahadevaS PAGN:VG SCAN:

ARTICLE IN PRESS

Available online at www.sciencedirect.com

ScienceDirect

Optik 1 (1111) 111–111

Optik Optics

www.elsevier.de/ijleo

High-capacity and security packet switching using the nonlinear effects in micro ring resonators

S. Mitatha[a], K. Dejhan[a], P.P. Yupapin[b,*], N. Pornsuwancharoen[c]

[a]*Faculty of Engineering, Research Center for Communication and Information Technology, Thailand*
[b]*Department of Applied Physics, Faculty of Science, Advanced Research Center for Photonics, King Mongkut's Institute of Technology Ladkrabang, Bangkok 10520, Thailand*
[c]*Department of Electronics, Faculty of Industry and Technology, Rajamangala University of Technology Isan, Sakon-nakorn Campus 47160, Thailand*

Received 28 January 2008; accepted 14 May 2008

Abstract

We propose a new design of secured packet switching generated by using nonlinear behaviors of light in a micro ring resonator. The use of chaotic signals generated by the micro ring resonator to form the filtering and packet switching characteristics is described, where the high-capacity and security switching using such form is presented. The key advantage is that the high capacity of communication data can be secured in the transmission link, where the nonlinear penalty of light traveling in the device is beneficial. For instance, the required information can be transmitted and retrieved by using the proposed packet switching scheme. In principle, the chaotic signals are generated by a Kerr effects nonlinear type of light in a micro ring resonator, where the control input power can be specified by the required output filtering signals. The ring radii used range between 10 and 20 μm, $\kappa = 0.0225$, $\alpha = 0.5$ dB and Q1 $n_2 = 2.2 \times 10^{-15}$ m^2/W. Simulation results obtained have been described based on the practical device parameters. Three models of the proposed devices have been simulated, the potential of using for the tunable band pass and band Q2 stop filters, in which high-capacity packet switching data can be performed, and the fs switching time is plausible.

Keywords: Packet switching; Chaotic filter; Tunable filter; Micro ring resonator

1. Introduction

Recently, Yupapin and Suwancharoen [1] have shown that the secured communication message in the present technology via the micro ring resonator device has promising realistic applications. Broad areas of research works in either theoretical or experimental works have been reported. One of the applications of the practical device using a micro ring radius of 10 μm has been reported [2,3]. The design of an add/drop device has also been recently proposed. The nonlinear behaviors of light in a micro ring resonator have been investigated and used for communication security [4,5]. Moreover, the frequency characteristics of the ring resonator-based filters in some way are complementary with respect to finite impulse response (FIR) filters, such as cascaded Mach–Zehnder or arrayed waveguide gratings, and have

*Corresponding author. Tel.: +23 264339; fax: +23 264354.
E-mail address: kypreech@kmitl.ac.th (P.P. Yupapin).

0030-4026/$ - see front matter © 2008 Elsevier GmbH. All rights reserved.
doi:10.1016/j.ijleo.2008.05.032

Please cite this article as: S. Mitatha, et al., High-capacity and security packet switching using the nonlinear effects in micro ring, Optik Int. J. Light Electron Opt. (2008), doi:10.1016/j.ijleo.2008.05.032

IJLEO : 50616

ARTICLE IN PRESS

2 S. Mitatha et al. / Optik ▮ (▮▮▮▮) ▮▮▮–▮▮▮

been studied [6], where cascaded resonators have shown frequency response with high rejections and narrow band pass. This feature can be advantageously combined with those of FIR filters to obtain very interesting transfer functions. A simple technique for the synthesis of band pass filters realized by cascading Fabry Pérot cavities or micro ring resonators has been reported [7]. The structure is called a direct coupled-resonators filter, because each resonator is directly coupled to the adjacent resonators. One of these applications is the so-called add/drop filter, using a four-port device capable of separating and/or combining communication channels in wide-band telecommunication systems. Furthermore, some methods have been described to obtain a wide pass band, large free spectral range and high finesse, where the series-coupled, and others to parallel-coupled have been applied [8,9]. A simple but very efficient single micro ring resonator and two-series-ring to parallel-coupled device is described [10], where it displays large finesse and high stop band attenuation.

In recent years, semiconductor micro ring resonators have received great interest as potential building blocks for optoelectronic integrated circuits due to their ultra compactness and small size, which can lead to high device integration densities. Moreover, the field buildup inside the ring cavity can be used for all optical signal-processing functions based on enhanced nonlinear effects [11]. In practice, the stop band filter can be created by a single waveguide ring resonator, where ultra-compact resonant silicon on insulator structures based on a 3-μm-diameter micro disk coupled to one or two waveguides have already been presented [2]. The micro ring resonator for an add/drop filter had a ring radius in the order of 10–50 μm. The application and design of an optical flip-flop device is an integrated InP/InGaAsP with a two-state coupled laser device. It is fabricated on an InP/InGaAsP material wafer, which contains active areas with 1550 nm emission wavelength, and an InGaAsP for semiconductor optical amplifiers. Another essential building block of an all-optical packet switch is optical flip-flop memories, which are used to store the switch decision information. An integrated optical flip-flop can control a wavelength converter to switch a 10 Gb/s data packet [12]. In this paper, we will present a different integrated optical flip-flop and its performance for 80 Gb/s all-optical packet switching has been presented by Liua et al. [13]. To date, the photonic approaches of packet switching have been motivated by the need for high-capacity optically transparent drop switches for ring and bus networks. The switching and/or routing fabric in recent demonstrations of photonic packet switching has generally been optical components. However, electronic components and circuits remain attractive alternatives to photonic devices in functions such as address processing, switch control, and buffer control and the chaotic quantum control. However, the filter response of the micro ring resonator can be synthesized by the combination of coupled and cascaded topologies. In addition, since the vertically coupled micro ring resonator is advantageous for dense integration due to its very compact element and cross-grid topology, it is easy to form the coupled and cascaded topologies without deteriorating the compactness [14].

In this paper, we report the design of packet switching and application for the band pass and band stop filters using the nonlinear behaviors of light in the micro ring resonators, where three forms of applications for chaotic signal filtering, encoding, and packet switching are proposed and discussed. These can be applied into the optical networks to encrypt and filter, and the required communication data can be retrieved. The ring parameters used are based on the practical device parameters as shown in references [2,3]. Simulation results obtained have shown the potential of application for secure communication links in the optical networks, where the high capacity of secure communication data can be performed.

2. Chaotic behaviors

Consider a micro ring resonator configuration as shown in Fig. 1, which is constructed by a single ring resonator (SRR) and a 2×2 optical coupler [1,4], the circumference of the micro ring is L. For the convenience of analysis, we assume that the complex electric field at each port as shown in Fig. 1(a) is $E(t)$, where $E_{in}(t)$ is the incoming light field of an input port and the transmitted light field to the output port is $E_{out}(t)$. While the rest of the fields $E_1(t)$ and $E_2(t)$ are the circulated fields inside the micro ring, Fig. 1(b) shows the series μ-ring resonator for design of the filtering device, and Fig. 1(c) shows the multi-users via the micro ring resonators in an optical network, where packet switching and filtering can be performed.

Here, the input light into the system is assumed to be monochromatic with constant amplitude and random phase modulation, which results in temporal coherence degradation. Hence, the input light field can be expressed as

$$E_{in}(t) = E_0 \exp^{j\phi_0(t)} \tag{2.1}$$

Eq. (2.2) is given by [2]

$$\left|\frac{E_{out}(t)}{E_{in}(t)}\right|^2 = (1-\gamma)\left[1 - \frac{(1-(1-\gamma)x^2)\kappa}{(1-x\sqrt{1-\gamma}\sqrt{1-\kappa})^2 + 4x\sqrt{1-\gamma}\sqrt{1-\kappa}\sin^2(\phi/2)}\right] \tag{2.2}$$

Please cite this article as: S. Mitatha, et al., High-capacity and security packet switching using the nonlinear effects in micro ring, Opt. Int. J. Light Electron. Opt. (2008), doi:10.1016/j.ijleo.2008.05.032

IJLEO : 50616

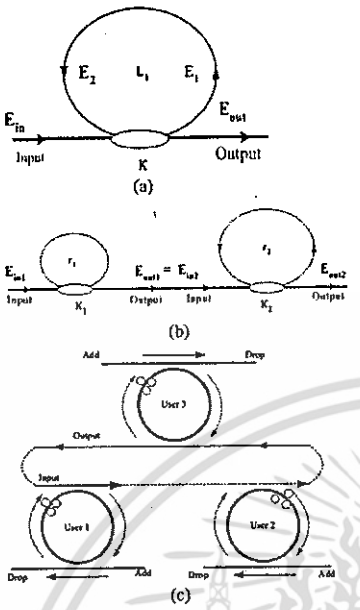

Fig. 1. A schematic of the micro ring resonators, (a) a micro ring resonator, (b) the serial micro ring resonators, and (c) the micro ring resonators in a network.

A close examination of Eq. (2.2) indicates that a ring resonator in the particular case is very similar to a Fabry Pérot cavity, which has an input and output mirror with a field reflectivity, $1-\kappa$, and a fully reflecting mirror, where n_0 and n_2 are the linear and nonlinear refractive indices, and the coupling coefficient is κ.

$$E_{out1} = (E_{in1})\sqrt{(1-\gamma)\left[1-\frac{(1-(1-\gamma)x^2)\kappa}{(1-x\sqrt{1-\gamma}\sqrt{1-\kappa})^2+4x\sqrt{1-\gamma}\sqrt{1-\kappa}\sin^2(\phi/2)}\right]} \tag{2.3}$$

When $E_{out1} = E_{in2}$ and $\kappa_1 = \kappa_2$:

$$E_{out}(t) = (E_{in2})\sqrt{(1-\gamma)\left[1-\frac{(1-(1-\gamma)x^2)\kappa}{(1-x\sqrt{1-\gamma}\sqrt{1-\kappa})^2+4x\sqrt{1-\gamma}\sqrt{1-\kappa}\sin^2(\phi/2)}\right]} \tag{2.4}$$

$x = \exp^{-\alpha L/2}$ represents the one roundtrip losses coefficient, $\phi_0 = kLn_0$ and $\phi_{NL} = kLn_2|E_1|^2$ are the linear and nonlinear phase shifts, and $k = 2\pi/\lambda$ is the wave propagation number in a vacuum.

This nonlinear behavior of light traveling in an SRR was investigated, where the parameters of the system were fixed to $\lambda_0 = 1.55\,\mu m$, $n_0 = 3.34$, $A_{eff} = 30\,\mu m^2$, $\alpha = 0.5\,dB$, where the practical bending loss of the waveguide fabricated by InGaAsP/InP is confirmed by reference [15], where the propagation loss is as low as $1.3 \pm .02\,dB/mm$ at $1.55\,\mu m$ [16], $\gamma = 0.1$, and $R_1 = 10\,\mu m$. The coupling coefficient of the micro ring resonator coupler was fixed in this investigation to $\kappa = 0.0225$. The nonlinear refractive index was $n_2 = 2.2 \times 10^{-15}\,m^2/W$ [8], and the 20,000 iterations of roundtrips inside the optical fiber ring were plotted. We assume that $\phi_L = 0$ for simplicity.

To design the nonlinear micro ring resonator, firstly, the nonlinear behavior of light in the ring needs to be characterized. The nonlinear behavior of the micro ring resonator with the roundtrips of 10,000 is as shown in Fig. 2. When the ring radius is $10\,\mu m$, the nonlinear effect does not occurred as shown in Fig. 2(a). It occurs when the ring radius is $20\,\mu m$ as shown in Fig. 2(b), where the filter characteristics are also shown.

In Fig. 3, the nonlinear effects and nonlinear behaviors of signal in the ring can be simultaneously generated, and the band pass and band stop filters can be performed. Fig. 3(a) shows the nonlinear effect of band stop filter where the roundtrips range between 9000 and 11,000. There are two side bands of band pass filters with roundtrips in the range of 7500 8800 and 11,500 12,500, respectively. In Fig. 3(b), with the roundtrips in the ranges of 8500 11,500, 8000 8800 and 11,500 12,000, the two band pass and band stop filters are seen. Similarly in Fig. 4(a) and (b), the band pass and band stop filters are shown, when the roundtrips are in the ranges 8500 10,500, 7500 8200, 11,800 12,500 and 9,000 12,000, 7500 8000, 8500 8700, 10,500 10,700, 12,000 12,500, respectively. A roundtrip time is $10^{-12}\,s$, when the ring radius is $10\,\mu m$.

From Fig. 1(b), Eq. (2.3) is obtained by using Eq. (2.2), which is given by

A close examination of Eq. (2.4) indicates that a ring resonator in the particular case is very similar to a Fabry Pérot cavity, which has an input and output mirror with a field reflectivity, $1-\kappa$, and a fully reflecting mirror, where n_0 and n_2 are the linear and nonlinear refractive indices, the coupling coefficient is κ. Here

Please cite this article as: S. Mitatha, et al., High capacity and security packet switching using the nonlinear effects in micro ring ... Opt. Intell. Light Electron. Opt. (2008), doi:10.1016/j.ijleo.2008.05.032

IJLEO : 50616

ARTICLE IN PRESS

4 S. Mitatha et al. / Optik ▮ (▮▮▮▮) ▮▮▮–▮▮▮

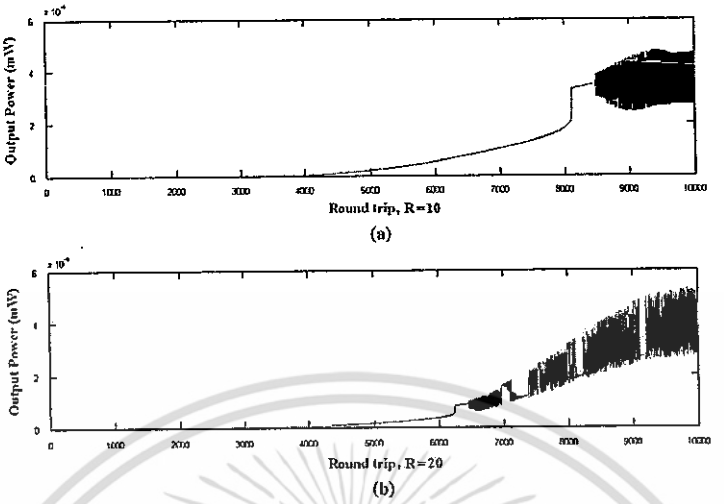

Fig. 2. The nonlinear behaviors of light in a micro ring resonator with (a) $R = 10\,\mu m$ and (b) $R = 20\,\mu m$.

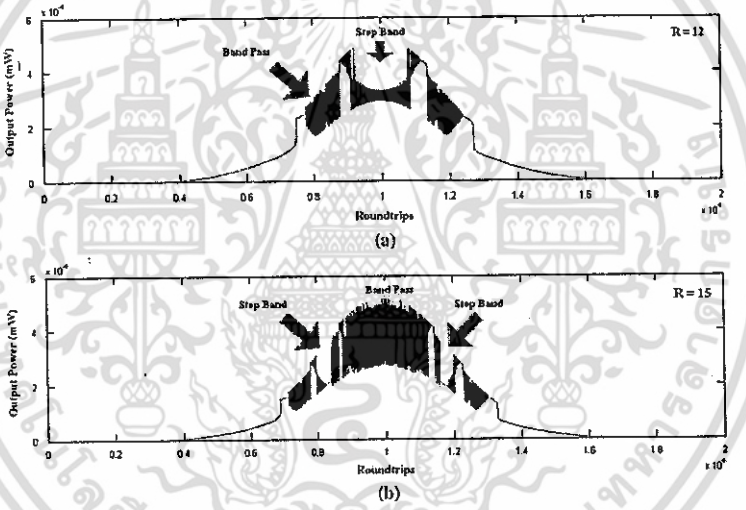

Fig. 3. The nonlinear behavior characteristics of band pass (a) and band stop (b) filters in the micro ring resonator, (a) $R = 12\,\mu m$ and (b) $R = 15\,\mu m$.

$x = \exp^{-\alpha L/2}$ represents the one roundtrip losses coefficient, $\phi_0 = kLn_0$ and $\phi_{NL} = kLn_2|E_1|^2$ are the linear and nonlinear phase shifts, respectively, and $\kappa = 2\pi/\lambda$ is the wave propagation number in vacuum.

Using Eqs. (2.3) and (2.4), the simulation results obtained are shown in Fig. 5(a c). Fig. 5(a) shows the behaviors of the band stop and band pass filters with a ring radius of 12 μm, and roundtrips of 9050–11,500. In

Please cite this article as: S. Mitatha, et al., High-capacity and security packet switching using the nonlinear effects in micro ring, Opt. Int. J. Light Electron. Opt. (2008), doi:10.1016/j.ijleo.2008.05.052

IJLEO : 50616

ARTICLE IN PRESS

S. Mitatha et al. / Optik 1 (2008) 120–230 5

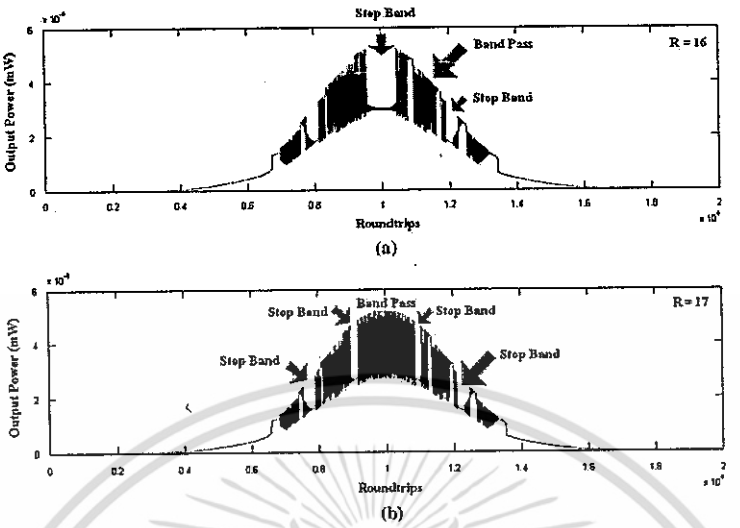

Fig. 4. The nonlinear behaviors characteristics of band pass (a) and band stop (b) filters in the micro ring resonator, (a) $R = 16\,\mu m$ and (b) $R = 17\,\mu m$.

Fig. 5(b) and (c) the band pass and band stop filters characteristics are shown, respectively. The serial ring output is shown in Fig. 5(c), which is obtained by using a device configured in Fig. 1(b). Similarly, the multi-filter characteristics can be seen in Fig. 6. However, the low level of signal to noise ratio may cause the problem in real applications.

3. Chaotic encoding and packet switching

The chaotic signals are generated by using Eq. (2.4), which can be used to form the digital codes as follows. The quantitatively present logic coding can be expressed by

$$u(v) = \begin{cases} 0, & v < 3.5\,\text{mW} \\ 1, & v \geq 3.5\,\text{mW} \end{cases} \quad (2.5)$$

For instance, when $u(v)$ represents the logic states, v is the signal power. The quantization and re-quantization can process the similar transfer characteristics. We assume that the quantizing involved is infinite, which means that the system input signal is never clipped by saturation of the quantizing. In this case, the corresponding transfer functions of the quantizing output to its input can be expressed analytically in terms of the quantizing step size as detailed in reference [17].

In practice, the design micro ring resonator with its suitable parameters can be used to generate the chaotic behaviors, which are being characterized and the chaotic codes implemented. For instance, we chose the chaotic signals with the optical power ranging from 1.8 to 1.82, 1.84 to 1.86 and 1.88 to 1.90 mW as shown in Fig. 7. The signal quantization can be further understood by using the approximation plots in which the chaotic signal can be encoded. These quantizing plots for various input powers range from 1.8 to 1.82 mW. These plots show the improvement of the approximation method as shown in Fig. 7(a) (c), and the deterioration until or the least-squares method as in Fig. 7(d) is introduced. The signal processing of the outputs using the approximation method is plotted, where (a) shows the relationship between the input and output signals, (b) the red line is the power reduction to be the threshold power of 3.5 mW, (c) the signal after threshold power condition uses, and (d) the output signal when the approximation method is applied, which the logical code with the logic state "1" or "0" generates. From the previous description, after the chaotic behaviors of the device are characterized, the next step is that the random code can be generated by controlling the input optical

Please cite this article as: S. Mitatha et al., High-capacity and security packet switching using the nonlinear effects in micro ring ..., Opt. Int. J. Light Electron. Opt. (2008), doi:10.1016/j.ijleo.2008.03.032

IJLEO : 50616

ARTICLE IN PRESS

6 S. Mitatha et al. / Optik ▮ (▮▮▮▮) ▮▮▮–▮▮▮

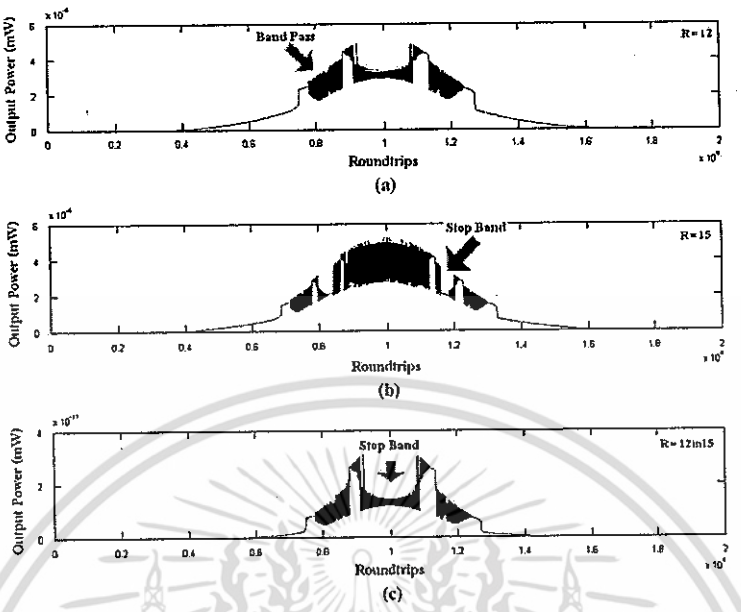

Fig. 5. The chaotic output power and the roundtrips of the micro ring at the roundtrips 20,000, (a) 12 μm, (b) 15 μm, (c) $R = 12$ μm in series with $R = 15$ μm.

power that enters the micro ring device. Then the required chaotic codes can be generated. However, in application, the consideration of the fiber ring resonators and the reliable optical source has become the key conditions. The chaotic coding creation can be processed as follows: (i) the chaotic signals can be generated within a fiber ring resonator by controlling the optical input power, which can be specified by the roundtrip number, i.e. time, (ii) to start the chaotic coding with the threshold power, where it is marked before averaging using the least-square method, (iii) the clipping signals are introduced, (iv) the chaotic code generation is completed by using the approximation and sampling methods.

The first chaotic codes generation is as shown in Fig. 8. The relationship between the output signals and roundtrips is as shown in Fig. 8(a), the chaotic behavior occurs when the roundtrips number is 10,000. Fig. 8(b) shows the threshold power is 3.5 mW, with the encoding roundtrips being from 9000 to 9050. Fig. 8(c) shows the clipping signals, 8(d) shows the clipping signals are performed by using the least-squares method, and 8(e) shows the chaotic codes are obtained using the approximation method, where the logic code obtained is [0111101010101101011110101110101101010101010101 1110101], there being 50 logic codes and a roundtrip time of 10^{-12} s. In general, the packet switching consists of the analog to digital converter (ADC) and photonic sampled and quantized ADC. The input signal is the analog signal, which is obtained from the chaotic signal, the output signal is the digital approximation (i.e. codes) [16]. The concepts of packet switching are scheduled as follows: first step: choosing the ring resonator filter band pass filter and band stop filter, second step: setting the range of the chaotic code; third step: choosing to the threshold power by sampling; and final step: quantizing the analog to digital approximation.

Fig. 9 shows the packet switching performed by the band pass filter, which occurred with the roundtrip ranges 9500 10,500, as shown in Fig. 9(a). To obtain the 100 bits, the selected roundtrips are 9900 10,000 to form the required digital codes [17] as shown in Fig. 9(b). The threshold power of 4.5 mW is used to perform the quantizing signals as shown in Fig. 9(c). The clipping signal using the least-squares method is applied in Fig. 9(d). The chaotic codes using the approximation method

Please cite this article as: S. Mitatha, et al., High-capacity and security packet switching using the nonlinear effects in micro ring ... Opt. Int. J. Light Electron Opt. (2008), doi:10.1016/j.ijleo.2008.05.032

IJLEO : 50616

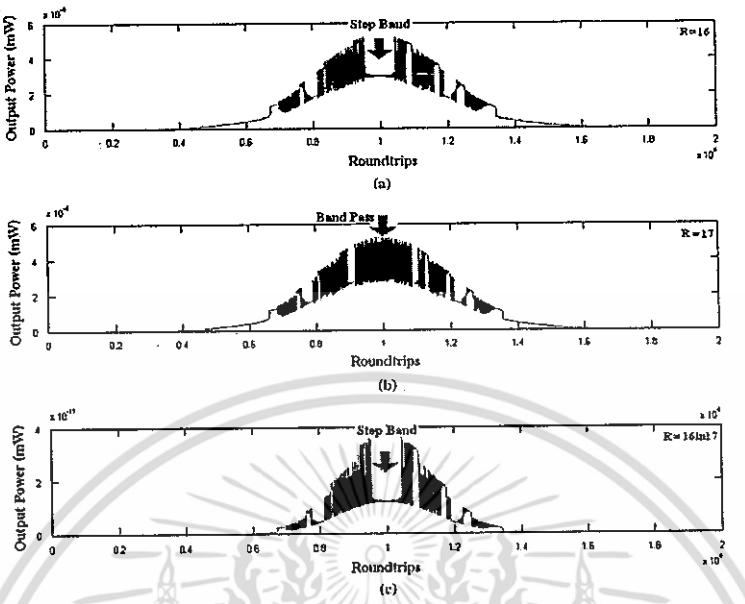

Fig. 6. The chaotic output power and roundtrips of the micro ring at the roundtrips of 20,000, (a) 16 μm, (b) 17 μm, (c) $R = 16$ μm in series with $R = 17$ μm.

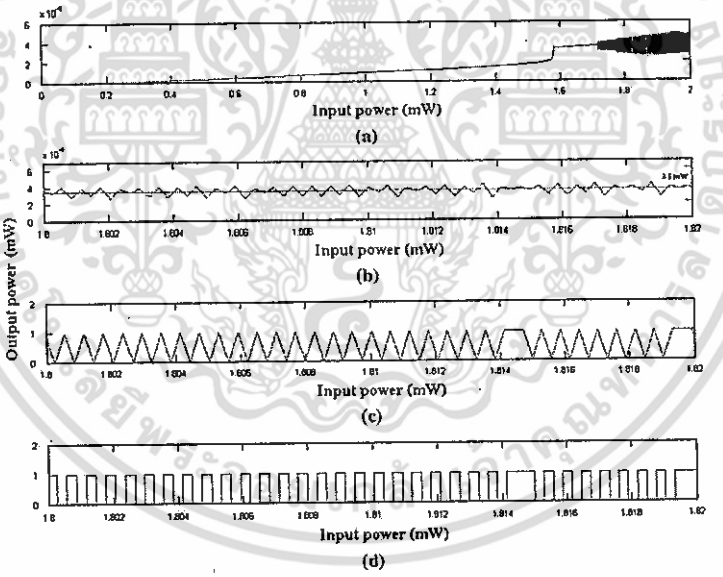

Fig. 7. The chaotic output power and digital codes using the approximation method.

IJLEO : 50616

ARTICLE IN PRESS

8 S. Mitatha et al. / Optik ▮ (▮▮▮▮) ▮▮▮–▮▮▮

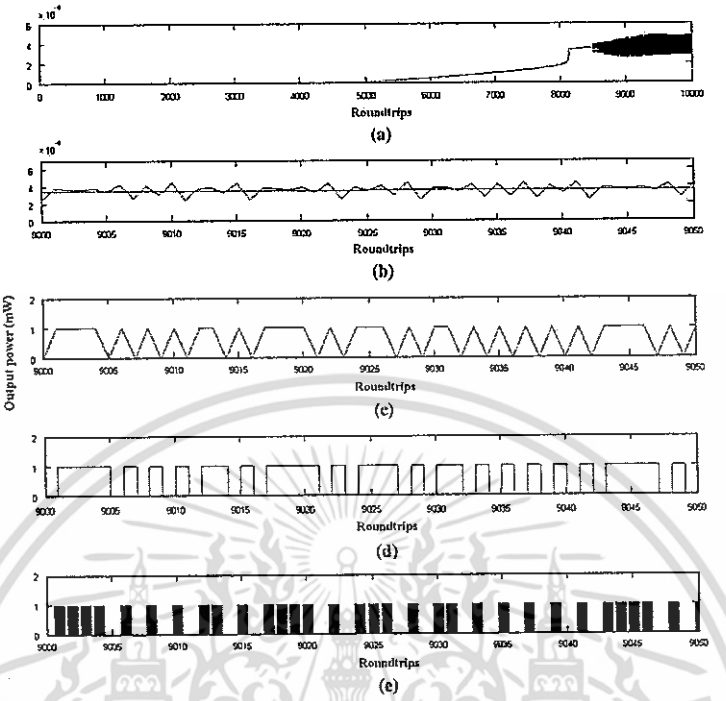

Fig. 8. The chaotic codes: [01111010101011010111101011010110101010101011110101].

is obtained in Fig. 9(e), where the logic code obtained is [000100000101000010100000000000100000100000000-1001001100010001000001001000001010100101000000100100010]. There are 100 logic codes, with a packet switching time of 10^{-12}s (a single bit time is 10^{-15}s). Similarly, the digital codes can be performed using the band stop filter characteristics as shown in Fig. 10. The digital code obtained is [010101011110000100101001 100000010100101010100110110101010010110100101000-0101011101010001010100101100001]. There are 100 logic codes.

In operation, the generated chaotic codes can be formed by quantizing the chaotic signals, which can be switched (On/Off) via the band pass or band stop filters to the specific users. This means the high-capacity and secured communication data can be performed in the optical networks. The simulation results obtained have shown that there are two schemes of the chaotic codes, which can be generated to obtain the 100 logical codes. The random process occurs when the random input is processed to control the optical chaotic signals, and the selected threshold powers. This means this scheme can be used to randomly process the chaotic codes. Further, the control function can also be implemented, which will be interesting for data encryption applications. This means the decryption will be allowed when the decryption codes are being given to the subscriptions clients only. To make more secure, the random control input power can be included in the design. Results obtained have shown that the ultra-fast switching time, i.e. bit time in the range of 10^{-15}s (fs), is achieved, which is fast compared with the electronic scheme.

Please cite this article as: S. Mitatha, et al., High-capacity and security packet switching using the nonlinear effects in micro ring..., Opt. Int. J. Light Electron. Opt. (2008), doi:10.1016/j.ijleo.2008.05.032

IJLEO : 50616

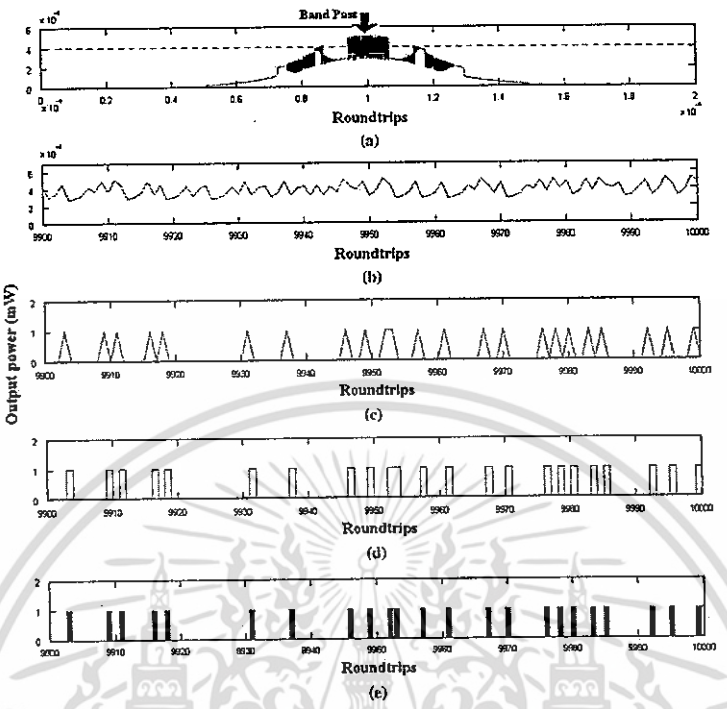

Fig. 9. The packet switching codes: [0001000001010000101000000000001000001000000001001001100010001000001001000001010100101000000100100010].1

4. Conclusion

We have proposed the use of a micro ring resonator to design the optical packet switching, which is useful, easy to design and to implement. Here the use of chaotic codes and packet switches can be performed and realized. The advantage of such a system is that the communication signals can be randomly chaotic encoded and switched for the specified users. The chaotic signals can be encoded using the synchronized technique, where the required message can be successfully decoded by subtracting the chaotic oscillation. This is operated by the receiver in the transmitted signal by using the least-squares method. We have demonstrated that the chaotic signal is logically encoded by using the waveforms of the transmitter and chaotic signals of the receiver output. Thus, we can conduct a secure transmission of a message and logical coding using chaotic quantizing and coding. In either case, the completed or generalized chaotic quantizing control and chaotic signals encoding can be applied to the systems for chaotic communications. However, the long-distance communication when the loss in optical power is the issue of implementation, then the optical repeater is required in the system, where the signal recovery and noise reduction are required to be taken into account. In practice, such a proposed device can be fabricated and implemented in the communication networks, which can form the high-capacity and secured packet of data using the chaotic encoding signals; for example, such a device can be applied to the mobile telephone hand set, computing system and telecommunication networks. For further application, the more advantageous method, called quantum chaotic encoding, may be the new area of investigation in the near future.

Please cite this article as: S. Mitatha, et al., High-capacity and security packet switching using the nonlinear effects in micro ring..., Opt. Int. J. Light Electron. Opt. (2008), doi:10.1016/j.ijleo.2008.05.032

IJLEO : 50616

ARTICLE IN PRESS

10 S. Mitatha et al. / Optik ▪ (▪▪▪▪) ▪▪▪–▪▪▪

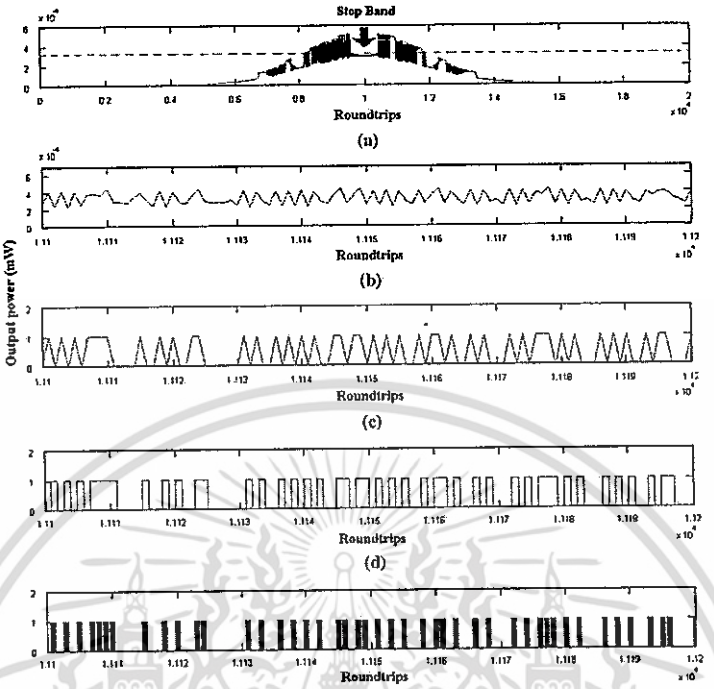

Fig. 10. The packet switching codes: [0101010111100001001010011000000101001010101001101010100101101001010000101011101010001010100101100001].

References

[1] P.P. Yupapin, W. Suwancharoen, Chaotic noise control and cancellation using a micro ring resonator incorporating an optical add/drop multiplexer, Opt. Commun. 280 (2007) 343–350.

[2] A. Morand, Y. Zhang, B. Martin, K.P. Huy, D. Amans, P. Benech, Ultra-compact microdisk resonator filters on SOI substrate, Opt. Exp. 14 (26) (2000) 12814–12821.

[3] V. Van, T.A. Ibrahim, P.P. Absil, F.G. Jhonson, R. Grover, P.T. Ho, Optical signal processing using nonlinear semiconductor microring resonators, IEEE J. Quantum Electron. 8 (2002) 705–713.

[4] P.P. Yupapin, P. Saeung, W. Suwancharoen, Coupler-loss and coupling-coefficient dependence of bistability and instability in a fiber ring resonator: nonlinear behaviors, J. Nonlinear Opt. Phys. Mater. (JNOPM) 16 (2007) 111–118.

[5] P.P. Yupapin, W. Suwanchareon, S. Suchat, Nonlinearity penalties and benefits of light traveling in a fiber optic ring resonator, Int. J. Light Electron Opt., doi: 10.1016/j.ijleo.2007.07.009.

[6] A. Melloni, M. Martinelli, Synthesis of direct-coupled-resonators band pass filter for WDM system, IEEE J. Lightwave Technol. 20 (2) (2002) 296–303.

[7] A. Melloni, M. Floridi, M. Martinelli, Synthesis of direct-coupled resonators band pass photonic filters, in: Proceedings of the LEOS 2000 13th Annual Meeting, 2000, pp. 704–705 November 13–16, ThC4.

[8] B.E. Little, S.T. Chu, J.V. Hryniewicz, P.P. Absil, Filter synthesis for periodically coupled micro ring resonators, Opt. Lett. 25 (5) (2000) 344–346.

[9] A. Melloni, Synthesis of a parallel-coupled ring-resonator filter, Opt. Lett. 26 (12) (2001) 917–919.

[10] Y. Kokubun, Wavelength selective integrated device by vertically coupled micro ring resonator filter: photonics based on wavelength integration and manipulation, IPAP Books 2 (2005) pp. 303–316

[11] E. Kehayas, L. Stampoulidis, H. Avramopoulos, Y. Liu, E. Tangdiongga, H.J.S. Dorren, 40 Gb/s all-optical packet clock recovery with ultra fast lock-in time and low inter-packet guard bands, Opt. Exp. 13 (2) (2005) 475–480.

Please cite this article as: S. Mitatha, et al., High-capacity and security packet switching using the nonlinear effects in micro ring ..., Opt. Int. J. Light Electron. Opt. (2008), doi:10.1016/j.ijleo.2008.05.032

IJLEO : 50616

[12] M. Takenaka, M. Raburn, K. Takeda, and Y. Nakano, All-optical packet switching by MMI-BLD optical flip-flop, in: Proceedings of 2006 OFC/NFOEC, Paper in OTHS3, Anaheim, California, USA, March 5–10, 2006.

[13] Y. Liua, E. Tangdionggaa, Z. Lia, S. Zhanga, M.T. Hilla, J.H.C. van Zantvoorta, F.M. Huijskensa, H. de Waardta, M.K. Smitb, A.M.J. Koonena, G.D. Khoea, H.J.S. Dorrena, Ultra-fast all-optical signal processing: towards optical packet switching, Proc. SPIE 6353 (2006) 635312-1–635312-12.

[14] S. Mikroulis, H. Simos, E. Roditi, A. Chipouras, D. Syvridis, 40-Gb/s NRZ and RZ operation of an all-optical AND logic gate based on a passive InGaAsP/InP micro ring resonator, IEEE J. Lightwave Technol. 24 (3) (2006) 1159–1164.

[15] T. Aizawa, K.G. Ravikumar, Y. Nagasawa, T. Sekiguchi, T. Watanabe, InGaAsP/InP NQW direction couple switch with small and low-loss bends for fiber array coupling, IEEE Photon. Technol. Lett. 6 (1994) 709–711.

[16] S. Xiao, M.H. Khan, H. Shen, M. Qi, Compact silicon micro ring resonators with ultra-low propagation loss in the C band, Opt. Exp. 15 (2007) 14467–14475.

[17] G.C. Valley, Photonic analog-to-digital converters, Opt. Exp. 15 (5) (2007) 1955–1982.

Please cite this article as: S. Mitatha, et al., High-capacity and security packet switching using the nonlinear effects in micro ring, Opt. Int. J. Light Electron. Opt. (2008), doi:10.1016/j.ijleo.2008.05.032

XML:ver:5.0.1 5 jena | IJLEO : 50612 | Prod.Type:FTP pp.1–9(col.fig.:NIL) | ED:JyothiG PAGN:dorthy SCAN:

ARTICLE IN PRESS

Available online at www.sciencedirect.com

ScienceDirect

ELSEVIER

Optik 1 (1111) 111–111

Optik Optics

www.elsevier.de/ijleo

Chaotic signal generation and coding using a nonlinear micro ring resonator

S. Mitatha[a], K. Dejhan[a], P.P. Yupapin[b,*], N. Pornsuwancharoen[c]

[a]*Faculty of Engineering, Research Center for Communication and Information Technology, Thailand*
[b]*Department of Applied Physics, Advanced Research Center for Photonics, Faculty of Science, King Mongkut's Institute of Technology Ladkrabang, Bangkok 10520, Thailand*
[c]*Department of Electronics, Faculty of Industry and Technology, Rajamangala University of Technology Isan, Sakon-nakorn Campus 47160, Thailand*

Received 20 December 2007; accepted 25 May 2008

Abstract

We propose a new digital encoding method using light pulses tracing in a micro ring resonator, where the randomly digital codes can be performed. The chaotic signals can be generated and formed by the logical pulses "1" or "0" by using the signal quantizing method, which can be randomly coded by controlling the specific optical input coupling powers, i.e. coupling coefficient (κ) and ring radii. Simulation results when the ring radius used is 10.0 μm, and the other selected parameters are close to the practical device values that are presented and discussed. The random codes can be generated by the random control of coupling powers, which can be transmitted and retrieved via the design filters by the specific clients. For instance, the controlled input power used is between 2.0 and 3.5 mW, whereas the quantizing threshold powers and the traveling roundtrips are 0.3–0.4 mW and 8000–10,000, respectively. In application, the required information can be generated, and the information can be securely transmitted in the public link.

Keywords: Nonlinear optical communication; Chaotic encoding; Chaotic communication

1. Introduction

Chaotic behavior has been studied as a nonlinear property in areas such as mathematics [1], physics electronics, and communications [2]. They have reported that the nonlinear behaviors can be accorded when the concerned parameters are suitable in similar cases, which is commonly known as a non-periodic behavior and become the penalty of the system. However, the benefit of such a property can also be accepted, for instance, the chaotic communication has recently attracted great interest because of its potential applications in secure and confidential communications, where it uses a noise-like broadband chaotic waveform as a carrier. Furthermore, the chaotic noise has been found useful in several areas of applications such as electronic communication [3], switching and control [4], and optical communication [5]. Where the present use of the benefit of such a nonlinear behavior, especially, in the military purpose for when the information is required to be kept confidential. In general, the

*Corresponding author. Tel.: +23 264339; fax: +23 264354.
E-mail address: kypreech@kmitl.ac.th (P.P. Yupapin).

0030-4026/$ - see front matter © 2008 Published by Elsevier GmbH.
doi:10.1016/j.ijleo.2008.05.028

Please cite this article as: S. Mitatha, et al., Chaotic signal generation and coding using a nonlinear micro ring..., Opt. Int. J. Light Electron Opt. (2008), doi:10.1016/j.ijleo.2008.05.028

IJLEO : 50612

ARTICLE IN PRESS

nonlinearity of the system involves behaviors such as chaos, bistability, and bifurcation, which can be generated in the electronic circuit and optical fiber [6,7], laser system [8], and optical waveguide [9]. One application is the use of the device known as a micro ring resonator, which can be formed by a waveguide or a fiber optic that has shown a very promising application. Moreover, when such a device is fabricated within the range of a micrometer scale [10,11], it can be used incorporating a system such as a mobile telephone hand set, computing system, and telecommunication networks. The secure communication systems based on chaos in a micro ring resonator were proposed by references [12,13]. The message coding and the nonlinear effect of the coding process and control chaotic signal encoding were studied. They consist of three methods, such as (1) control input power (mW); (2) control threshold power (mW); and (3) timing control.

The chaotic encoding methods are processed by sampling, quantizing, and chaotic synchronization. The chaotic signal generation and cancellation using a micro ring resonator have been recently reported [7]. In this paper, we have proposed the extended details of our previous work, where the other point of view from its applications is the chaotic switching of the optical output which can be formed by the digital codes. The selected input signals can be used to control the required chaotic encoding, which can be distributed into the optical transmission link. The most important advantage of the proposed system is the easy implementation compared to the well-known secure communication technique called quantum cryptography [14], which will be extremely difficult in the realistic system, while the requirement in terms of security is acceptable. Eventually, the required information can be retrieved when the decode technique and the tunable filters are employed by the required clients. The basic theory of a micro ring resonator is reviewed, the chaotic quantizing and coding and control are presented in detail.

2. Operating principles

A simple device schematic diagram is as shown in Fig. 1, when the light from a monochromatic light source is launched into a ring resonator with a constant light field amplitude (E_0) and random phase modulation (ϕ_0), which results in a chronological coherence degradation.

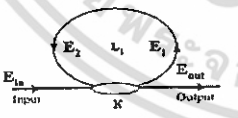

Fig. 1. A schematic diagram of the micro ring resonator.

Hence forth, the input light field (E_{in}) can be expressed as

$$E_{in}(t) = E_0 \exp^{j\phi_0(t)} \tag{2.1}$$

Eq. (2.2) is given by [7]

$$\left|\frac{E_{out}(t)}{E_{in}(t)}\right|^2 = (1-\gamma) \times \left[1 - \frac{(1-(1-\gamma)x^2)\kappa}{(1-x\sqrt{1-\gamma}\sqrt{1-\kappa})^2 + 4x\sqrt{1-\gamma}\sqrt{1-\kappa}\sin^2(\phi/2)}\right] \tag{2.2}$$

In addition, the optical fields E_1 and E_2 represent the right and left hand circulations in a ring resonator, respectively. A close examination of Eq. (2.2) indicates that a ring resonator in the particular case is very similar to a Fabry–Perot cavity, which has an input and output mirror with a field reflectivity, $1-\kappa$, and a fully reflecting mirror. Where n_0 and n_2 are the linear and nonlinear refractive indices, and the coupling coefficient is κ. Where $x = \exp(-\alpha L/2)$ represents a roundtrip losses coefficient, $\phi_0 = kLn_0$ and $\phi_{NL} = kLn_2|E_1|^2$ are the linear and nonlinear phases that shift, respectively; $k = 2\pi/\lambda$ is the wave propagation number in vacuum.

This nonlinear behavior of light traveling in a single ring resonator is described. When the parameters of the system are fixed to $\lambda_0 = 1.55\,\mu m$, $n_0 = 1.54$, $A_{eff} = 30\,\mu m^2$, the waveguide ring resonator loss (α) is 0.5 dB/mm. The practical bending loss of the waveguide fabricated by InGaAsP/InP is confirmed by reference [15], where the propagation loss is as low as $1.3 \pm .02$ dB/mm at 1.55 μm [16], the fractional coupler intensity loss (γ) is 0.1, and $R_1 = 10\,\mu m$. The coupling coefficient of the fiber coupler is fixed to $\kappa = 0.0225$. The nonlinear refractive index used is $n_2 = 2.2 \times 10^{-15}\,m^2/W$ [7], and the data of 10,000 iterations of roundtrips inside the optical micro ring are plotted. We assume that $\phi_L = 0$ for simplicity; however, the change in phase is slightly altered by the optical output [9], which means the dispersion can be neglected when the resonant output has occurred. The chaotic signals are generated by using Eq. (2.2), which can be electronically formed by the digital codes as the following details. The quantitatively present logic coding can be expressed by,

$$u(v) = \begin{cases} 0 \ldots\ldots v < 3.5\,mW \\ 1 \ldots\ldots v \geq 3.5\,mW \end{cases} \tag{2.3}$$

Furthermore, when $u(v)$ represents the logic states, v is the signal power. The quantization and re-quantization can be processed by similar transfer characteristics. We assume that the quantizing involved is infinite, which means that the system input signal is never clipped by saturation of the quantizing. In this case, the corresponding transfer functions of the quantizing output to its input can be expressed analytically in terms of the quantizing step size as detailed in references [17,18]. The chaotic signals mentioned below can be used to form the

Please cite this article as: S. Mitatha, et al., Chaotic signal generation and coding using a nonlinear micro ring, Opt. Int. J. Light Electron. Opt. (2008), doi:10.1016/j.ijleo.2008.05.028

digital codes. Fig. 2 illustrates a flow chart of the chaotic encoding procedures. When the program is operated, i.e. "START," then the program logical coding begins. Firstly, the reduction of the threshold and maximum powers is required, which are ranged between 3.5 and 4 mW. Secondly, "Yes" and "NO" form the logics "1" and "0", respectively. Lastly, "END" is the process of the final step. In practice, the design micro ring resonator with its suitable parameters can be used to generate the chaotic signals, which can be electronically coded. For example, the chaotic signals with the optical power ranges are 1.8–1.82, 1.84–1.86 and 1.88–1.90 mW as shown in Fig. 3.

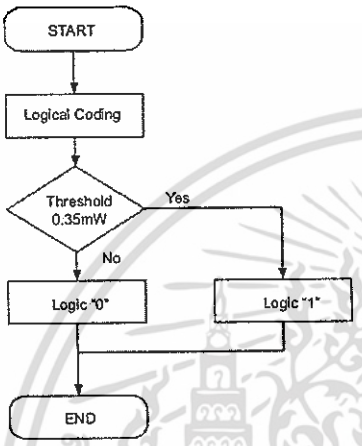

Fig. 2. A diagram of a chaotic coding algorithm.

The signal quantization can be further understood by using the approximation method in which the chaotic signal can be encoded. The quantizing plots of the various input powers are ranged from 1.8 to 1.82 mW as shown in Fig. 3. These plots show the improvement of the approximation method as shown in Fig. 3(a–c), and deterioration until or the least-square method in Fig. 3(d) is introduced. The signal processing of the output using the approximation method is plotted. Where (a) shows the relationship between the input and output signals; (b) the red line (straight line) is the power reduction with the threshold power of 3.5 mW; (c) the signal after threshold power condition uses; and (d) the output signal of when the approximation method is employed. The logical code with the logic state "1" or "0" is generated from the previous description, after the chaotic behaviors of the device are characterized; the next step is that random coding can be generated by controlling the input optical power, which then enters into the micro ring device. The required chaotic codes can be electronically generated. However, in application, the fiber ring resonator parameters and the reliable optical source have become the key conditions.

3. Chaotic coding and control

The chaotic coding generation can be processed as the following. Firstly, the chaotic signals can be generated within the fiber ring resonator by controlling the optical input power into a ring resonator, which can be specified

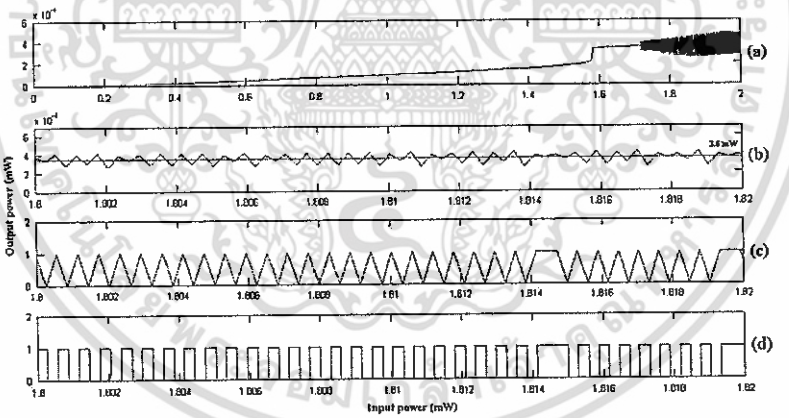

Fig. 3. The chaotic signal and coding using the approximation method.

Please cite this article as: S. Mitatha, et al., Chaotic signal generation and coding using a nonlinear micro ring, Opt. Int. J. Light Electron Opt. (2008), doi:10.1016/j.ijleo.2008.03.028

by the roundtrip numbers, i.e. circulation time. Secondly, the electronically encoding processes are performed by the following steps: (i) chaotic coding with the threshold power is marked by using the least-square method; (ii) the clipping signals is introduced; and (iii) the chaotic code generation is completed by using the approximation and sampling methods. The first chaotic code generation is as shown in Fig. 4, where Fig. 4(a) shows the relationship between the output signals and roundtrips, in which the chaotic behavior occurs when the roundtrips are 10,000, and the optical power is 0.5 mW. In Fig. 4 (b) the threshold power is 3.5 mW, and the encoding roundtrips are ranged between 9000 and 9050.

The 'he' clipping signals shown in Fig. 4 (c e) are the clipping signals using the least-square method and the chaotic codes using the approximation method. The logic codes are [0111101010101101011110101110101101010101010111-10101], which are 50 logic codes, and a roundtrip time is found to be 29×10^{-12} s, i.e. ps.

Similarly, Figs. 5 8 are the results which are described as the following figure captions. Fig. 5(a), the optical output power is 0.5 mW, with 10,000 roundtrips, where the threshold power is 0.40 mW with the encoding roundtrips that range between 9000 and 9050 as shown in Fig. 5(b); Fig. 5(c) shows the clipping signals, and the least-squares method is applied as shown in Fig. 5(d). There are 50 logic codes obtained with a bit time of 29×10^{-12} s as shown in Fig. 5(e). In Fig. 6(a) the input optical power is 2 mW with 10,000 roundtrips, and the output power is 0.5 mW (b). The red line is the threshold power, which is 0.30 mW within the encoding ranges and that range between 9000 and 9025 roundtrips. (c) The clipping signal using the threshold power without the least-squares method, (d) the clipping signals using the threshold power with the least-squares method, (e) the chaotic codes obtained using the approximation method in which there are 25 logic codes. The roundtrip time is 29×10^{-12} s. In Fig. 7(a) the input power is 2.00 mW within 10,000 roundtrips, the output power is 0.5 mW. In Fig. 7(b) the threshold power is 0.30 mW, within the encoding ranges between 9000 and 9025 roundtrips. Fig. 7 (c) and (d) shows the clipping signals without and with least-squares methods. The chaotic codes using the approximation method is as shown in Fig. 7(e). There are 25 logic codes; moreover, the roundtrip time is 29×10^{-12} s. In Fig. 8(a) the input power is 2.00 mW within 10,000 roundtrips, and the output power is 0.5 mW. In Fig. 8(b) the red line is the threshold power (0.3 mW), which is shown within the encoding ranges between 8975 and 9000 roundtrips. The clipping signals without and with the least-squares methods are shown in Fig. 8(c e), which show that the chaotic codes using the approximation method, there are 25 logic codes, and the roundtrip time is 29×10^{-12} s.

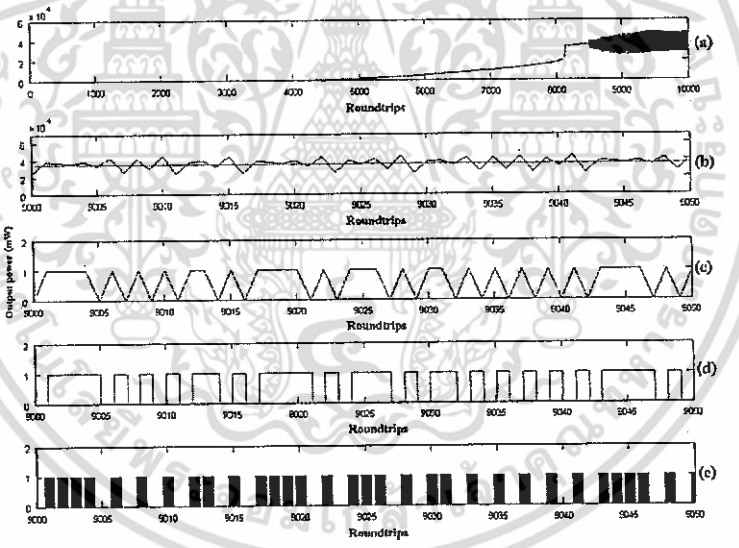

Fig. 4. Chaotic codes: [0111101010101101011110101110101101010101010111101011.

Please cite this article as: S. Mitaiha, et al., Chaotic signal generation and coding using a nonlinear micro ring, Opt. Int. J. Light Electron Opt. (2008), doi:10.1016/j.ijleo.2008.05.028

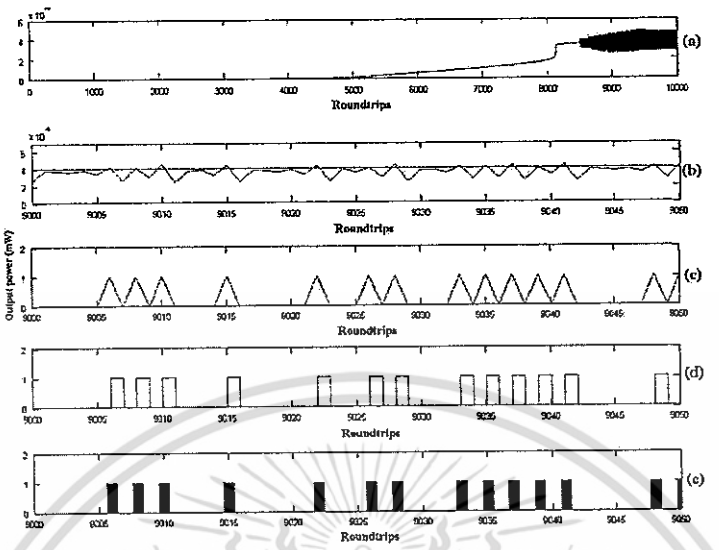

Fig. 5. Chaotic codes: [0000001010100001000000100010100001010101010000000101].

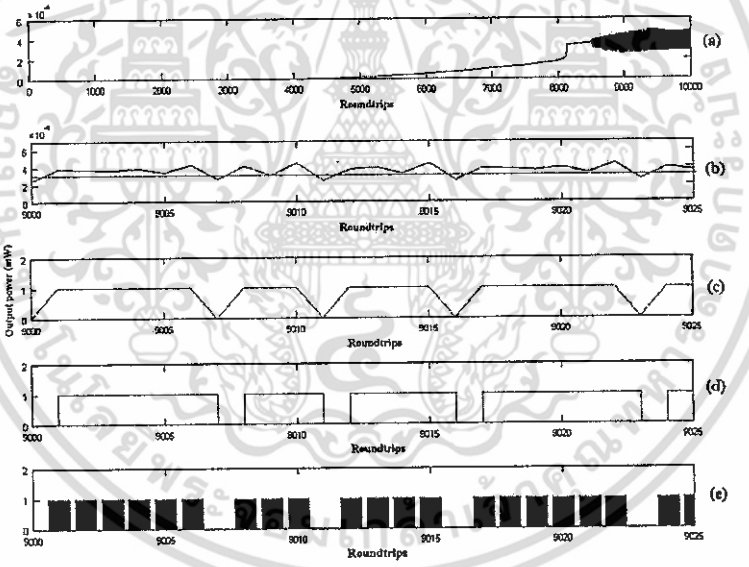

Fig. 6. Chaotic codes: [0111111011101111011111011].

Please cite this article as: S. Mitatha, et al., Chaotic signal generation and coding using a nonlinear micro ring, Opt. Int. J. Light Electron. Opt. (2008), doi:10.1016/j.ijleo.2008.05.022

IJLEO : 50612

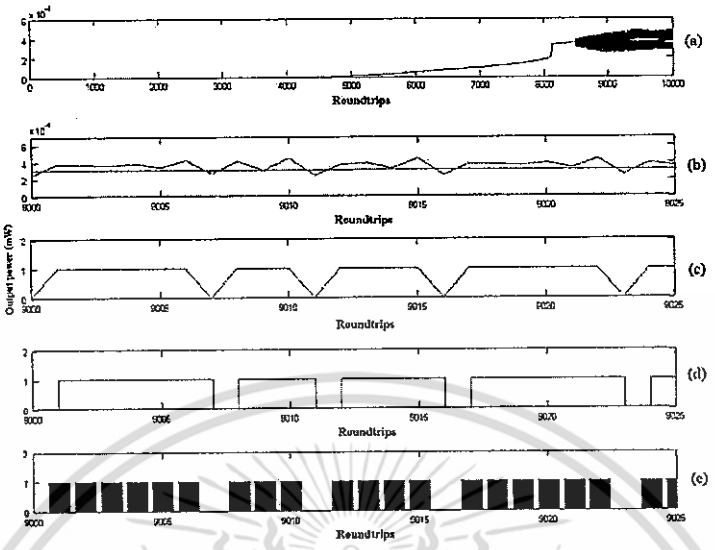

Fig. 7. Chaotic codes: [0111111011101111011111011].

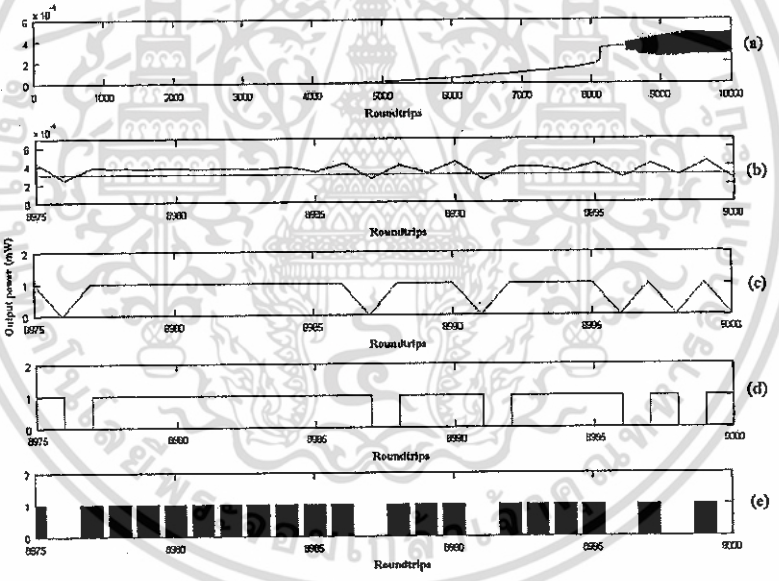

Fig. 8. Chaotic codes: [10111111111110111011101010].

Please cite this article as: S. Mitatha, et al., Chaotic signal generation and coding using a nonlinear micro ring-4 Opt. Int. J. Light Electron. Opt. (2008), doi:10.1016/j.ijleo.2008.05.028

IJLEO : 50612

ARTICLE IN PRESS

S. Mitatha et al. / Optik ▮ (▮▮▮▮) ▮▮▮–▮▮▮ 7

4. Discussion and conclusion

From Fig. 9, the chaotic signals are generated by using the micro ring part, while the chaotic codes (digital codes) are electronically performed by the encryption data. The signals are multiplexed and transmitted via either wire or wireless links to the required receivers. The transmitted signals are received and de-multiplexed, where the synchronously decryption to the encryption data is processed before the chaotic codes being intercepted by the specific users via the design chaotic filters. Finally, the required signals can be retrieved by the previous scheme, i.e. chaotic cancellation [7]. Using Eq. (2.2), the simulation results obtained are shown in Fig. 10, where Fig. 10(a) shows the behaviors of the band stop and band pass filters with a ring radius of 12 μm, roundtrips of 9050 11,500. In Fig. 10(b) and (c), the band stops and band pass filters' characteristics of the different ring radii, and the serial rings configuration are shown. Similarly, the multi-filter characteristics can be seen in Fig. 11. However, the low level of the upper and lower side bands of the signals may cause a problem

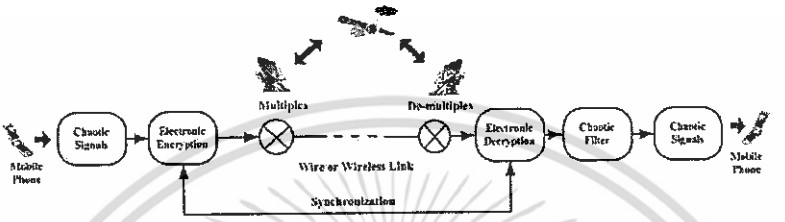

Fig. 9. The schematic diagram of the synchronous encryption and the encryption system.

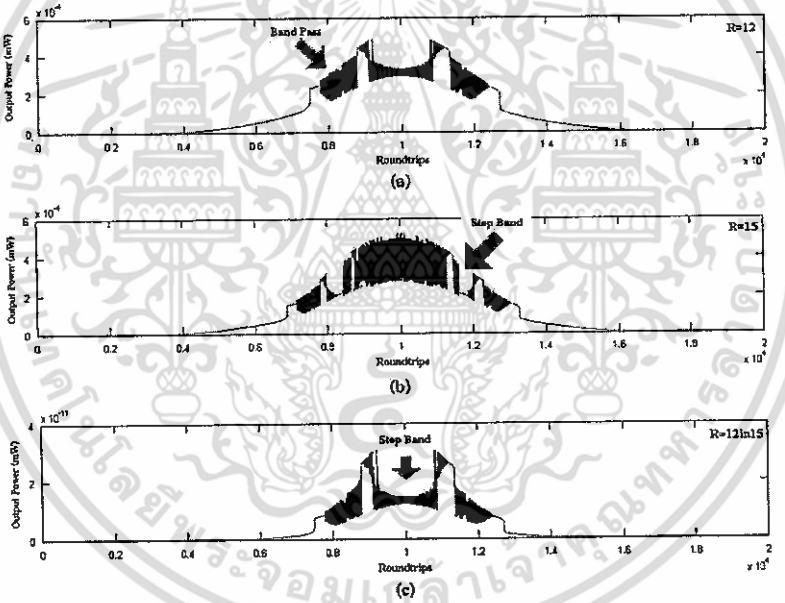

Fig. 10. The chaotic filter characteristics and roundtrips of the micro ring at the roundtrips of 20,000, (a) $R = 12\,\mu m$, (b) $R = 15\,\mu m$, (c) $R = 12\,\mu m$ in series with $R = 15\,\mu m$.

Please cite this article as: S. Mitatha, et al., Chaotic signal generation and coding using a nonlinear micro ring, Opt. Int. J. Light Electron. Opt. (2008), doi:10.1016/j.ijleo.2008.03.028

IJLEO : 50612

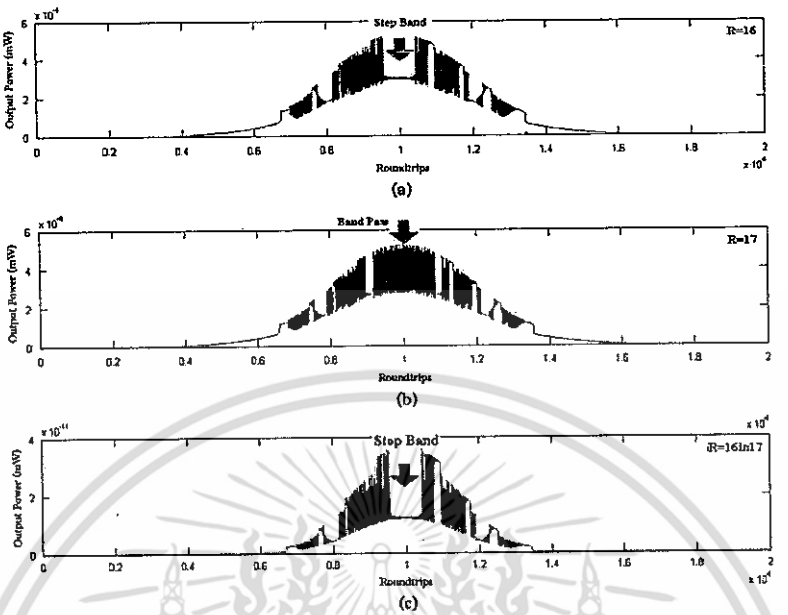

Fig. 11. The chaotic filter characteristics and roundtrips of the output signal using micro ring at the roundtrips of 20,000, (a) $R = 16\,\mu m$, (b) $R = 17\,\mu m$, (c) $R = 16\,\mu m$ in series with $R = 17\,\mu m$.

of low-level signal to noise ratio in real applications. The serial rings results have shown better S/N than the single ring configurations.

We have proposed the use of a micro ring resonator to generate the chaotic codes, where the advantages of such a device are (i) the signals are randomly encoded, (ii) easy to design and implement, (iii) the control optical power could be selected, and finally (iv) the tunable filters can be employed. In an application, such a proposed device can be fabricated and implemented in the communication. For example, a mobile telephone hand set, a computing system, and telecommunication networks. The chaotic signals can be encoded by using the electronically synchronized technique, where the required message can be successfully decoded by subtracting the chaotic oscillation. This is operated by the receiver on the transmitted signal by using the least-squares method. We have demonstrated that the chaotic signal is logically encoded by using the waveforms of the transmitter and chaotic signal of the receiver output. Thus, we can conduct a secure transmission of a message by logical coding using the electronic quantizing, and coding by using the micro ring incorporating in the communication transmission. In either case, the completed or generalized chaotic quantizing control and chaotic signals encoding can be applied to the systems for chaotic communications for a long distance communication when the loss in the optical power is the issue of implementation. Therefore, such a proposed technique can overcome the problem of signal degradation because the digital signal can be recovered more easily than the analog ones. In practice, the optical repeater is required into the system, where the signal recovery and noise reduction are required to be taken into account. For further application, the more advantageous method, called quantum chaos, may be the new area of investigation in the near future.

References

[1] P.P. Yupapin, P. Saenng, W. Suwancharoen, J. Nonlinear Opt Phys Mater 16 (2007) 111.
[2] C. Juang, T.M. Hwang, J. Juang, Wen-Wei Lin, IEEE J. Quantum Electron. 36 (2000) 300.
[3] X. Wang, M. Zhan, X. Gong, C.H. Lai, Ying-Cheng Lai, Phys. Lett. A 334 (2005) 30.
[4] P.M. Alsing, A. Gavrielides, V. Kovanis, R. Roy, K.S. Thornburg Jr., Phys. Rev. E 56 (1997) 6302.

Please cite this article as: S. Mitatha et al., Chaotic signal generation and coding using a nonlinear micro ring..., Opt. Int. J. Light Electron. Opt. (2008), doi:10.1016/j.ijleo.2008.05.028

IJLEO : 50612

[5] P.P. Yupapin, W. Suwancharoen, Opt. Commun. 280 (2007) 343.
[6] R. Gang, X. Jiapin, W.H. Hui, J. Lu, IEEE J. Commun Circuit Syst. 2 (2004) 809.
[7] E. Genin, L. Larger, Jean-Pierre Goedgebuer, M.W. Lee, R. Ferriere, X. Bavard, IEEE J. Quantum Electron. 40 (2004) 294.
[8] S. Sivaprakasam, K.A. Shore, IEEE J. Quantum Electron. 36 (2000) 35.
[9] V. Van, T.A. Ibrahim, P.P. Absil, F.G. Jhonson, R. Grover, P.T. Ho, IEEE J. Quantum Electron. 8 (2002) 705.
[10] A. Morand, Y. Zhang, B. Martin, K.P. Huy, D. Amans, P. Benech, Opt. Exp. 14 (2000) 12814.
[11] V. Van, T.A. Ibrahim, P.P. Absil, F.G. Jhonson, R. Grover, P.T. Ho, IEEE J. Quantum Electron. 8 (2002) 705.
[12] J. Garcia-Gjaivo, R. Roy, Phys. Rev. Lett. 86 (2001) 5204.
[13] E. Bollt, Ying-Cheng Lai, C. Grebogi, Phys. Rev. Lett. 79 (1997) 3787.
[14] S. Suchat, W. khunnam, P.P. Yupapin, Opt. Eng. 46 (2007) 100502.
[15] T. Aizawa, K.G. Ravikumar, Y. Nagasawa, T. Sekiguchi, T. Watanabe, IEEE Photon. Technol. Lett. 6 (1994) 709.
[16] S. Xiao, M.H. Khan, H. Shen, M. Qi, Opt. Express 15 (2007) 14467.
[17] R.A. Wannamaker, S.P. Lipshitz, J. Vanderkooy, J.N. Wright, IEEE Trans. Signal Process. 48 (2000) 499.
[18] G.C. Valley, Opt. Express 15 (2007) 1955.

Please cite this article as: S. Mitatha, et al., Chaotic signal generation and coding using a nonlinear micro ring... Opti Int. J. Light Electron. Opt. (2008), doi:10.1016/j.ijleo.2008.05.028.

Microwave and
Optical Technology Letters

A Simultaneous Fast and Slow Light Generation via Nonlinear Micro Ring Resonators for Optical Wireless Links

Journal:	*Microwave and Optical Technology Letters*
Manuscript ID:	MOP-08-0893
Wiley - Manuscript type:	Research Article
Date Submitted by the Author:	25-Jun-2008
Complete List of Authors:	Yupapin, PP; King Mongkut's Institute of Technology Ladkrabang, Applied Physics Mitatha, Somsak; King Mongkut's Institute of Technology Ladkrabang, Computer Engineering Dejhan, Kobchai; King Mongkut's Institute of Technology Ladkrabang, Telecommunication Engineering
Keywords:	Harmonic generation , Fast and slow lights, Frequency converter, Optical wireless link

scholarONE™
Manuscript Central

John Wiley & Sons

A Simultaneous Fast and Slow Light Generation via Nonlinear Micro Ring Resonators for Optical Wireless Links

S. Mitatha[1], K. Dejhan[1], P.P. Yupapin[2] and N. Pornsuwancharoen[3]

[1]Faculty of Engineering, Research Center for Communication and Information Technology
[2]Advanced Research Center for Photonics, Department of Applied Physics, Faculty of Science
King Mongkut's Institute of Technology Ladkrabang, Bangkok 10520, Thailand
[3]Department of Electronics, Faculty of Industry and Technology, Rajamangala University of Technology Isan
Sakon-nakorn Campus, Sakon-nakorn 47160, Thailand
Corresponding author: <kypreech@kmitl.ac.th>

Abstract:

We firstly propose a new system of the simultaneous fast and slow light generation using a soliton pulse propagating within the nonlinear micro ring resonators. The nonlinear Kerr effect induces the spreading frequency bands within the micro ring device, where the chaotic filtering characteristics can be employed by using the appropriate micro ring parameters. Results obtained have shown that the wide spreading of frequency bands can be generated and selected to form the optical wireless communication links. In this work, the selected down-link and up-link frequency bands are 500 MHz and 2 GHz, respectively. The proposed system can be implemented within the mobile telephone hand set, where the two different carriers in the same frequency bands can be selected to form the up-down-link converters, which means that the frequency converter can be performed within a single system.

Keywords: Harmonic generation, Fast and slow lights, Frequency converter, Optical wireless link

Mobile telephone has been brought to the world for two decades, where there are some technologies involved in many areas of research. Up to date, the searching for new devices and technologies are still needed. For instance, Yupapin and Suwancharoen have reported the use of chaotic signals generated by micro ring resonator for communication security [1], where the transmission signals could be secured by using the analog or digital methods. The increasing in the channel capacity could be achieved by the technique called the chaotic encoding and packet switching [2], where the information could be secured with highly capacity [3, 4]. Recently, Chaiyasoonthorn et al [5] have reported the interesting results when the ultrafast pulse with pulse width of as could be easily generated by using a soliton pulse travelling in the nonlinear micro ring resonators. The interesting idea is that the system is very small which is capable to implement within the mobile telephone hand set, whereas the required applications can be employed. In this work, we present the other application, where the technique of up-link and down-link can be integrated within a small device called the micro ring devices. Several systems of optical wireless up-down-link converters have been reported [6, 7], however, there is no such a system that can be performed the link within a single system. Our proposed system can be implemented within the mobile telephone handset, where the links can be performed by using the frequency bands generated by the technique called chaotic filtering, where the required frequency bands can be selected and used. Results obtained have shown the good potential application for mobile telephone up-link and down-link device.

Optical soliton is recognized as a powerful laser pulse, which is used to generate the chaotic filter characteristics, especially, when it propagates within the nonlinear micro ring resonators [5]. When the soliton pulse is input into the multi-stage micro ring resonators as shown in Fig. 1, the input optical field (E_{in}) in the form of soliton pulse is expressed by an Eq. (1).

$$E_{in} = A\,Sech\left[\frac{T}{T_0}\right]\exp\left[\left(\frac{z}{2L_D}\right)\right] \qquad (1)$$

Where A and z are the optical field amplitude and propagation direction, respectively. $L_D = T_0^2 / |\beta_2| i$ is the dispersion length of the soliton pulse. This solution describes a pulse that keeps its temporal width invariant as it propagates and thus is called a temporal soliton. T_o is known, once we can find the proper peak intensity $\left(\frac{|\beta_2|}{\gamma T_0^2}\right)$ that will make this pulse a soliton. For example, when the micro ring resonator at the 1550 nm

wavelength, with a 12 W peak power, then $T_o = 50ns$ long, which is a pulse of about 2 millimeter long (in z). For the soliton pulse in the micro ring device, a balance should be achieved between the dispersion lengths $L_D = \frac{T_o^2}{|\beta_2|}$ and the nonlinear length $L_{NL} = \frac{1}{\gamma \psi_0}$, which are the length scales over which dispersive or nonlinear effects make the beam become wider or narrower. For a soliton pulse, there is the balance between the two and hence $L_D = L_{NL}$.

$$n = n_0 + n_2 I = n_0 + (\frac{n_2}{A_{eff}})P, \quad (2)$$

where n_0 and n_2 are the linear and nonlinear refractive indexes, respectively. I and P are the optical intensity and optical field power, respectively. The effective mode core area of the device is A_{eff}.

Thus, the normalized output of the light field can be expressed as,

$$\left|\frac{E_{out}}{E_{in}}\right|^2 = (1-\gamma)^2 \left[1 - \frac{\kappa\left[1-(1-\gamma)^2 x^2\right]}{1+(1-\gamma)^2(1-\kappa)x - 2(1-\gamma)\sqrt{1-\kappa}\, x \cos\phi}\right]. \quad (3)$$

The close form of equation (3) indicates that a ring resonator in the particular case to very similar to a Fabry-Perot cavity, which has an input and output mirror with a field reflectivity, 1-κ, and a fully reflecting mirror. Where n_0 and n_2 are the linear and nonlinear refractive indices, the coupling coefficient is κ. Where $x = \exp^{-\frac{\alpha L}{2}}$ represents the one roundtrip losses coefficient, $\phi_0 = kLn_0$ and $\phi_{NL} = kLn_2\left|E_{in}\right|^2$ are the linear and nonlinear phase shifts, $k = 2\pi/\lambda$ is the wave propagation number in a vacuum, respectively.

In this work, the key point is that the two different frequencies can be simultaneously generated, where the up-down-link converters can be simultaneously operated within a single system. The proposed system of the simultaneous fast and slow light generation is as shown in Fig. 1. The single mode soliton pulse is become many modes (noisy signals) after circulating within the first micro ring device due to the nonlinear Kerr effects of light within the micro ring resonator. The chaotic filtering characteristics of the signals are formed by the other ring resonators within the system. However, in practice, the evidence of such a device in realistic application is required and found in reference [8]. By using the material parameters of *InGaAsP/InP*, the specified frequency bands can be obtained by using the appropriate ring parameters, finally, we ended up with the following details. The soliton waveform with the center frequency at 2 GHz is input into the first micro ring resonator (R1). The optical power is fixed to 550 mW, $f_0 = 2$ GHz, $n_0 = 3.34$, $n_2 = 2.2 \times 10^{-17}$ m^2W^{-1}, $A_{eff} = 0.50$ μm^2, $\alpha = 0.5$ $dBmm^{-1}$, $\gamma = 0.1$, with 20,000 roundtrips. The chaotic signals are generated within the first ring (R1), where the broad frequency band is observed in ring R2. The clearer filtering signals are seen in ring R3 and R4. Fig. 2 shows graph of the simultaneous fast and slow light generation for up-down-link converters. Where the parameters are R1 = 10 μm, κ1 = 0.9713, R2 = 10 μm, κ2 = 0.9718, R3 = 10 μm, κ3 = 0.9718, R4 = 15 μm, κ4 = 0.9728. The down-link and up-link converters are shown in Figs. 3 and 4, respectively. Fig. 3 shows graph of fast and slow light generation for down-link converter. Where the parameters used are R1 = 10 μm, κ1 = 0.9713, R2 = 10 μm, κ2 = 0.9718, R3 = 10 μm, κ3 = 0.9718,R4 = 15 μm, κ4 = 0.9728. Fig. 4 shows graph of fast and slow light generation for up-link converter. When the parameters used are R1 = 10 μm, κ1 = 0.9713, R2 = 10 μm, κ2 = 0.973, R3 = 10 μm, κ3 = 0.9732, R4 = 15 μm, κ4 = 0.9777. In application, the upstream and downstream communication information can be linked via a single system of devices as shown in Fig. 1, for the up-down-link converters. In principle, the communication signals are formed by the signal interchanging devices known as Electrical to Optical (E/O) and Optical to Electrical (O/E) converters. In the system the up-link and down-link frequency bands can be simultaneously generated, therefore, the next step is that the specified frequency band will be selected (filtered) to form the required link converters. By using the proposed system, the wide range of the spread wavelength domain can also be generated and available, which means that the wavelength multiplexing, especially, dense wavelength division multiplexing (DWDM) via optical wireless link is plausible. Moreover, the use of the quantum key distribution via optical wireless link is confirmed by Suchat et al [9]. However, they have proposed the system of fiber optic ring resonator. By using our proposed system, the quantum key distribution can be generated within the micro ring device which will be able to use with the mobile telephone, therefore, the message can be kept in secret via quantum cryptography. This is shown the indication that the perfect security via mobile telephone network is plausible.

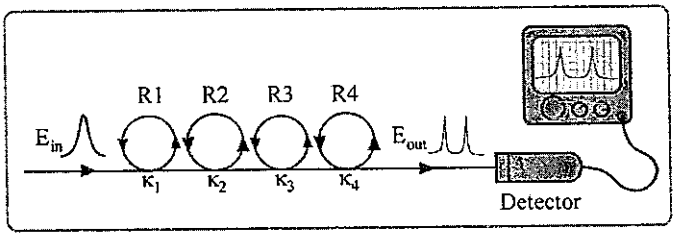

Fig. 1. The schematic diagram of a simultaneous fast and slow light generation. Rs: ring radii, and κs: coupling coefficients.

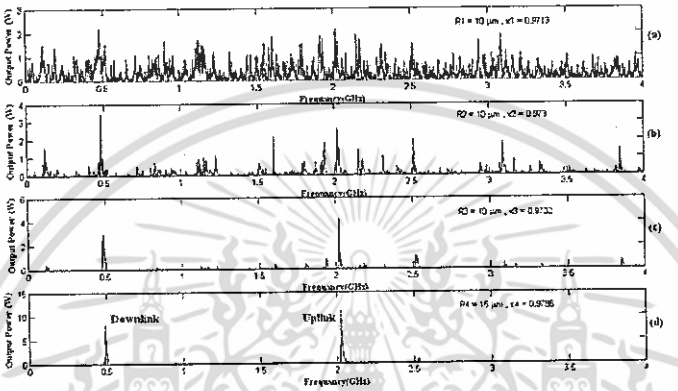

Fig. 2. Graph of simultaneous fast and slow light generation for up-down-link converters, (a) noisy chaotic signals, (b) frequency bands, (c) filtering signals, (d) Up-down-link signals.

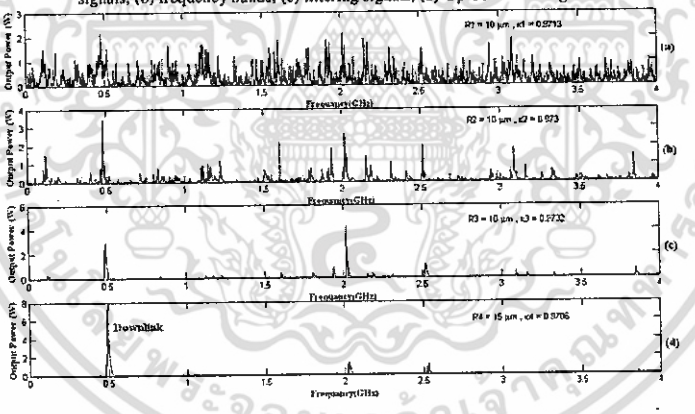

Fig. 3. Graph of fast and slow light generation for down-link converter, (a) noisy chaotic signals, (b) frequency bands, (c) filtering signals, (d) down-link signal(500MHz).

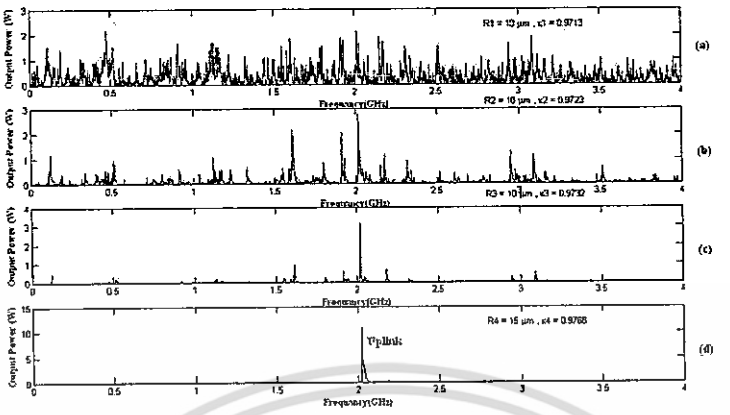

Fig. 4. Graph of fast and slow light generation for up-link converter, (a) noisy chaotic signals, (b) frequency bands, (c) filtering signals, (d) up-link signal(2GHz).

In conclusion, we have proposed the very interesting results that the simultaneous fast and slow light could be generated by using the nonlinear micro ring devices. The system is consisted by a series of four nonlinear micro ring devices. We have shown that the two different frequency bands could be generated and selected, which they are normally used in the up-down-link converters in optical wireless link system. The key advantages of the system are the simultaneous generation of up and down link frequency bands, and the frequency band generation can be formed in the single system. The optical power in the system is generated by using a soliton pulse within the nonlinear Kerr type micro ring devices. Therefore, the remaining optical power is able to perform the link. Further, there are more frequency bands available, which is suitable to implement more applications.

References

[1] P.P. Yupapin, P. Saeung and W. Suwancharoen, Guided Wave Optics and Photonics: Micro Ring Resonator Design for Telephone Network Security, Nova Science Publishers, New York, 2008.
[2] P.P. Yupapin and W. Suwanchroen, A Novel Technology for Mobile Telephone Networks and Security, Mobile Telephones : Networks, Applications, and Performance, Editors : Alvin C. Harper and Raymond V. Buress, Nova Science Publishers, New York, 2008.
[3] S. Mitatha, K. Dejhan, P.P. Yupapin and N. Pornsuwancharoen, International Journal of Light and Electron Optics, 2008.[Article in press]
[4] S. Mitatha, K. Dejhan, P.P. Yupapin and N. Pornsuwancharoen, International Journal of Light and Electron Optics, 2008.[Article in press]
[5] S. Chaiyasoonthorn, O. Saneujit, W. Suwancharoen and P.P. Yupapin, J. Advance Materials Research, 2008. [Article in press].
[6] M.T. Zhou, J.D. Zhang, A.B. Sharma, Y. Zhang, S. Xiao, M. Fujise, Opt. Commun., 269, 69(2007).
[7] M.T. Zhou, Q.J. Wang, B. Luo, Y.X. Guo, L.C. Ong, Y. Zhang, Y.C. Soh, R. Miura, Opt. Commun. 281, 2572(2008).
[8] Y. Kokubun, Y. Hatakeyama, M. Ogata, S. Suzuki, and N. Zaizen, IEEE J. of Selected Topics in Quantum Electronics 11, 4(2005).
[9] S. Suchat, W. Khannam and P.P. Yupapin, Opt. Eng. 46, 100502-1(2007).

BIOGRAPHY

Name: **Mr. Somsak Mitatha**

Organization: Department of Computer Engineeing, Faculty of Engineering
King Mongkut's Institute Technology Ladkrabang(KMITL)
Bangkok, Thailand 10520.
Email Address: kmsomsak@kmkitl.ac.th, kmsomsak@hotmail.com

Educations:

Year	Degree	Major	Institution	Country
1987	B.Ind.Eng	Technology Television Engineering	KMITL	Thailand
1995	M.Eng	Electrical Engineering	KMITL	Thailand

Profession Experiences:

1985 - 1996 Lecturer at Department of Computer Engineering, Faculty of Engineering King Mongkut's Institute Technology Ladkrabang(KMITL).

1996-1999 Assistance Professor of Department of Computer Engineering, Faculty of Engineering, King Mongkut's Institute Technology Ladkrabang(KMITL).

1999- Present Associate Professor of Department of Computer Engineering, Faculty of Engineering, King Mongkut's Institute Technology Ladkrabang(KMITL).

1999-2003 Head Department of Computer Engineering, Faculty of Engineering King Mongkut's Institute Technology Ladkrabang(KMITL).

2004-2005 JICA Third Country Expert (Computer Engineering) in Faculty of Engineering, National of University Laos(NOUL), Vientiane, Laos PDR.

2006-2007 Associate Dean of Faculty of Engineering King Mongkut's Institute Technology Ladkrabang(KMITL).

Text Book: Somsak Mitatha, "Digital Circuits and Logic Design", Faculty of Engineerig, King Mongkut's Institute Technology Ladkrabang, 340 pages, 1st Editions, July 2004 (Thai version)

Research Fields: Computer Hardware Design, Pattern Recognition, Image Processing, Optical Communication, Speech Recognition.